

Universiteit
Leiden
The Netherlands

Identification of neural and non-neural contributors to joint stiffness in upper motor neuron disease

Gooijer-van de Groep, K.L. de

Citation

Gooijer-van de Groep, K. L. de. (2019, June 20). *Identification of neural and non-neural contributors to joint stiffness in upper motor neuron disease*. Retrieved from https://hdl.handle.net/1887/74470

Version:	Not Applicable (or Unknown)
License:	Leiden University Non-exclusive license
Downloaded from:	https://hdl.handle.net/1887/74470

Note: To cite this publication please use the final published version (if applicable).

Cover Page



Universiteit Leiden



The following handle holds various files of this Leiden University dissertation:
http://hdl.handle.net/1887/74470

Author: Gooijer-van de Groep, K.L. de
Title: Identification of neural and non-neural contributors to joint stiffness in upper motor neuron disease
Issue Date: 2019-06-20

Identification of neural and non-neural contributors to joint stiffness in upper motor neuron disease

Novel tools for diagnosis and follow-up



Karin L. de Gooijer-van de Groep

Identification of neural and non-neural contributors to joint stiffness in upper motor neuron disease

Novel tools for diagnosis and follow-up

Karin L. de Gooijer-van de Groep

This research is supported by the Dutch Technology Foundation (STW), which is part of the Dutch National Organization for scientific research (NWO) and partly funded by the Ministry of Economic Affairs, Agriculture and Innovation (ROBIN project, grant nr. 10733).

Financial support for printing of this thesis was generously sponsored by Motekforce Link B.V. and TMSi B.V.

Cover design & Layout: Loes Kema and Karin de Gooijer-van de Groep

Print: GVO drukkers & Vormgevers B.V.

ISBN: 978-94-6332-499-1

©2019 K.L. de Gooijer-van de Groep

Identification of neural and non-neural contributors to joint stiffness in upper motor neuron disease

Novel tools for diagnosis and follow-up

Proefschrift

ter verkrijging van

de graad van Doctor aan de Universiteit Leiden

op gezag van Rector Magnificus prof.mr. C.J.J.M. Stolker

volgens besluit van het College voor Promoties

te verdedigen op donderdag 20 juni 2019

klokke 10:00 uur

door

Karine Lamberthe de Gooijer-van de Groep

geboren te Nijkerk

in 1984

Promotor

Prof dr. J.H. Arendzen

Co-promotoren

Dr. Ir. J.H. de Groot

Dr. C.G.M. Meskers (VU Medisch Centrum)

Leden promotiecommissie

Prof. dr. T.P.M. Vliet Vlieland

Prof. dr. ir. J. Harlaar (VU Medisch Centrum, TU Delft)

Prof. dr. K. Desloovere (KU Leuven)

To wisdom belongs the intellectual apprehension of things eternal; to knowledge, the rational apprehension of things temporal

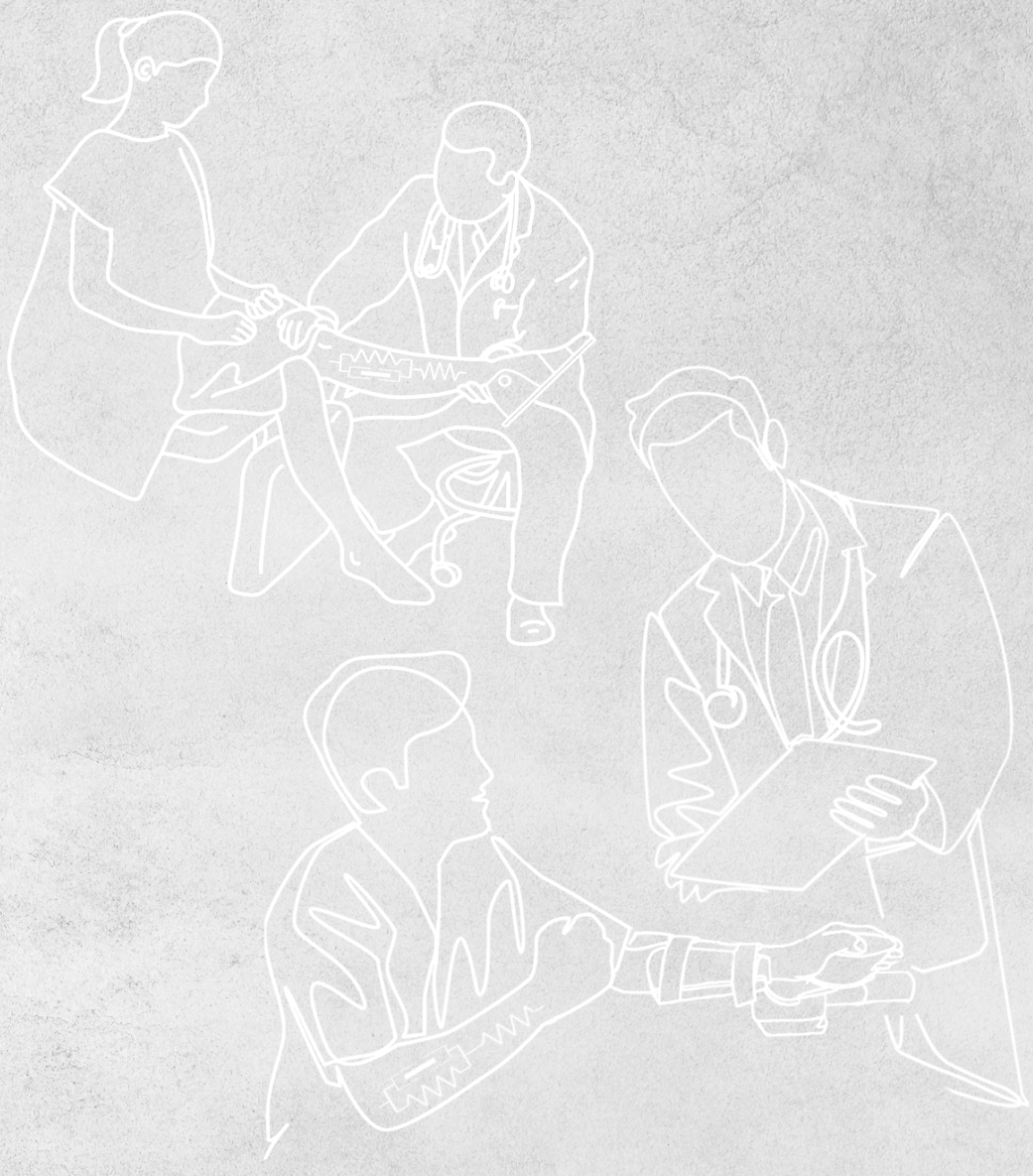
St. Augustine, 354-430

Content

1. Introduction	9
2. Differentiation between non-neural and neural contributors to ankle joint stiffness in cerebral palsy	17
3. Non-invasive assessment of ankle muscle force-length characteristics post-stroke	35
4. Estimation of tissue stiffness, reflex activity, optimal muscle length and slack length in stroke patients using an electromyography driven antagonistic wrist model	65
5. Early shortening of wrist flexor muscles coincides with poor recovery after stroke	97
6. Estimating the effects of botulinum toxin A therapy post-stroke: evidence for reduction of background muscle activation	119
7. Summary and general discussion	137
8. Nederlandse samenvatting – summary in Dutch	149
List of publications	169
Dankwoord	171
Curriculum Vitae	173

CHAPTER 1

Introduction



In upper motor neuron diseases, like spinal cord injury, multiple sclerosis, cerebral palsy and stroke, motor areas in the brain and/or spinal cord are damaged or fail to develop normally. Cerebral palsy is due to abnormal development or damage in the developing brain and occurs in about 2 per 1000 life births[1;2]. Stroke is now the second leading cause of death worldwide and third most common cause of disability-adjusted life-years[3-5] and the incidence of stroke increases with the graying of the society[6;7]. Improvement in acute stroke care results in a greater proportion of patients surviving stroke, but consequently a larger number of people that needs to deal with stroke related disabilities. Activities of daily living and quality of life are affected by motor, cognitive, speech and language disorders, depression and dementia[8;9]. Interfering motor disorders are stiffness, i.e. increased resistance to movement, decreased range of motion, flexion deformity resulting in a shift of joint rest angle towards flexion and paresis, i.e. the inability to voluntarily and selectively generate muscle strength and power[10].

Rehabilitation interventions at the ICF[11] level of body functions and structures focus on reduction of stiffness and maintenance or increasing joint range of motions and correction of abnormal joint rest angle shifts. Clinically, the combination of stiffness and muscle over-activity is often called “spasticity”, but the definition is under debate[10;12]. In stroke about 20-30% of all patients suffer from spasticity[13]. Spasticity was assumed to originate from neurally induced reflexive stiffness, i.e. velocity dependent resistance of joint to passive stretching, according to the definition of Lance[14]. However nowadays it becomes accepted that in “spasticity”, the neural and non-neural components intermingle[15-17]. Neural and non-neural tissue components continuously interact within a closed loop: The tight coupling between afferent sensory information, the central neural system, efferent commands and motor properties[16;18]. Neural activity may modulate tissue properties; tissue shortening may alter reflexive thresholds. Moreover, the neural and non-neural properties are environment- and task dependent[10;16].

This poses a challenge to assess and quantify the neural, i.e. reflexive stiffness and involuntary background activation, and non-neural, i.e. muscle shortening and stiffening, components[15;19]. At these contributors selective treatment should be aimed, i.e. either targeted at the neural component or at the non-neural component. The clinical Ashworth and Tardieu tests[20-22] are applied to quantify the joint stiffness by the observer while manually rotating the joint throughout its range of motion. These clinical tests do not differentiate between the neural

reflexive and non-neural tissue components, besides being notoriously insensitive, ordinal and insufficient valid and reliable as a measure for spasticity[16;23;24].

The neural and non-neural components can be disentangled using a system identification and parameter estimation approach (SIPE). System identification uses robotic devices to deliver precise force and position perturbations to a joint to allow for assessment of input- output relations which can be used to describe the properties of a system[18;25-27]. Subsequent neuromuscular modeling allows for describing the neuromuscular system into clinically interpretable parameters. Linear SIPE techniques have been applied for analysis of the underlying neuromuscular system in patients with dystonia and stroke[28;29] and analysis of standing balance in Parkinson's disease and healthy elderly[30-32]. In these SIPE techniques, the non-linearity, e.g. increased resistance against movement near the maximal range of motion, of the (neuromuscular) system is described by a linear technique. Use of these linear techniques requires small deviations of e.g. joint angle and muscle contraction. These small deviations in movements and contraction do not resemble functional movement. Furthermore, the non-linear force-length and force-velocity properties of the connective and contractile tissue and the quantification of thresholds of spinal reflexes require non-linear methods[16;33;34]. Non-linear models were applied to predict recorded forces from ramp-and-hold joint perturbations by optimizing parameter values of the model of the wrist and ankle in healthy subjects and to discriminate groups of patient with stroke from controls[35;36].

Non-linear models are necessary to quantify underlying neural and non-neural contributors of increased joint stiffness, diminished range of motion and shift of joint rest angle. This quantification is important for understanding of underlying mechanisms of functional recovery and the effect of therapy on the underlying components to diminish or eventually prevent impairments of movement function.

The aim of the present thesis is:

1. To quantify neural reflexive and non-neural tissue contributors in patients with upper motor neuron disease to understand underlying pathophysiological mechanism of increased joint stiffness, diminished range of motion and shifted joint rest angle. Therefore, an instrumented and EMG driven non-linear neuromuscular modeling approach is developed and validated that allows for high precision quantification of behavior of the neuromuscular system and by disentanglement of its underlying components (chapter 2, 3 and 4).
2. The method will be used to understand underlying mechanisms of functional recovery and the effect of therapy in stroke:
    a) The development of aforementioned components over time will be analyzed in the sub-acute phase post-stroke to address possible targeted preventive measures and to improve understanding of underlying mechanisms of functional recovery (chapter 5).
    b) The effect of botulinum toxin A treatment on the neural reflexive and non-neural tissue properties in patients post-stroke will be determined to make a first step in predicting which patients will benefit from this therapy (chapter 6).

The present thesis was founded on two research projects, i.e. ROBIN (STW) and Explicit Stroke (ZonMw). ROBIN (ROBot aided system identification: novel tools for diagnosis and assessment in Neurological rehabilitation) aimed to develop the required tools for applying SIPE techniques to clinical practice. The techniques developed in ROBIN were applied to clinical data obtained in Explicit-Stroke. The Explicit-Stroke project was a multi-center randomized controlled trial which studied the effect of early therapy on post-stroke recovery of the upper limb[37;38]. It further aimed to understand the underlying mechanisms of upper extremity functional recovery, encompassing brain plasticity by fMRI[39] and end-point wrist neuromechanics by haptic robotics[40;41].

References

(1) Prevalence and characteristics of children with cerebral palsy in Europe. *Dev Med Child Neurol* 2002;44:633-640.

(2) Odding E, Roebroeck ME, Stam HJ. The epidemiology of cerebral palsy: incidence, impairments and risk factors. *Disabil Rehabil* 2006;28:183-191.

(3) Murray CJ, Vos T, Lozano R et al. Disability-adjusted life years (DALYs) for 291 diseases and injuries in 21 regions, 1990-2010: a systematic analysis for the Global Burden of Disease Study 2010. *Lancet* 2012;380:2197-2223.

(4) Lozano R, Naghavi M, Foreman K et al. Global and regional mortality from 235 causes of death for 20 age groups in 1990 and 2010: a systematic analysis for the Global Burden of Disease Study 2010. *Lancet* 2012;380:2095-2128.

(5) World Health Organization. The top 10 causes of death. 24-5-2018. Online Source.

(6) Sanossian N, Ovbiagele B. Prevention and management of stroke in very elderly patients. *Lancet Neurol* 2009;8:1031-1041.

(7) Krishnamurthi RV, Feigin VL, Forouzanfar MH et al. Global and regional burden of first-ever ischaemic and haemorrhagic stroke during 1990-2010: findings from the Global Burden of Disease Study 2010. *Lancet Glob Health* 2013;1:e259-e281.

(8) Skolarus LE, Burke JF, Brown DL, Freedman VA. Understanding stroke survivorship: expanding the concept of poststroke disability. *Stroke* 2014;45:224-230.

(9) Crichton SL, Bray BD, McKevitt C, Rudd AG, Wolfe CD. Patient outcomes up to 15 years after stroke: survival, disability, quality of life, cognition and mental health. *J Neurol Neurosurg Psychiatry* 2016;87:1091-1098.

(10) van der Krogt HJ, Meskers CG, de Groot JH, Klomp A, Arendzen JH. The gap between clinical gaze and systematic assessment of movement disorders after stroke. *J Neuroeng Rehabil* 2012;9:61.

(11) World Health Organization. *International Classification of Functioning, Disability and Health: ICF*. 2011.

(12) Dressler D, Bhidayasiri R, Bohlega S et al. Defining spasticity: a new approach considering current movement disorders terminology and botulinum toxin therapy. *J Neurol* 2018;265:856-862.

(13) Sommerfeld DK, Gripenstedt U, Welmer AK. Spasticity after stroke: an overview of prevalence, test instruments, and treatments. *Am J Phys Med Rehabil* 2012;91:814-820.

(14) Lance JW. Spasticity: Disordered Motor Control. In: Feldman R, Young R, Koella W, eds. *Symposium Synopsis*. C: Year Book Medical Publishers; 1980;485-495.

(15) Dietz V, Sinkjaer T. Spastic movement disorder: impaired reflex function and altered muscle mechanics. *Lancet Neurol* 2007;6:725-733.

(16) Meskers CG, de Groot JH, de Vlugt E, Schouten AC. NeuroControl of movement: system identification approach for clinical benefit. *Front Integr Neurosci* 2015;9:48.

(17) van den Noort JC, Bar-On L, Aertbelien E et al. European consensus on the concepts and measurement of the pathophysiological neuromuscular responses to passive muscle stretch. *Eur J Neurol* 2017;24:981-e38.

(18) van der Helm FC, Schouten AC, de Vlugt E, Brouwn GG. Identification of intrinsic and reflexive components of human arm dynamics during postural control. *J Neurosci Methods* 2002;119:1-14.

(19) Burne JA, Carleton VL, O'Dwyer NJ. The spasticity paradox: movement disorder or disorder of resting limbs? *J Neurol Neurosurg Psychiatry* 2005;76:47-54.

(20) Ashworth B. Preliminary trial of carisoprodol in multiple sclerosis. *Practitioner* 1964;192:540-542.

(21) Tardieu C, Huet dlT, Bret MD, Tardieu G. Muscle hypoextensibility in children with cerebral palsy: I. Clinical and experimental observations. *Arch Phys Med Rehabil* 1982;63:97-102.

(22) Haugh AB, Pandyan AD, Johnson GR. A systematic review of the Tardieu Scale for the measurement of spasticity. *Disabil Rehabil* 2006;28:899-907.

(23) Lorentzen J, Grey MJ, Crone C, Mazevet D, Biering-Sorensen F, Nielsen JB. Distinguishing active from passive components of ankle plantar flexor stiffness in stroke, spinal cord injury and multiple sclerosis. *Clin Neurophysiol* 2010;121:1939-1951.

(24) Fleuren JF, Voerman GE, Erren-Wolters CV et al. Stop using the Ashworth Scale for the assessment of spasticity. *J Neurol Neurosurg Psychiatry* 2010;81:46-52.

(25) Kearney RE, Stein RB, Parameswaran L. Identification of intrinsic and reflex contributions to human ankle stiffness dynamics. *IEEE Trans Biomed Eng* 1997;44:493-504.

(26) van der Kooij H, van der Helm FC. Observations from unperturbed closed loop systems cannot indicate causality. *J Physiol* 2005;569:705.

(27) Schouten AC, de Vlugt E, Van Hilten JJ, van der Helm FC. Design of a torque-controlled manipulator to analyse the admittance of the wrist joint. *J Neurosci Methods* 2006;154:134-141.

(28) Schouten AC, Van de Beek WJ, Van Hilten JJ, van der Helm FC. Proprioceptive reflexes in patients with reflex sympathetic dystrophy. *Exp Brain Res* 2003;151:1-8.

(29) Meskers CG, Schouten AC, de Groot JH et al. Muscle weakness and lack of reflex gain adaptation predominate during post-stroke posture control of the wrist. *J Neuroeng Rehabil* 2009;6:29.

(30) Boonstra TA, Schouten AC, van Vugt JP, Bloem BR, van der Kooij H. Parkinson's disease patients compensate for balance control asymmetry. *J Neurophysiol* 2014;112:3227-3239.

(31) Engelhart D, Pasma JH, Schouten AC et al. Impaired standing balance in elderly: a new engineering method helps to unravel causes and effects. *J Am Med Dir Assoc* 2014;15:227.

(32) Pasma JH, Engelhart D, Maier AB et al. Reliability of System Identification Techniques to Assess Standing Balance in Healthy Elderly. *PLoS One* 2016;11:e0151012.

(33) Klomp A, de Groot JH, de Vlugt E, Meskers CG, Arendzen JH, van der Helm FC. Perturbation amplitude affects linearly estimated neuromechanical wrist joint properties. *IEEE Trans Biomed Eng* 2014;61:1005-1014.

(34) Klomp A, de Vlugt E, de Groot JH, Meskers CGM, Arendzen JH, van der Helm FCT. Perturbation velocity affects linearly estimated neuromechanical wrist joint properties. *J Biomech* 2018;74:207-212.

(35) Van Eesbeek S, de Groot JH, van der Helm FC, de Vlugt E. In vivo estimation of the short-range stiffness of cross-bridges from joint rotation. *J Biomech* 2010;43:2539-2547.

(36) de Vlugt E, de Groot JH, Schenkeveld KE, Arendzen JH, van der Helm FC, Meskers CG. The relation between neuromechanical parameters and Ashworth score in stroke patients. *J Neuroeng Rehabil* 2010;7:35.

(37) Kwakkel G, Meskers CG, van Wegen EE et al. Impact of early applied upper limb stimulation: the EXPLICIT-stroke programme design. *BMC Neurol* 2008;8:49.

(38) Kwakkel G, Winters C, van Wegen EE et al. Effects of Unilateral Upper Limb Training in Two Distinct Prognostic Groups Early After Stroke: The EXPLICIT-Stroke Randomized Clinical Trial. *Neurorehabil Neural Repair* 2016;30:804-816.

(39) Buma FE, Raemaekers M, Kwakkel G, Ramsey NF. Brain Function and Upper Limb Outcome in Stroke: A Cross-Sectional fMRI Study. *PLoS One* 2015;10:e0139746.

(40) Klomp A, van der Krogt JM, Meskers CGM et al. Design of a concise and comprehensive protocol for post stroke neuromechanical assessment. *J Bioengineer & Biomedical Sci* 2012.

(41) van der Krogt HJ, Klomp A, de Groot JH et al. Comprehensive neuromechanical assessment in stroke patients: reliability and responsiveness of a protocol to measure neural and non-neural wrist properties. *J Neuroeng Rehabil* 2015;12.

CHAPTER 2

Differentiation between non-neural and neural contributors to ankle joint stiffness in cerebral palsy

Authors:
Karin L de Gooijer-van de Groep, Erwin de Vlugt,
Jurriaan H de Groot, Hélène CM van der Heijden-Maessen,
Dennis HM Wielheesen, Rietje (M) S van Wijlen-Hempel,
J Hans Arendzen, Carel GM Meskers



J Neuroeng Rehabil 2013 Jul 23; 10:81

Abstract

Spastic paresis in cerebral palsy (CP) is characterized by increased joint stiffness that may be of neural origin, i.e. improper muscle activation caused by e.g. hyperreflexia or non-neural origin, i.e. altered tissue viscoelastic properties (clinically: “spasticity” vs. “contracture”). Differentiation between these components is hard to achieve by common manual tests. We applied an assessment instrument to obtain quantitative measures of neural and non-neural contributions to ankle joint stiffness in CP.

Twenty-three adolescents with CP and eleven healthy subjects were seated with their foot fixated to an electrically powered single axis footplate. Passive ramp-and-hold rotations were applied over full ankle range of motion (RoM) at low and high velocities. Subject specific tissue stiffness, viscosity and reflexive torque were estimated from ankle angle, torque and triceps surae EMG activity using a neuromuscular model.

In CP, triceps surae reflexive torque was on average 5.7 times larger (p=.002) and tissue stiffness 2.1 times larger (p=.018) compared to controls. High tissue stiffness was associated with reduced RoM (p<.001). Ratio between neural and non-neural contributors varied substantially within adolescents with CP. Significant associations of SPAT (spasticity test) score with both tissue stiffness and reflexive torque show agreement with clinical phenotype.

Using an instrumented and model-based approach, increased joint stiffness in CP could be mainly attributed to higher reflexive torque compared to control subjects. Ratios between contributors varied substantially within adolescents with CP. Quantitative differentiation of neural and non-neural stiffness contributors in CP allows for assessment of individual patient characteristics and tailoring of therapy.

Background

Cerebral palsy (CP) comprises a variety of non-progressive upper motor neuron (UMN) lesions occurring in the developing fetal or infant brain. The resulting movement and posture disorders are generally characterized by loss of muscle strength, i.e. paresis, improper muscle activation by e.g. increased reflexes and loss of coordination by e.g. flexion synergies. In addition, changes of tissue viscoelastic properties may modulate the characteristics of the primary motor disorders[1;2]. Spastic CP is the most common type of CP[3], which is characterized by increased joint stiffness (resistance to movement). Increased joint stiffness in the relaxed condition can be of either neural (hyperreflexia, "spasticity") or non-neural origin (altered tissue viscoelastic properties "contracture")[4]. Treatment of spastic CP is generally aimed at diminishment of joint stiffness in order to improve passive and active joint range of motion. In case of suspected neural origin, therapy is aimed at reducing muscle activation and blocking the stretch reflex loop by botulinum toxin[5], intra thecal baclofen[6] or selective dorsal rhizotomy[7]. In case of suspected non-neural origin, i.e. changes in viscoelastic properties of muscle and connective tissues, corrective casting, splinting and surgical lengthening can be applied[8]. Current manual tests, like the Ashworth[9] and Tardieu[10], are based on the paradigm of increased reflex activity as a result of neural damage, leading to a velocity dependent joint resistance or spasticity[11]. This paradigm is however an oversimplification[4]. Inherently, by manual testing, it is not possible to quantitatively discriminate between underlying neural and non-neural contributors to joint stiffness as each of these contributors may generate a velocity dependent joint resistance. This makes the selection of treatment aiming at the dominant contributor difficult.

De Vlugt et al.[12] developed an instrumented method to quantify neural and non-neural contributors to joint stiffness for the ankle joint in patients with chronic stroke. The ankle was rotated in a precise and controlled way using a robotic manipulator. Using neuromuscular modeling, the key neural and non-neural contributors to ankle joint stiffness were quantified from recorded ankle torque and EMG of leg (below the knee) muscles. Compared to healthy subjects, patients with stroke showed increased tissue stiffness and to a lesser extent increased reflex activity.

The objective of the present study was to quantify neural and non-neural contributors to ankle joint stiffness in patients with spastic CP and to assess its validity and reliability. A quantitative discrimination between the neural and non-neural components of joint stiffness in CP gives

insight in pathophysiological mechanisms and may provide a strong instrument for development of tailored intervention strategies and their follow-up.

Methods

Participants

Twenty-three adolescents with CP (mean age (SD) and range: 14.9 (2.4) y, 12-19 y, fifteen male) were recruited from the outpatient clinics of the Rijnlands Rehabilitation Centre and the Department of Rehabilitation Medicine of the Leiden University Medical Centre, Leiden, the Netherlands. Table 2.1 provides the patient characteristics. Inclusion criteria comprised diagnosis of spastic CP and a gross motor function[13] (GMFCS) of I, II or III. Patients with a GMFCS of IV were excluded because of possible interference of the outcome with muscle disuse or atrophy. Other exclusion criteria were concomitant neurological diseases, orthopedic problems of the lower extremities, casting, botulinum toxin A injections within the previous 4 months, previous orthopedic surgery or tendon and tissue surgery of the leg, orthopedic surgery of other body parts within the last 12 months, previous selective dorsal rhizotomy or intra thecal baclofen treatment and inability to participate in the tests. Eleven healthy subjects (mean age (SD) and range: 15.1 (2.1) y, 12-18 y, six males), matched for age and sex, were recruited as a control group. Required sample size estimation was based on previous data[12]. The medical ethics committee of the Leiden University Medical Centre approved the study. Written informed consent was obtained from participants.

Instrumentation

Subjects were seated with their foot fixated onto an electrically powered single axis footplate (Nissan Motor Company, Japan). Subjects were seated with their hip and knee positioned at approximately 80° and 70° of flexion respectively (Figure 2.1). The thigh was held in place through the seat support of the chair; movement of the shank in cranial- caudal direction was ensured by careful aligning axis of rotation of the motor with the ankle axis. Movement of the shank in medio-lateral was limited by fixation of the thigh. The ankle was positioned at zero degrees onto the footplate of the manipulator, perpendicular to the leg (neutral position). A

positive rotation of the manipulator was defined to equal dorsiflexion of the foot and a negative rotation, plantar flexion of the foot. Range of motion of the manipulator was mechanically constrained to plus and minus 30 degrees with respect to the neutral position.

Table 2.1: *Characteristics of study population.*

Characteristics of study population	**Cerebral palsy (N = 23)**	**Healthy subjects (N=11)**
Age, years (SD)	14.9 (2.4)	15.1 (2.1)
Male gender, n (%)	15 (65)	6 (55)
Unilateral, n (%)	8 (35)	Na
GMFCS* I, II, III, n (%)	20 (87), 2 (9), 1 (4)	Na
Ashworth, median (range)	1 (0-2)***	Na
SPAT, median (range)**	2 (0-3)***	Na

* GMFCS = Gross Motor Function Classification System **SPAT = Spasticity test

***From one patient data is missing

The axis of rotation of the ankle and footplate were aligned by visually minimizing knee translation in the sagittal plane during manual rotation of the footplate. The motor was driven to rotate the ankle by either a torque for the assessment of ankle range of motion (RoM), or by a position to impose ramp-and-hold (RaH) rotational stretches of the triceps surae for the identification of joint stiffness. During movement, flat foot placement was ensured by visual inspection. Muscle activation of the tibialis anterior (TA) and triceps surae muscles (TS: soleus, lateral and medial gastrocnemius) was recorded by surface electrodes (electromyography, EMG), using a Delsys Bagnoli 4 system (Delsys, Boston MA, USA). Inter electrode distance was 10 mm. EMG signals were sampled at 2500 Hz, online band pass filtered (20-450 Hz) and offline rectified and low pass filtered (3th-order Butterworth) at 20 Hz. Reaction torque and ankle rotational angle were recorded at 250 Hz sample rate and low pass filtered at 20 Hz (3th-order Butterworth).

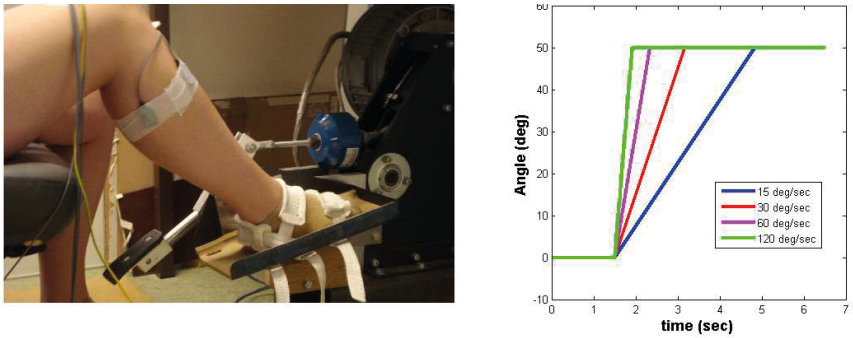


Figure 2.1: *Measurement set-up (left) and applied ankle joint rotations (right). Ankle joint rotations were applied at 4 different velocities over the individual range of motion.*

Protocol

Measurements were performed on the most affected ankle of each patient and at the right ankle in case of controls. Maximum plantar and dorsal flexion angles were assessed by a gradually increasing flexion torque from 0 to a maximum value of 15 Nm. RoM was defined as the difference between the maximum plantar and dorsal flexion angle and used as boundary for the subsequent RaH rotations. During the RaH rotations, the ankle was rotated at 4 different angular velocities (15, 30, 60, 120 deg/sec) over the individually assessed RoM, starting in maximal plantar flexion. RaH rotations were started at random time instants. The hold phase lasted 4 seconds after which the ankle was moved back again to the neutral position. Time to cover a complete RaH rotation did not exceed 15 sec. Rest periods of about 30 sec were introduced between each RaH rotation to avoid hysteresis effects[14]. All RaH rotations were performed twice. Thus, the complete experimental procedure consisted of 1 RoM and 2 times 4 RaH rotations. Subjects were asked to remain relaxed during the entire experiment and not actively resist any motion. EMG prior to RaH rotation was offline checked to be between minus and plus 3 times standard deviation from the lowest EMG value over the whole signal as determined by a moving average procedure (window width 1 sec.). RaH rotations not fulfilling this requirement were discarded from further analysis.

Model description and validation

To distinguish between the neural and non-neural contributions to ankle joint stiffness, a nonlinear neuromuscular model of the ankle joint was used by which the ankle torque was predicted and matched to the measured ankle torque using EMG and ankle angle as input. The model included a Hill-type muscle model to describe the torque contribution from muscle activation induced by stretch reflexes. Hill-type models account for the effect of muscle length and lengthening velocity on muscle force. Passive torque from viscoelasticity (parallel elastic element) was modeled by exponential force-length and force-velocity functions. Tendon stiffness (series elastic element) was assumed to be infinitely stiff[12]. The full description of the model can be found in de Vlugt et al.[12]. The model was fitted to the measured ankle torque defined within a time frame starting 0.5 sec before the start of the ramp till 0.5 sec after the end of the ramp, which was in the hold phase. Model parameters where estimated for each single RaH rotation by minimizing the quadratic difference (error function) between the measured and predicted ankle torque. The validity of the model was determined for each RaH rotation by the variance accounted for (VAF):

$$VAF = \left(1 - \frac{\sum_{i=1}^{n} (T_{measured,i} - T_{model,i})^2}{\sum_{i=1}^{n} T_{measured,i}^{\ 2}} \right) * 100\% \qquad (2.1)$$

With i the sample time and n the number of data points used for the parameter estimation. $T_{measured,i}$ is the measured ankle reaction torque and $T_{model,i}$ the predicted ankle torque. Those rotations exhibiting a VAF score lower than the mean VAF over all rotations minus 2 times standard deviation were excluded from analysis.

Primary outcome parameters were RoM, tissue stiffness and viscosity and torque from triceps surae (TS) and tibialis anterior (TA) stretch reflexes. As passive tissue stiffness and viscosity strongly depend on joint angle, values at the maximal common dorsal flexion angle of all subjects were calculated for inter-subject analysis. This particular angle was chosen as

exhibiting probably the largest contrast between subjects[12]. Model simulations and data analyses were performed in MATLAB (The Mathworks Inc., Natick MA). An extensive validity and reliability analysis of the used method and the estimated model parameters was performed previously[12].

Statistical analysis

Difference in RoM between patients with CP and healthy controls was tested using an unpaired t-test. A linear mixed model was used to determine the difference in primary outcome variables between healthy controls and patients with CP (random factor) and to assess the effect of velocity (fixed, repeated factor). Stepwise linear regression procedures and one-way ANOVA with Bonferroni correction were applied to assess associations of primary outcome variables with RoM and secondary outcome variables i.e. speed of ankle rotation, age, gender, GMFCS[13], Ashworth[9] and spasticity test (SPAT)[15] scores. Inter-trial variability was assessed using intraclass correlation coefficients (ICC, 2-way mixed model). Statistical analysis was performed using SPSS 17.0 (SPSS Inc.) and GraphPad Prism 5 (Graphpad Software) with a significant level of .05.

Results

One subject (healthy) could not complete the RaH measurement due to insufficient relaxation and in this particular case only the RoM was used. In 2 other healthy subjects 1 RaH rotation had to be excluded due to technical problems. In total, 16 of the 256 RaH rotations from 9 subjects (8 CP), were excluded due to poor model fits (10, 4% of 256 RaH rotations) or insufficient relaxation (6, 2 % of 256 RaH rotations). The VAF of the remaining RaH rotations was above 98.9%, meaning that the model could well describe ankle torque dynamics.

Range of motion

RoM in dorsiflexion was significantly smaller in CP (t=2.10, p=.044), see Figure 2.2 (top left). Of all subjects, 4 patients with CP (12%) and 7 healthy controls (64%) had a RoM of at least 60 deg. The smallest maximal dorsal flexion angle among all subjects was 2 deg.

Non-neural contributors to joint stiffness: tissue stiffness and viscosity

Tissue stiffness was independent of velocity (F=0.35, df=3, p=.79) and was significantly larger in CP compared to healthy controls (F=6.28, df=1, p=.018), see Figure 2.2 (bottom left). There was a large variation in tissue stiffness within the CP group. Viscosity decreased with angular velocity (F=9.86, df=3, p<.001). We found no significant difference between the groups regarding ankle viscosity (F=1.35, df=1, p=.254).

Neural contributor to joint stiffness: reflexive torque

TS reflexive torque (Figure 2.2, top right) was higher in CP than in healthy controls (F=11.6, df=1, p=.002) and the difference increased with velocity (F=4.61, df=3, p=.009). TS reflexive torque showed a large variation within the group with CP. TA reflexive torque was not significantly different between CP and healthy controls (F=2.864, df=1, p=.104) and did not change with velocity (F=0.602, df=3, p=.620).

Relation tissue stiffness and range of motion

Tissue stiffness at the lowest ankle rotation speed appeared to be the best predictor of ankle RoM (β=-0.45 se 0.06, p<.001, Figure 2.3) with a total explained variance of 84%.

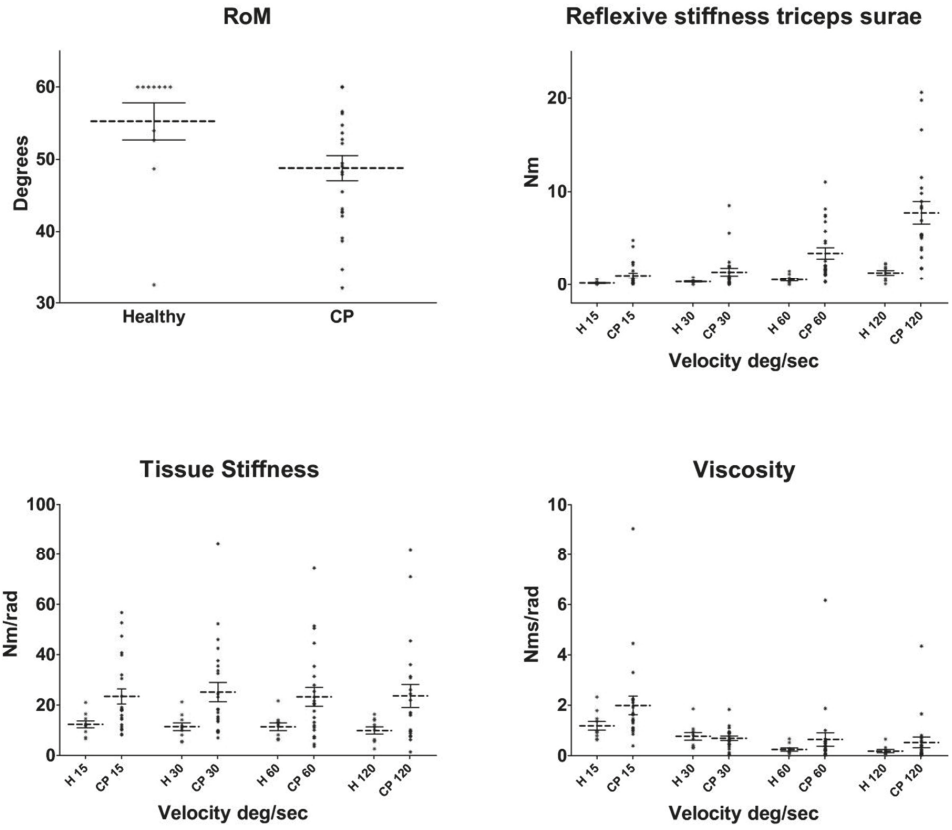


Figure 2.2: *Primary outcome parameters. Range of motion (top left), triceps surae reflexive stiffness (top right), tissue stiffness (bottom left) and viscosity (bottom right) for patients with cerebral palsy (CP) and healthy controls (H). The dotted line gives the mean value with the corresponding standard error. Each dot represents an individual result of a subject. Tissue stiffness and viscosity were determined at the same ankle angle for all subjects, which was 2 deg ankle dorsal flexion.*

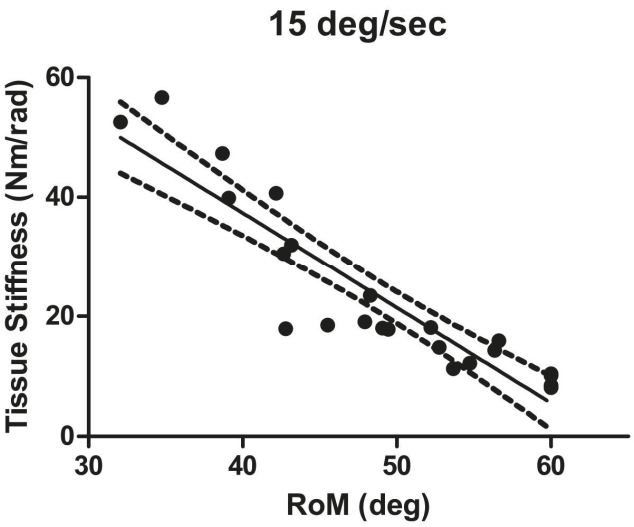


Figure 2.3: *Relation between tissue stiffness and range of motion for adolescents with cerebral palsy (CP). Tissue stiffness (15 deg/sec) was determined at 2 deg ankle dorsal flexion. Each dot represents the result of an individual subject. A linear regression line with its 95% confidence interval is fitted through the data. The total explained variance was 84%.*

Relation tissue stiffness and reflexive torque

For patients with CP, tissue stiffness at the lowest ankle rotation speed (15 deg/sec) was on average 4.2 times higher than reflexive torque at the highest ankle rotation speed (120 deg/sec) with a standard deviation of 3.3 indicating a substantially variation between subjects. Total explained variation of reflexive torque (120 deg/sec) by tissue stiffness (15 deg/sec) was 38%. Association between tissue stiffness and reflexive torque was low (ICC: less than .5).

Relation with clinical phenotype

Using stepwise linear regression SPAT score was the only variable that was significantly associated with tissue stiffness (β=15.8 *se* 4, p=.001). For reflexive torque, both SPAT score and age were significant positive contributors (β=3.8 *se* 1.46, p=.02 and β=0.88 *se* 0.41, p=.049). Tissue stiffness (15 deg/sec, p=.002), TS reflexive torque (120 deg/sec, p=.032) and RoM (p=.001) differed significantly with respect to SPAT but not Ashworth score (Figure 2.4).

Reliability

Tissue stiffness showed a good conformity between the two repetitive RaH rotations especially at the lowest ankle rotation speed: ICC .93 at 15 deg/sec. For reflexive torque, inter-trial reliability was especially good at the highest ankle rotation speed: ICC .80 at 120 deg/sec. Reliability was similar for CP and healthy subjects.

Discussion

Ankle joint stiffness in CP was successfully separated into its neural and non-neural components using an instrumented and model-based approach. Compared to healthy subjects, patients with CP showed a smaller RoM, higher TS reflexive torque and higher tissue stiffness. Ratios between contributors varied substantially within the group with CP.

Higher tissue stiffness and smaller range of motion in cerebral palsy

Previously, in larger groups of children with CP, RoM was associated with level of spasticity as expressed by Ashworth score and GMFSC I-II[16-19]. Decreased RoM in CP is explained by increased passive tissue stiffness[17], likely originating from changes in the mechanical property of fiber bundles and/or fewer sarcomeres (in series) which might result in increased sarcomere length[20-22] or actively, i.e. hypertonia[23]. In vivo measurements in CP show that muscles appeared to undergo much higher stresses with increased muscle length[21] and torque-angle relationships are much steeper in CP[24], which is supported in our study by the correlation between tissue stiffness and RoM (Figure 2.3). RoM measurements at low speed may therefore represent passive tissue stiffness, i.e. “static” contracture[23]. Note that despite the instruction to the subjects to relax, tissue stiffness may be modulated by a constant level of (increased muscle activation)[25]. Separation of these components requires further effort.

Clinical implication: variation in tissue stiffness and reflexive torque

Even in this relatively mild affected group of adolescents with CP, a large inter-subject variation was found for the ratio between TS reflexive torque and tissue stiffness. Association between the two was low. This variation is the rationale for pursuing the development of personalized therapy. A variation in CP may be induced by ageing and the corresponding growth spurt in puberty since we measured adolescents in a wide age range (12-19 years). It was suggested previously that the role of passive stiffness may increase over reflex activity with age in children with spastic diplegic CP[26] and that the range of dorsiflexion of the ankle joint in CP decreases on average 19 deg during the first 18 years of life[18]. We found an association of reflex activity but not tissue stiffness with age in the present study. The present study was however not designed to study age effects.

Correlation of SPAT score with both tissue stiffness and reflexive torque underlines the fact that it is difficult to split the neural and non-neural component with the manual tests such as SPAT. In future work we will measure more patients and with a wider range of GMFCS and SPAT scores to study this correlation more extensively.

The present and former[12] studies show that the instrumented approach can be used in different patient groups to quantitatively determine neural and non-neural contributors of ankle joint stiffness.

Non-neural and neural components in cerebral palsy compared to stroke

TS reflexive torque was more dominant in CP than in stroke[12]. For the patients with an Ashworth score of 1, the ratio between TS reflexive torque at the highest ankle rotation speed and tissue stiffness at the lowest ankle rotation speed was for CP three times higher than for stroke (CP ≈ 0.3 and stroke ≈ 0.1). In contrast to stroke, viscosity was not significantly increased in CP. RoM was smaller in stroke compared to CP, reflecting also the higher tissue stiffness component in the stroke group. CP differs from stroke by onset of the disease with respect to age. The main question is whether the differences between stroke and CP may be explained by purely an age effect or whether there might be etiological differences.

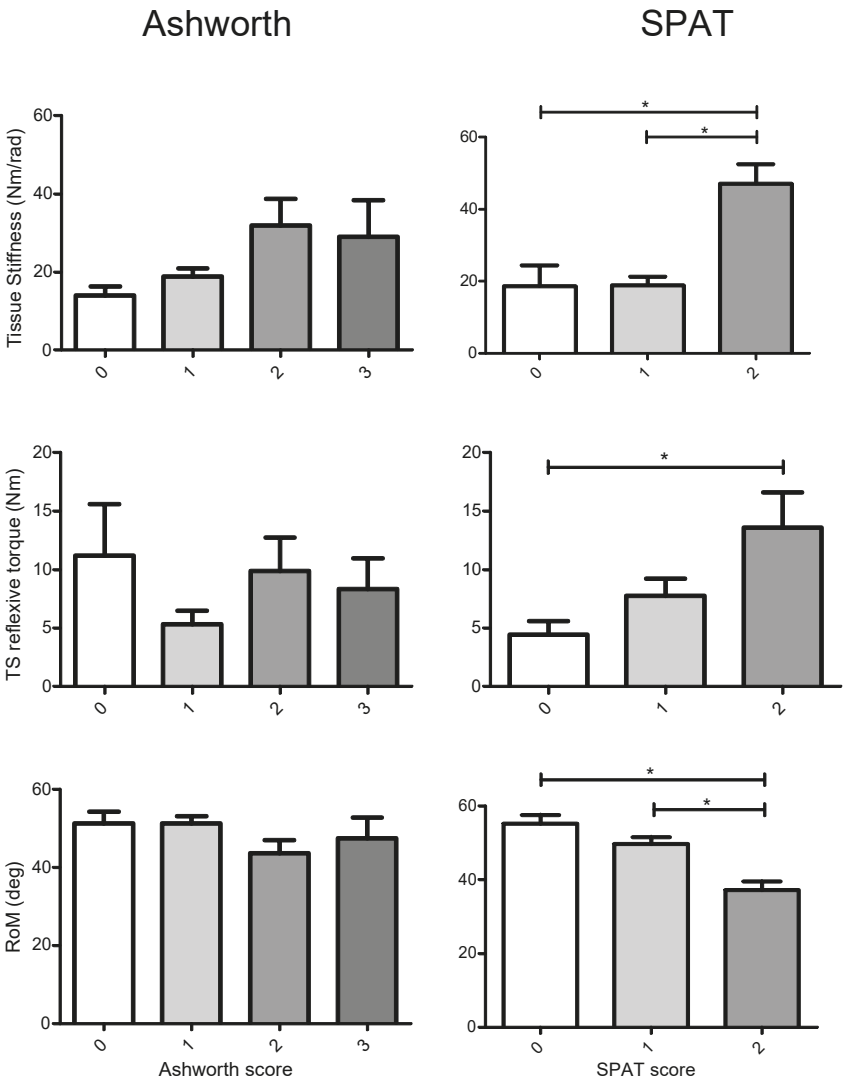


Figure 2.4: *Relation of outcome parameters with Ashworth and spasticity test (SPAT). Mean with standard error for tissue stiffness (15 deg/sec), triceps surae (TS) reflexive torque (120 deg/sec) and range of motion (RoM) for groups of patients with different Ashworth and SPAT scores. *significantly different ($p<.05$) by one-way ANOVA with a Bonferroni post-hoc test.*

Reliability and validity

Tissue stiffness and reflexive torque could both be reliably estimated: tissue stiffness especially at the low ankle rotation speed and reflexive torque at the high speeds. This illustrates the feasibility of the method to distinguish contributors to joint stiffness on an individual basis. As expected, reflexive torque and not tissue stiffness was significantly influenced by ankle rotation speed and especially tissue stiffness was associated with RoM at low speed. Significant associations of SPAT score with both tissue stiffness and reflexive torque show agreement with clinical phenotype.

Limitations

We selected patients with CP with a relatively high GMFSC score (median of 1) to create a homogenous population. This limits validity of the present study and prevents more extensive elaboration of the relation with clinical phenotype which will be important for goal directed therapy. There were only 3 patients with a GMFCS score higher than 1, so correlations of GMFCS with neuromuscular parameters could not be studied well. The present study did not differentiate contributions of gastrocnemius and soleus and was performed at 1 knee angle. Joint stiffness should also be assessed in relation to functional movements, like walking using static and dynamic measurements[27]. In this study we were able to split neural and non-neural contributors to increased joint stiffness. However, the neural component in this study comprised only the reflex activity and not cross bridge dynamics and background muscle activity during passive (and active) conditions. Achilles tendon stiffness was assumed to be of a magnitude greater than the total (active and passive) muscle stiffness for the current conditions applied in this study[28] and was taken in our model as infinitely stiff, considering the low torque and passive conditions[12] applied in the present study.

Future work will comprise the assessment of Achilles tendon stiffness by ultrasound measurements, the assessment of joint stiffness as a function of ankle rotation angle in a more detailed way, measurements at different knee angles and under functional (loaded) conditions.

Conclusion

Using a novel instrumented assessment technique, patients with CP showed a smaller RoM and higher tissue stiffness and reflexive torque compared to control subjects. Good reliability and validity of the assessment technique combined with considerable intra-individual variance are a base for individual tailored therapy.

Acknowledgements

This research is supported by the Dutch Technology Foundation STW, which is part of the Netherlands Organisation for Scientific Research (NWO) and partly funded by the Ministry of Economic Affairs, Agriculture and Innovation.

References

(1) Goldstein M. The treatment of cerebral palsy: What we know, what we don't know. *J Pediatr* 2004;145:S42-S46.

(2) Rosenbaum P, Paneth N, Leviton A et al. A report: the definition and classification of cerebral palsy April 2006. *Dev Med Child Neurol Suppl* 2007;109:8-14.

(3) Prevalence and characteristics of children with cerebral palsy in Europe. *Dev Med Child Neurol* 2002;44:633-640.

(4) Dietz V, Sinkjaer T. Spastic movement disorder: impaired reflex function and altered muscle mechanics. *Lancet Neurol* 2007;6:725-733.

(5) Sheean G. Botulinum toxin should be first-line treatment for poststroke spasticity. *J Neurol Neurosurg Psychiatry* 2009;80:359.

(6) Albright AL, Barron WB, Fasick MP, Polinko P, Janosky J. Continuous intrathecal baclofen infusion for spasticity of cerebral origin. *JAMA* 1993;270:2475-2477.

(7) Mittal S, Farmer JP, Al-Atassi B et al. Long-term functional outcome after selective posterior rhizotomy. *J Neurosurg* 2002;97:315-325.

(8) Thompson AJ, Jarrett L, Lockley L, Marsden J, Stevenson VL. Clinical management of spasticity. *J Neurol Neurosurg Psychiatry* 2005;76:459-463.

(9) Ashworth B. Preliminary trial of carisoprodol in multiple sclerosis. *Practitioner* 1964;192:540-542.

(10) Gracies JM, Marosszeky JE, Renton R, Sandanam J, Gandevia SC, Burke D. Short-term effects of dynamic lycra splints on upper limb in hemiplegic patients. *Arch Phys Med Rehabil* 2000;81:1547-1555.

(11) Lance JW. Spasticity: Disordered Motor Control. In: Feldman R, Young R, Koella W, eds. *Symposium Synopsis*. C: Year Book Medical Publishers; 1980;485-495.

(12) de Vlugt E, de Groot JH, Schenkeveld KE, Arendzen JH, van der Helm FC, Meskers CG. The relation between neuromechanical parameters and Ashworth score in stroke patients. *J Neuroeng Rehabil* 2010;7:35.

(13) Palisano R, Rosenbaum P, Walter S, Russell D, Wood E, Galuppi B. Development and reliability of a system to classify gross motor function in children with cerebral palsy. *Dev Med Child Neurol* 1997;39:214-223.

(14) Gajdosik RL, Lentz DJ, McFarley DC, Meyer KM, Riggin TJ. Dynamic elastic and static viscoelastic stress-relaxation properties of the calf muscle-tendon unit of men and women. *Isokinetics and Exercise Science* 2006;14:33-44.

(15) van den Noort JC, Scholtes VA, Harlaar J. Evaluation of clinical spasticity assessment in cerebral palsy using inertial sensors. *Gait Posture* 2009;30:138-143.

(16) Shortland AP, Harris CA, Gough M, Robinson RO. Architecture of the medial gastrocnemius in children with spastic diplegia. *Dev Med Child Neurol* 2002;44:158-163.

(17) Alhusaini AA, Crosbie J, Shepherd RB, Dean CM, Scheinberg A. Mechanical properties of the plantarflexor musculotendinous unit during passive dorsiflexion in children with cerebral palsy compared with typically developing children. *Dev Med Child Neurol* 2010;52:e101-e106.

(18) Hagglund G, Wagner P. Spasticity of the gastrosoleus muscle is related to the development of reduced passive dorsiflexion of the ankle in children with cerebral palsy. *Acta Orthop* 2011;82:744-748.

(19) McDowell BC, Salazar-Torres JJ, Kerr C, Cosgrove AP. Passive range of motion in a population-based sample of children with spastic cerebral palsy who walk. *Phys Occup Ther Pediatr* 2012;32:139-150.

(20) Tabary JC, Tabary C, Tardieu C, Tardieu G, Goldspink G. Physiological and structural changes in the cat's soleus muscle due to immobilization at different lengths by plaster casts. *J Physiol* 1972;224:231-244.

(21) Smith LR, Lee KS, Ward SR, Chambers HG, Lieber RL. Hamstring contractures in children with spastic cerebral palsy result from a stiffer extracellular matrix and increased in vivo sarcomere length. *J Physiol* 2011;589:2625-2639.

(22) de Vlugt E, de Groot JH, Wisman WH, Meskers CG. Clonus is explained from increased reflex gain and enlarged tissue viscoelasticity. *J Biomech* 2011.

(23) Hof AL. Changes in muscles and tendons due to neural motor disorders: implications for therapeutic intervention. *Neural Plast* 2001;8:71-81.

(24) Tardieu C, Huet dlT, Bret MD, Tardieu G. Muscle hypoextensibility in children with cerebral palsy: I. Clinical and experimental observations. *Arch Phys Med Rehabil* 1982;63:97-102.

(25) Burne JA, Carleton VL, O'Dwyer NJ. The spasticity paradox: movement disorder or disorder of resting limbs? *J Neurol Neurosurg Psychiatry* 2005;76:47-54.

(26) Pierce SR, Prosser LA, Lauer RT. Relationship between age and spasticity in children with diplegic cerebral palsy. *Arch Phys Med Rehabil* 2010;91:448-451.

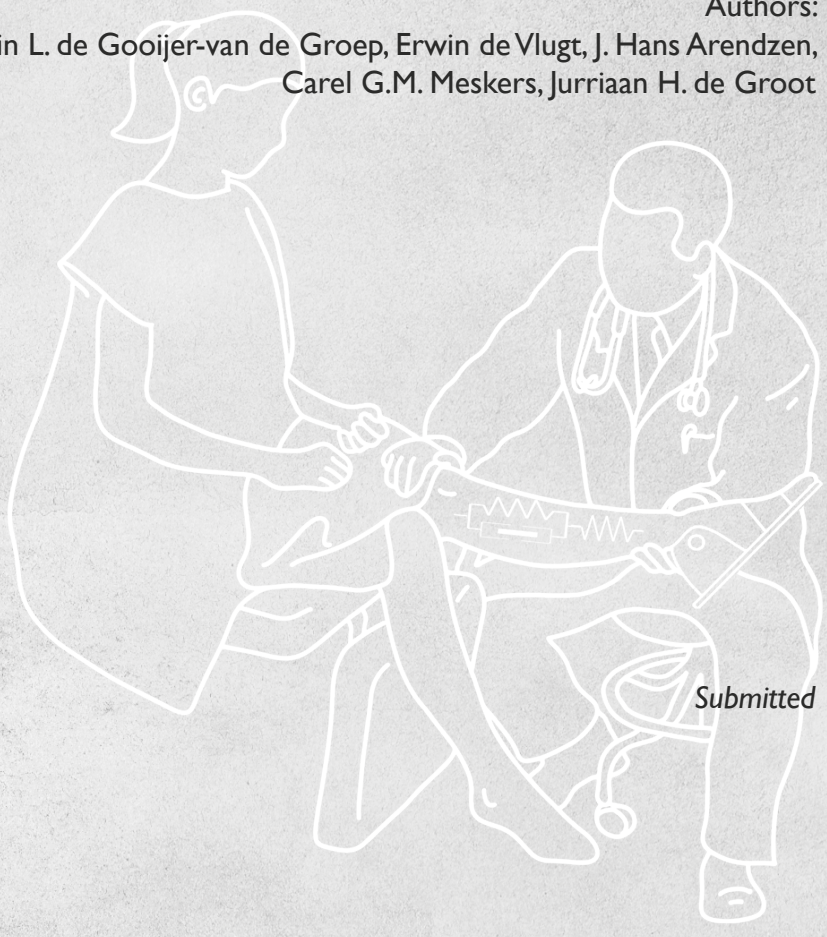
(27) Desloovere K, Molenaers G, Feys H, Huenaerts C, Callewaert B, Van de Walle P. Do dynamic and static clinical measurements correlate with gait analysis parameters in children with cerebral palsy? *Gait Posture* 2006;24:302-313.

(28) Kubo K, Kanehisa H, Fukunaga T. Is passive stiffness in human muscles related to the elasticity of tendon structures? *Eur J Appl Physiol* 2001;85:226-232.

CHAPTER 3

Non-invasive assessment of ankle muscle force-length characteristics post-stroke

Authors:
Karin L. de Gooijer-van de Groep, Erwin de Vlugt, J. Hans Arendzen, Carel G.M. Meskers, Jurriaan H. de Groot



Submitted

Abstract

Non-invasive estimation of the neural reflexive and non-neural tissue contributors viz. passive and active muscle force length characteristics, to increased joint stiffness after central neural motor lesions like stroke will contribute to fundamental understanding, clinical diagnosis, development and evaluation of therapy. Hereto we proposed an electromyography (EMG)-driven model approach.

Ramp-and-hold ankle rotations were applied and torques were measured by a robotic manipulator in 13 patients post-stroke (> 6 months, 59.9, SD 7.1 years) and 15 age matched healthy volunteers (64.0, SD 1.2 years). Stiffness coefficient and slack length of the passive and optimal length of the active force-length characteristics of triceps surae and tibialis anterior muscles were estimated together with the neural reflexive torque by minimizing the least squares difference between measured and simulated torque. Internal model validity, test-retest reliability, sensitivity and external validity were addressed.

Internal model validity was good and test-retest reliability fair to good. Model parameters were sensitive for knee angles and disease. The neural reflexive torque, the stiffness coefficient and the slack length of the triceps surae were increased in patients post-stroke.

Valid, reliable and sensitive estimations of passive and active force-length characteristics next to neural reflexive torque could be estimated non-invasively from applied position and recorded torque signals using an EMG-driven ankle model. Increased ankle joint stiffness was explained by both an increased triceps surae stiffness and an increased reflexive torque.

Introduction

Upper motor neuron diseases, like stroke and cerebral palsy, may result in an increased resistance of the ankle to dorsiflexion under passive conditions, generally in combination with muscle weakness and an equinovarus malposition of the foot[1-4]. This combination of symptoms affects the functional ability of the patient in e.g. locomotion, and originates from altered neural input to the ankle muscles (hyperreflexia, "spasticity") and non-neural tissue changes (stiffer and shorter muscles)[5]. Clinical treatment focuses on reducing the neural input e.g. by botulinum toxin infiltration[6-8] and/or addressing the tissue contribution to increased joint stiffness by corrective casting, splinting or surgical lengthening[9-11]. Non-invasive quantification of underlying contributors to increased joint stiffness post-stroke is important for proper and tailored patient referral to therapeutic strategies and high resolution follow-up[12;13] yet cannot reliably be achieved by current clinical tests[14].

Model driven approaches have been developed to quantitatively estimate the neural reflexive torques and non-neural peripheral tissue stiffness and viscosity contributing to ankle and wrist joint stiffness[4;15;15-21]. The clinical validity of these methods was demonstrated in patients with stroke[4;15;17;21], cerebral palsy[16;20;22], multiple sclerosis and spinal cord injury[17]. The passive and active force-length relationships represent the properties of the connective and contractile tissues. It is of importance to address these properties in patients longitudinally[13;23] as the temporal changes of these properties[24-26] needs further evaluation[27].

This study aims to estimate the passive and active tissue properties, i.e. the stiffness coefficient and slack length of the passive force-length relationship and the optimal length of the active force-length relationship, of the triceps surae and tibialis anterior muscles non-invasively in patients and healthy volunteers using an electromyography (EMG)-driven neuromuscular modeling approach, expanding on previous work[4;15;20;22]. To address the clinical potential of the method, we determined internal model validity ($VAF \geq 99\%$; $SEM \leq 0.1$), test-retest reliability ($ICC \geq 0.4$), and sensitivity next to external validity (*MDC*). The sensitivity of the model is assessed by comparing outcome measures between flexed and extended knee. Knee angle affects the relative contribution of the soleus (mono-articular ankle muscle) and the lateral and medial gastrocnemii (bi-articular ankle-knee muscles). With the knee in flexion, the contribution of the soleus is dominant. With the knee extended, a combined contribution of the

triceps muscles is expected to be observed in the passive and active force-length parameters (slack length, optimal length). Knee angle is expected to have no influence on the passive and active force-length parameters of the tibialis anterior. External validity is assessed by comparing healthy subjects to patients post-stroke and using the minimal detectable change (*MDC*) of healthy subjects. It is expected that patients differ from healthy subjects by an increased peripheral tissue stiffness due to stiffer and shortened muscles of the triceps surae and an increased reflexive torque of the triceps surae. Individual observations are compared to the clinical Ashworth score and it is expected that especially patients with a high Ashworth score (>2) have deviated outcome measures as defined by the *MDC*. To show the potential for longitudinal observations, e.g. to evaluate treatment, the *MDC* of stroke patients is assessed.

Methods

Study setting and participants

Thirteen chronic stroke patients (115 months post-stroke, mean age 59.9 SD 7.1 years, 6 male, Table 3.1) and 15 healthy volunteers (mean age 64.0 SD 1.2 years, 8 male) were included in the study. Patients with clinically determined increased ankle stiffness were selected from the outpatient clinic of the department of rehabilitation medicine of the Leiden University Medical Center (LUMC). Exclusion criteria were concomitant neurological and/or orthopedic disorders, any new medical intervention within the last four months having possible interference with ankle joint stiffness; surgery of leg/foot within the last 12 months and total paralysis of the ankle. The medical ethics committee of the LUMC approved the study (P12.125, NL4083.058.12). Written informed consent was obtained from all participants.

Measurement protocol

Participants were measured during two consecutive visits within a time interval of 1-2 weeks. Each participant underwent two measurement sessions during the first visit, and one session during the second visit. At each session, measurements were performed at two knee flexion angles (20°, 70°) in order to discriminate the relative contribution of the gastrocnemius

components of the triceps surae. During each visit, the Ashworth score[28] was determined by an independent physician.

Table 3.1: *Characteristics of included patients.*

ID	Age	Sex	Lesion	Months post-stroke	Passive dorsal RoM	Ashworth
1	56	F	Hemorrhage L	72	19.5	3
2	65	F	Hemorrhage L	368	18.4	2
3	60	F	Ischemia L	177	9.7	1
4	65	M	Hemorrhage R	204	23.8	0
5	57	M	Ischemia R	108	7.3	4
6	51	F	Ischemia R	80	1.2	1
7	46	F	Ischemia R	11	13.2	3
8	70	M	Hemorrhage R	14	3.3	4
9	57	M	Ischemia L	6	19.5	1
10	57	M	Ischemia R	153	6.8	0
11	67	M	Ischemia R	76	13.7	2
12	69	F	Ischemia R	42	27.2	2
13	59	F	Ischemia R	185	23.5	3

F: female, M: male, L: left hemisphere, R: right hemisphere

Instrumentation

Participants were seated on a car seat with their foot fixated onto an electrically powered single axis rotating footplate (Achilles, MOOG FCS Inc., Nieuw-Vennep, The Netherlands, Figure 3.1). The footplate was aligned visually at 25° plantar flexion with respect to the line connecting the head of the fibula and the lateral malleolus.

Muscle activation of the tibialis anterior (*tib*) and triceps surae muscles (*tri*: soleus, SOL; lateral gastrocnemius, GL; medial gastrocnemius, GM) was recorded using surface electromyography (EMG, Porti, TMSi B.V. Oldenzaal, The Netherlands) according to the SENIAM guidelines[29] (Appendix 3A). Dorsal- and plantar flexion (positive and negative rotation respectively) was limited by individually pre-set manipulator hardware and software stops. During ramp-and-hold (RaH) movements, EMG, torque and angle were simultaneously recorded. EMG signals

were sampled at 1000 Hz, offline high pass filtered (20Hz, 3th-order Butterworth), rectified and low pass filtered (20 Hz zero overshoot filter). Rest EMG, i.e. the minimal EMG determined for each muscle by applying a moving window of 8 ms, was subtracted from the total EMG because it was assumed not to contribute to ankle torque (noise). Torque and ankle angle were sampled at 1024 Hz and low pass filtered (20 Hz zero overshoot filter) and resampled to 1000 Hz.

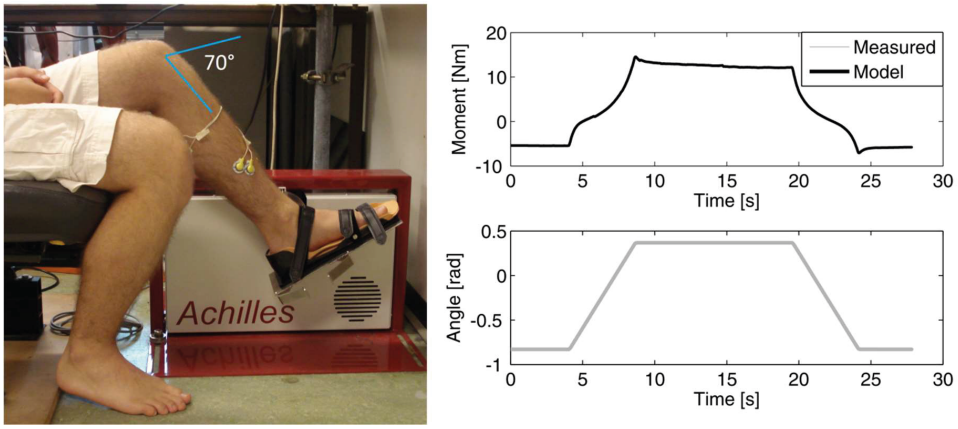


Figure 3.1: *Left: Measurement set-up. Measurements were performed at 70° (see figure) or 20° knee flexion. Right: Example of imposed angular rotation (bottom) and torque response with model fit (top row) for a healthy participant (extended knee, 15°/sec VAF=99.97%).*

Protocol

Measurements were performed at the right ankle (healthy volunteers) or at the hemiparetic side (patients). Maximum dorsal- and plantar flexion angles within the predefined tolerated range of motion (RoM) were assessed by imposing torques of 15 Nm (dorsiflexion) and -7.5 Nm (plantar flexion). The resulting RoM defined the boundaries for the subsequent RaH rotations.

During the RaH measurements, the ankle was rotated at two different angular velocities, $15°.s^{-1}$ and $100°.s^{-1}$, starting from maximal plantar flexion and ending at maximal dorsiflexion (first ramp). After a hold phase the ankle was moved back to the maximal plantar flexion angle (second ramp, Figure 3.1). RaH rotations were started at random (thus unpredictable) time instants. A single session thus comprised one RoM assessment and four RaH trials (twice for

each velocity) per knee angle. Participants were asked not to actively resist or to move with any motion.

Biomechanical model

A biomechanical model-based on a previous developed Hill-type muscle element ankle model[4] was adapted to estimate parameters of the passive and active force-length relationship of the connective and contractile tissue contribution of the triceps surae and tibialis anterior (Appendix 3B).

The net ankle torque, T_{mod}, applied onto the manipulator was estimated based on 15 parameters (Appendix 3A) describing the inertial torque (I), the torque generated by the plantar flexors (tri) and the torque generated by the dorsiflexors (tib) as a function of time (t) and the combined gravitational torque of the foot and foot plate as a function of ankle angle (θ) (Eq. 3.1):

$$T_{mod}(t) = I\ddot{\theta}(t) + T_{tri}(t) - T_{tib}(t) + T_{grav}(\theta) \quad (3.1)$$

The measured joint torque (T_{meas}) was simulated (T_{mod}) from ankle position and EMG by optimizing 15 parameters (Appendix 3) using a least squares gradient search algorithm (*lsqnonlin*, *MATLAB*). Primary outcome measures were:

1) Slack length ($l_{p,slack,m}$) and stiffness coefficient (k_m) for both dorsiflexors (m=tib) and plantar flexors (m=tri), represent the passive force-length relation of the parallel connective tissues. The higher k_m, the stiffer the muscle; the lower $l_{p,slack,m}$ the shorter the muscle.
2) Optimal length ($l_{opt,m}$), i.e. the length at which the activated plantar (tri) and dorsiflexor (tib) muscles generate their maximum force.
3) Peripheral tissue stiffness (K_{joint}) selectively derived from the (parallel) connective tissue model components at angle position $\theta = 0^o$, i.e. foot perpendicular to the lower leg.
4) Reflexive torque $T_{reflex,m}$, i.e. the root mean square of the active muscle torque for the observed trial

Simulation and analysis was performed in *MATLAB* (The Mathworks Inc., Natick MA) and statistical analysis was performed using IBM SPSS statistics 22 and GraphPad Prism 6.

Internal model validity, test-retest reliability, sensitivity and external validity

Internal model validity: Model fit and parameter reliability

The model fit was indicated by the torque variance accounted for (*VAF*), estimated for each trial:

$$VAF = \left(1 - \frac{\sum\left((T_{meas} - T_{mean}) - (T_{\mathrm{mod}} - T_{mean})\right)^2}{\sum (T_{meas} - T_{mean})^2}\right) * 100\% \qquad (3.2)$$

with T_{mean} being the average of T_{mod} and T_{meas}. *VAF* values less than 99% were disregarded from analysis for test-retest reliability, sensitivity and external validity.

The standard error of the mean (*SEM*) represents the parameter reliability and is based on the partial derivatives of each parameter to the error function[4]. Low *SEM* values indicated that the specific parameter has substantial contribution to the error function. High values may indicate high co-variances or over-parameterization. *SEM* values were estimated for each trial before rejection based on low *VAF* value.

For interpretation of the results we defined the following inclusion demands: Optimal lengths ($l_{opt,m}$) were only included in the analysis in case of sufficient muscle activity, i.e. reflexive torque, $T_{reflex,m}$ larger than .75 Nm, combined with *SEM*'s lower than 0.1 Nm and for optimal length values that did not meet predefined parameter boundaries. Optimal tibialis length ($l_{opt,tib}$) was excluded from further analysis when the model parameter G_{tib}, i.e. EMG weighting factor of tibialis anterior, was extremely high ($>1*10^8$) thereby introducing noise amplification. This was not an issue for the optimal triceps surae length ($l_{opt,tri}$) because three EMG weighting factors were used to define the triceps surae muscle activation.

Test-retest reliability

Repeated measures were averaged for each participant for comparison between sessions on the same day and between days. Between-trial reliability of consecutive trials within a session, between-session reliability (on the same day) and between-day reliability with 1-2 weeks in between were assessed using the intra-class correlation coefficient (*ICC* using the two-way

mixed model for absolute agreement and interpreted according to Fleiss[30] (>.75 excellent, .4-.75 fair to good, <.4 poor).

Sensitivity for knee angle

Repeated measures were averaged for each participant to compare groups of participants. Optimal length estimates were averaged for 15°.s^{-1} and 100°.s^{-1} observations. A paired t-test was used to compare outcome measures between flexed and extended knee condition in healthy subjects and stroke patients.

External validity

A linear mixed model was used to determine the difference in model parameters between healthy controls and stroke patients after transforming data to obtain a normal distribution using the square root of the estimated primary outcome measures. Data from the slow trials (15°.s^{-1}) were used to estimate non-neural parameters while for the reflexive torques data from the fast trials (100°.s^{-1}) were used, as reliability for passive parameters proved to be highest for slow movements and reflexive torques proved to be highest for fast movements[22]. Individual observations were compared to the clinical Ashworth score. The minimal detectable change (*MDC*)[31;32] with a 95% confidence interval was used to identify deviated parameters in patients post-stroke relative to healthy volunteers, i.e. parameters exceeding the mean value +/- *MDC*. *MDC* values were calculated using the standard error of measurement (S_{EM}) using *ICC* from healthy participants calculated between sessions on different days, Eq. 3.3:

$$S_{EM} = SD * \sqrt{1 - ICC} \tag{3.3}$$

$$MDC = 1.96 * \sqrt{2} * S_{EM} \tag{3.4}$$

MDC values were also calculated based on *ICC* from stroke patients to determine the potential for longitudinal observations to e.g. identify the effect of treatment.

Results

From three patients and one healthy volunteer, the data of the second visit was missing or excluded due to muscular pain, measurement problems and medication possibly influencing muscle function. In total 640 trials from 28 participants were included for analysis of internal model validity. The requirements of sufficient muscle activation to optimal length analysis were met for 345 trials of 27 participants (13 stroke patients). Eight trials (1.25%) were excluded due to low *VAF* values not exceeding 99%. Data from 24 participants (10 patients) were available to assess between-day reliability. In 25 sessions of eight (out of 28) participants, RaH's were not performed over the whole [-7.5–15 Nm] RoM at dorsiflexion (7 times, 5 participants) and plantar flexion (22 times, 5 participants). In these cases, safety stops were set at smaller ranges because of e.g. pain or discomfort. Dorsal passive RoM of patients post-stroke, 16.5° (*SD* 8.7) was reduced (p=.025) compared to healthy participants, 25.5° (*SD* 9.2).

Detailed overview of all model parameter estimates and *SEM* values are presented in Appendix 3A. Median *VAF* values of all 640 trials, i.e. including *VAF* < 99% observations, was 99.9% for both knee angles. Median *SEM* values were equal or below 0.1 for all estimated parameters except the EMG weighting factors.

Test-retest reliability of model parameters varied dependent on ankle rotation speed and knee angle and was fair to excellent for parameters related to the passive force-length of the triceps (k_{tri}, $l_{p,slack,tri}$) (Table 3.2). For the optimal length of the triceps ($l_{opt,tri}$), test-retest reliability was fair to good except for between-trial reliability with extended knee. Test-retest reliability for reflexive torque of the triceps ($T_{reflex,tri}$) was poor at 15°.s^{-1} between days for the extended knee condition. Test-retest reliability of the peripheral tissue stiffness (K_{joint}) was in all cases higher than 0.8 and excellent in 6 out of 12 conditions (*ICC*>.9).

For healthy volunteers, peripheral tissue stiffness was higher in extended knee condition compared to flexed knee condition (P=.017) and slack length (P<.001), stiffness coefficient (P=.003) and optimal length (P=.024) of the triceps surae were increased in flexed knee condition (Figure 3.2, Table 3.3 and Table 3.4). There were no significant changes for the parameters involved in the passive and active force-length relationship of the tibialis anterior.

Table 3.2: *Intraclass correlation coefficients over observations of controls and patients for flexed and extended knee for movement velocity of 15°.s-1 and 100°.s-1. For analysis of the optimal lengths the parameters per knee angle were averaged due to small number of trials as not all trials met the requirements of sufficient muscle activation to estimate* $l_{opt,m}$.

	Between-trial		**Between-session**		**Between-day**	
	15°.s^{-1}	100°.s^{-1}	15°.s^{-1}	100°.s^{-1}	15°.s^{-1}	100°.s^{-1}
Flexed knee						
k_{tri} [m^{-1}]	.636	.811	.948	.903	.937	.598
k_{tib} [m^{-1}]	.763	.716	.875	.845	.662	.773
$l_{slack,tri}$ [m]	.683	.563	.812	.778	.705	.564
$l_{slack,tib}$ [m]	.883	.859	.922	.839	.484	.775
$l_{opt,tri}$ [m]*	.600		.735		.565	
$l_{opt,tib}$ [m]*	.569		.476		.050	
K_{joint} [Nm.rad^{-1}]	.909	.986	.846	.861	.833	.823
$T_{reflex,tri}$ [Nm]	.722	.701	.839	.908	.707	.719
$T_{reflex,tib}$ [Nm]	.074	.390	.578	.805	.165	.246
Extended knee						
k_{tri} [m^{-1}]	.848	.646	.909	.755	.694	.530
k_{tib} [m^{-1}]	.585	.747	.617	.846	.679	.387
$l_{slack,tri}$ [m]	.739	.578	.831	.830	.689	.423
$l_{slack,tib}$ [m]	.604	.722	.553	.760	.736	.385
$l_{opt,tri}$ [m]*	.333		.756		.470	
$l_{opt,tib}$ [m]*	.736		.097		.158	
K_{joint} [Nm.rad^{-1}]	.916	.989	.899	.919	.930	.878
$T_{reflex,tri}$ [Nm]	.506	.631	.647	.775	.110	.647
$T_{reflex,tib}$ [Nm]	.732	.788	.690	.883	.203	.546

**Parameters per knee angle were averaged*

Table 3.3: *Model outcome parameters (mean, SD) for healthy and stroke participants for flexed and extended knee condition.*

	Flexed knee		**Extended knee**	
	Healthy	**Stroke**	**Healthy**	**Stroke**
k_{tri} [m^{-1}]	270 (33)	328 (73)	252 (37)	321 (65)
k_{tib} [m^{-1}]	210 (47)	188 (58)	204 (31)	197 (42)
$l_{slack,tri}$ [m]	.022 (.0028)	.023 (.0029)	.019 (.0029)	.022 (.0030)
$l_{slack,tib}$ [m]	.067 (.0065)	.060 (.015)	.066 (.0048)	.064 (.0068)
$l_{opt,tri}$ [m]	.050 (.0054)	.046 (.0058)	.046 (.0042)	.043 (.0042)
$l_{opt,tib}$ [m]	.072 (.0050)	.074 (.015)	.073 (.011)	.081 (.0097)
K_{joint} [$Nm.rad^{-1}$]	53 (39)	94 (65)	65 (42)	103 (80)
$T_{reflex,tri}$ [Nm]	.85 (.39)	1.6 (1.1)	1.1 (.48)	2.0 (1.2)
$T_{reflex,tib}$ [Nm]	.61 (.46)	.79 (.97)	1.4 (1.4)	.76 (1.0)

Reflexive torque of the tibialis anterior in extended knee condition was increased (P=.013) compared to the flexed knee condition. In patients post-stroke, optimal muscle length of the triceps surae was smaller (P=.016) and reflexive torque of the triceps surae higher (P=.003) in extended knee condition compared to flexed knee condition. Parameters involved in the passive force-length relationship of the triceps surae, i.e. the stiffness coefficient (k_{tri}) and the slack length ($l_{p,slack,tri}$), and the reflexive torque ($T_{reflex,tri}$) of the triceps surae were higher in patients post-stroke relative to healthy volunteers (Figure 3.2, Table 3.3 and Table 3.4). No significant differences were found for the optimal length of the triceps surae and all tibialis anterior parameters between stroke patients and healthy controls. Based on calculated *MDC*s, individual patients could be identified with respect to healthy volunteers (Table 3.5). The variability in terms of individual parameters was high, as illustrated in Figure 3.2B.

Non-neural tissue properties tended to be more prominent for the low Ashworth scores (0, 1 and 2) and reflexive torque for the high Ashworth scores (3 and 4) (Table 3.6). *MDC*s of stroke patients were comparable with *MDC*s of healthy subjects (Table 3.7). Only for the reflexive torque of tibialis and slack length of tibialis in flexed knee condition, the *MDC* was more than two times higher in the stroke patients group than in the control group.

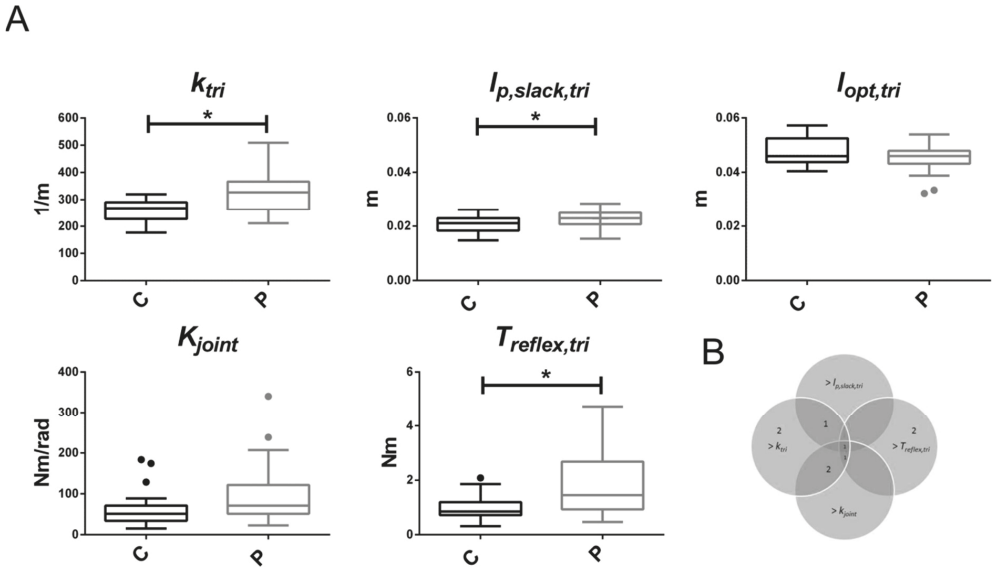


Figure 3.2: *A: Comparison between stiffness coefficient (k_{tri}), slack length ($l_{p,slack,tri}$), optimal length ($l_{opt,tri}$), peripheral tissue stiffness (K_{joint}) and reflexive torque ($T_{reflex,tri}$) of the triceps surae between healthy participants (H) and stroke patients (P). Figures show boxplots. Asterisks denote significant differences ($p<.05$). B: The Venn diagram of outcome parameters for extended knee. Values indicate nine patients with deviated values for one or more outcome measures. The patient with increased stiffness coefficient (k_{tri}), slack length ($l_{p,slack,tri}$), tissue stiffness (K_{joint}) and reflexive torque ($T_{reflex,tri}$) also had an smaller optimal length ($l_{opt,tri}$).*

Table 3.4: *P-values for comparison between participant group and knee angle (flexed =70º, extended = 20º).*

	Healthy vs Stroke*	**Flexed versus extended knee****	
		Healthy	**Stroke**
k_{tri} [m^{-1}]	**.003**	**.003**	.38
k_{tib} [m^{-1}]	.319	.63	.40
$l_{slack,tri}$ [m]	**.046**	**<.001**	.22
$l_{slack,tib}$ [m]	.157	.79	.16
$l_{opt,tri}$ [m]	.243	**.024**	**.016**
$l_{opt,tib}$ [m]	.509	.82	.13
K_{joint} [Nm.rad^{-1}]	.051	**.017**	.44
$T_{reflex,tri}$ [Nm]	**.011**	.087	**.003**
$T_{reflex,tib}$ [Nm]	.354	**.013**	.87

** Statistical analysis: linear mixed model **Statistical analysis: paired t-test*

Table 3.5: *Minimal detectable change (MDC) and threshold (Th) to determine "deviated" values in stroke. The number of patients identified as deviated from healthy controls are indicated per parameter. The threshold and minimal detectable change for the optimal length of the tibialis anterior for the flexed knee condition was not determined because the intraclass correlation coefficient was zero for this parameter.*

	Flexed knee			**Extended knee**		
	Th;	***MDC***	**# deviating patients**	**Th**	***MDC***	**# deviating patients**
k_{tri} [m^{-1}]	> 301	32.3	**7**	> 318	65.3	**7**
k_{tib} [m^{-1}]	< 134	75.5	**3**	< 141	6.8	**2**
$l_{slack,tri}$ [m]	> .0267	.0047	**1**	> .0254	.0060	**2**
$l_{slack,tib}$ [m]	< .0547	.0119	**3**	< .0580	.0079	**2**
$l_{opt,tri}$ [m]	< .0357	.0133	**1**	< .0379	.0083	**1**
$l_{opt,tib}$ [m]	-		-	<.0429	.0287	**0**
K_{joint} [Nm.rad^{-1}]	> 119	64.7	**4**	>114	48.1	**4**
$T_{reflex,tri}$ [Nm]	> 1.97	1.07	**5**	> 2.70	1.55	**4**
$T_{reflex,tib}$ [Nm]	> 1.72	1.08	**3**	> 3.99	2.59	**0**

Table 3.6: *Ashworth scores related to outcome measures. Percentage of patients with Ashworth score that show deviated values on outcome measures.*

Ashworth score	K_{joint}	k_{tri}	$l_{slack,tri}$	$l_{opt,tri}$	$T_{reflex,tri}$
0 (n=2)	50%	50%	0%	0%	0%
1 (n=3)	67%	100%	0%	0%	33%
2 (n=3)	0%	67%	33%	0%	0%
3 (n=3)	0%	33%	0%	0%	67%
4 (n=2)	50%	50%	50%	50%	100%

Table 3.7: *Intraclass correlation coefficients (ICC) and minimal detectable changes (MDC) of stroke patients. The ICC and MDC for the optimal length of the tibialis anterior for the extended knee condition were not determined because the intraclass correlation coefficient was negative for this parameter.*

	Flexed knee		**Extended knee**	
	ICC	***MDC***	***ICC***	***MDC***
k_{tri} [m^{-1}]	.937	49.1	.567	122
k_{tib} [m^{-1}]	.613	100	.777	56.4
$l_{slack,tri}$ [m]	.76	.0043	.728	.0046
$l_{slack,tib}$ [m]	.44	.030	.776	.00875
$l_{opt,tri}$ [m]	.658	.011	.234	.012
$l_{opt,tib}$ [m]	.947	.0086	-	-
K_{joint} [Nm.rad^{-1}]	.925	46.7	.955	49.9
$T_{reflex,tri}$ [Nm]	.8	1.26	.665	2.02
$T_{reflex,tib}$ [Nm]	.153	3.1	.182	2.54

Discussion

The aim of this study was to estimate the passive and active tissue properties, i.e. the stiffness coefficient and slack length of the passive force-length relationship and the optimal length of the active force-length relationship, of the triceps surae and tibialis anterior muscles non-invasively in patients and healthy volunteers. Valid, reliable and sensitive estimations of passive and active force-length characteristics next to neural reflexive torque could be obtained using an EMG-driven ankle model. Increased ankle joint stiffness was explained by an increase in triceps stiffness next to an elevated reflexive torque, but not by a shorter triceps surae. Values for minimal detectable change were such that individual patients could be discerned from healthy volunteers further substantiating the clinical potential of the method.

Internal model validity

With the extension of the model relative to the preceding model of de Vlugt et al. (2010) additional parameters were introduced which generally resulted in a higher goodness of fit, but at a risk of over-parameterization. The internal model validity indicated high *VAF* values in 98% of the cases without being over-parameterized as indicated by the low *SEM*s.

Test-retest reliability

Ramp velocity affected the test-retest reliability for tissue parameters and reflexive torque differently with optimal validity with velocities of $15°.s^{-1}$ and $100°.s^{-1}$ respectively. Sensitivity for the ramp velocity on the test-retest reliability of the outcome measures was also observed in patients with cerebral palsy[20;22]. The test-retest reliability of the triceps surae was higher than the test-retest reliability of the tibialis anterior, especially for the reflexive torque and optimal muscle length.

Sensitivity to knee angle

Changing the knee angle induces changes in the bi-articular muscle length and thus in the relative contribution of the mono-articular soleus and the bi-articular gastrocnemii and affected as expected the passive and active force-length characteristics of the bi-articular triceps surae in contrast to the mono-articular tibialis anterior thereby increasing the peripheral tissue stiffness in extended knee condition as was also shown in literature[33;34].

External validity

Patients post-stroke showed an increased stiffness coefficient of the triceps surae in combination with an increased triceps surae slack length and increased reflexive torque of the triceps surae. Difference between stroke patients and healthy volunteers for the stiffness coefficient suggests the presence of tissue changes after stroke coinciding with increased reflexive torque of the triceps as prior observed in the ankle[4;17] and wrist[15;18;27]. Stiffening of the muscle may be due to a change in collagen compound and/or structure in the extracellular matrix as was found in cerebral palsy[26]. It can be speculated that stiffer tissue in series with proprioceptive organs (muscle spindles and golgi tendon organs) may result in higher efferent responses and consequently higher reflexive torques.

Increased slack length in patients post-stroke may be the result of reduced pennation angle as a consequence of muscle atrophy[35]. Pennation angles are not separately addressed by the current approach.

The combination of the stiffness coefficients and slack muscle lengths of the triceps surae and tibialis anterior, determines the peripheral tissue stiffness. It is important to be aware that conclusions on joint stiffness depend on the ankle angle at which participants are compared. The difference in ankle angle of 3° dorsiflexion in our previous study[4] and 0° dorsiflexion in the current study, may explain why significant differences of K_{joint} were only found in the first study and not just in the current study (P=.051).

Estimation of the stiffness coefficient and slack length of the passive force-length relationship in either triceps surae or tibialis anterior in patients helps to better characterize the underlying tissue changes of increased peripheral tissue stiffness (stiffened and/or shortened). Different combinations of neural reflexive and non-neural tissue parameters were found but overall, a high Ashworth score coincided with a high reflexive torque. Using the *MDC* values of healthy subjects, deviated parameters were found in both flexed and extended knee condition and can be used to identify deviated neural reflexive and non-neural tissue properties in patients. This method might be helpful in muscle specific treatment selection by measuring at different knee angles dependent on the muscle of interest, e.g. to assess the non-neural tissue parameters of the soleus, the patient can be measured in flexed knee condition.

MDC values of the passive and active force-length characteristics of stroke patients being 2-7 times smaller than the average parameter values showed the potential for longitudinal observations e.g. to evaluate treatment.

Limitations and recommendations

The series elastic muscle tendon and the pennation angle both affect the (optimal) length characteristic of a muscle, but were not yet included within the model. Van de Poll showed by simulation, that including an Achilles tendon did not significantly affects the model parameters[36]. Pennation angle is a potential covariate of the length parameters, and affects the passive and active force-length characteristics of the model structure. Increased slack length in patients post-stroke may also be the result of a reduced pennation angle compared to healthy volunteers as a consequence of muscle atrophy[35]. Further addressing pennation (or muscle fiber length) requires direct observations, e.g. by ultrasound recordings.

Rest EMG, i.e. the minimal EMG determined for each muscle, was subtracted from the total EMG because assumed not to contribute to ankle torque. However, important information of background muscle activation, which might be elevated in stroke patients[37], was discarded. In case of increased background activation this might be accounted for by other parameters, e.g. the peripheral tissue stiffness, muscle stiffness coefficient and (optimal) muscle length, due to changed pennation angle.

Conclusion

A non-invasive EMG-driven neuromuscular modeling approach was demonstrated to estimate the properties of the passive and active force-length relationship of the triceps surae and tibialis anterior next to neural reflexive torque in patients and healthy volunteers. The model provided for valid, reliable and sensitive parameters and can be used to identify deviated neural reflexive and non-neural tissue properties in stroke patients. Non-invasive quantification of underlying contributors to increased joint stiffness post-stroke is important for proper and tailored patient referral to therapeutic strategies and high resolution follow-up.

Acknowledgements

We would like to thank all patients and healthy volunteers who participated in the study; all rehabilitation specialists of the Leiden University Medical Center for recruitment of the patients and clinical assessment; Chantal Hofman and Jasper Mulder for conducting the experiment and recruitment of patients and healthy volunteers; Stijn Van Eesbeek for technical assistance. We thank the Department of Medical Statistics at the LUMC for assistance in statistical analysis. This research is supported by the Dutch Technology Foundation STW, which is part of the Netherlands Organisation for Scientific Research (NWO) and partly funded by the Ministry of Economic Affairs, Agriculture and Innovation (ROBIN project, grant nr. 10733).

References

(1) Mayer NH, Esquenazi A, Childers MK. Common patterns of clinical motor dysfunction. *Muscle Nerve Suppl* 1997;6:S21-S35.

(2) Harlaar J, Becher JG, Snijders CJ, Lankhorst GJ. Passive stiffness characteristics of ankle plantar flexors in hemiplegia. *Clin Biomech* 2000;15:261-270.

(3) Ada L, Canning CG, Low SL. Stroke patients have selective muscle weakness in shortened range. *Brain* 2003;126:724-731.

(4) de Vlugt E, de Groot JH, Schenkeveld KE, Arendzen JH, van der Helm FC, Meskers CG. The relation between neuromechanical parameters and Ashworth score in stroke patients. *J Neuroeng Rehabil* 2010;7:35.

(5) Dietz V, Sinkjaer T. Spastic movement disorder: impaired reflex function and altered muscle mechanics. *Lancet Neurol* 2007;6:725-733.

(6) Gracies JM, Singer BJ, Dunne JW. The role of botulinum toxin injections in the management of muscle overactivity of the lower limb. *Disabil Rehabil* 2007;29:1789-1805.

(7) Simpson DM, Gracies JM, Graham HK et al. Assessment: Botulinum neurotoxin for the treatment of spasticity (an evidence-based review): report of the Therapeutics and Technology Assessment Subcommittee of the American Academy of Neurology. *Neurology* 2008;70:1691-1698.

(8) Sheean G. Botulinum toxin should be first-line treatment for poststroke spasticity. *J Neurol Neurosurg Psychiatry* 2009;80:359.

(9) Mortenson PA, Eng JJ. The use of casts in the management of joint mobility and hypertonia following brain injury in adults: a systematic review. *Phys Ther* 2003;83:648-658.

(10) Thompson AJ, Jarrett L, Lockley L, Marsden J, Stevenson VL. Clinical management of spasticity. *J Neurol Neurosurg Psychiatry* 2005;76:459-463.

(11) Renzenbrink GJ, Buurke JH, Nene AV, Geurts AC, Kwakkel G, Rietman JS. Improving walking capacity by surgical correction of equinovarus foot deformity in adult patients with stroke or traumatic brain injury: a systematic review. *J Rehabil Med* 2012;44:614-623.

(12) Kwakkel G, Meskers CG. Botulinum toxin A for upper limb spasticity. *Lancet Neurol* 2015.

(13) Meskers CG, de Groot JH, de Vlugt E, Schouten AC. NeuroControl of movement: system identification approach for clinical benefit. *Front Integr Neurosci* 2015;9:48.

(14) Fleuren JF, Voerman GE, Erren-Wolters CV et al. Stop using the Ashworth Scale for the assessment of spasticity. *J Neurol Neurosurg Psychiatry* 2010;81:46-52.

(15) de Gooijer-van de Groep K, de Vlugt E., van der Krogt HJ et al. Estimation of tissue stiffness, reflex activity, optimal muscle length and slack length in stroke patients using an electromyography driven antagonistic wrist model. *Clin Biomech* 2016;35:93-101.

(16) Willerslev-Olsen M, Lorentzen J, Sinkjaer T, Nielsen JB. Passive muscle properties are altered in children with cerebral palsy before the age of 3 years and are difficult to distinguish clinically from spasticity. *Dev Med Child Neurol* 2013;55:617-623.

(17) Lorentzen J, Grey MJ, Crone C, Mazevet D, Biering-Sorensen F, Nielsen JB. Distinguishing active from passive components of ankle plantar flexor stiffness in stroke, spinal cord injury and multiple sclerosis. *Clin Neurophysiol* 2010;121:1939-1951.

(18) Wang R, Herman P, Ekeberg O, Gaverth J, Fagergren A, Forssberg H. Neural and non-neural related properties in the spastic wrist flexors: An optimization study. *Med Eng Phys* 2017;47:198-209.

(19) Jalaleddini K, Golkar MA, Kearney RE. Measurement of Dynamic Joint Stiffness from Multiple Short Data Segments. *IEEE Trans Neural Syst Rehabil Eng* 2017;25:925-934.

(20) Sloot LH, van der Krogt MM, de Gooijer-van de Groep KL et al. The validity and reliability of modelled neural and tissue properties of the ankle muscles in children with cerebral palsy. *Gait Posture* 2015.

(21) Lindberg PG, Gaverth J, Islam M, Fagergren A, Borg J, Forssberg H. Validation of a new biomechanical model to measure muscle tone in spastic muscles. *Neurorehabil Neural Repair* 2011;25:617-625.

(22) de Gooijer-van de Groep KL, de Vlugt E, de Groot JH et al. Differentiation between non-neural and neural contributors to ankle joint stiffness in cerebral palsy. *J Neuroeng Rehabil* 2013;10:81.

(23) Wisdom KM, Delp SL, Kuhl E. Use it or lose it: multiscale skeletal muscle adaptation to mechanical stimuli. *Biomech Model Mechanobiol* 2015;14:195-215.

(24) Gao F, Zhang LQ. Altered contractile properties of the gastrocnemius muscle poststroke. *J Appl Physiol (1985)* 2008;105:1802-1808.

(25) Gao F, Grant TH, Roth EJ, Zhang LQ. Changes in passive mechanical properties of the gastrocnemius muscle at the muscle fascicle and joint levels in stroke survivors. *Arch Phys Med Rehabil* 2009;90:819-826.

(26) Smith LR, Lee KS, Ward SR, Chambers HG, Lieber RL. Hamstring contractures in children with spastic cerebral palsy result from a stiffer extracellular matrix and increased in vivo sarcomere length. *J Physiol* 2011;589:2625-2639.

(27) de Gooijer-van de Groep KL, de Groot JH, van der Krogt H, de Vlugt E, Arendzen JH, Meskers CGM. Early Shortening of Wrist Flexor Muscles Coincides With Poor Recovery After Stroke. *Neurorehabil Neural Repair* 2018;1545968318779731.

(28) Ashworth B. Preliminary trial of carisoprodol in multiple sclerosis. *Practitioner* 1964;192:540-542.

(29) Hermens HJ, Freriks B, Disselhorst-Klug C, Rau G. Development of recommendations for SEMG sensors and sensor placement procedures. *J Electromyogr Kinesiol* 2000;10:361-374.

(30) Fleiss J.L. The measurement of interrater agreement. *Statistical methods for rates and proportions*. New York: John Wiley & Sons; 1981;212-236.

(31) Haley SM, Fragala-Pinkham MA. Interpreting change scores of tests and measures used in physical therapy. *Phys Ther* 2006;86:735-743.

(32) de Vet HC, Terwee CB, Knol DL, Bouter LM. When to use agreement versus reliability measures. *J Clin Epidemiol* 2006;59:1033-1039.

(33) Cresswell AG, Loscher WN, Thorstensson A. Influence of gastrocnemius muscle length on triceps surae torque development and electromyographic activity in man. *Exp Brain Res* 1995;105:283-290.

(34) Le Sant G, Nordez A, Andrade R, Hug F, Freitas S, Gross R. Stiffness mapping of lower leg muscles during passive dorsiflexion. *J Anat* 2017;230:639-650.

(35) Ramsay JW, Buchanan TS, Higginson JS. Differences in Plantar Flexor Fascicle Length and Pennation Angle between Healthy and Poststroke Individuals and Implications for Poststroke Plantar Flexor Force Contributions. *Stroke Res Treat* 2014;2014:919486.

(36) van de Poll KD. *Estimating ankle muscle parameters.* TU Delft, The Netherlands; 2016.

(37) Burne JA, Carleton VL, O'Dwyer NJ. The spasticity paradox: movement disorder or disorder of resting limbs? *J Neurol Neurosurg Psychiatry* 2005;76:47-54.

Appendix 3A: Supplementary tables

Table 3A**:** *Electrode placement according to seniam guidelines (www.seniam.org)*

Muscle	**Location**
Tibialis anterior	At 1/3 on the line between the tip of the fibula and the tip of the medial malleolus.
Soleus	At 2/3 of the line between the medial condylis of the femur to the medial malleolus.
Gastrocnemius medialis	On the most prominent bulge of the muscle.
Gastrocnemius lateralis	At 1/3 of the line between the head of the fibula and the heel.

Table 3B: *Description of model parameters (n=15) and optimization values (initial value and min and max)*

Model parameters	**Description**	**Initial value**	**[Min Max]**
M	Mass [kg]	1.5	[1.2 3]
k_{tri}, k_{tib}	Stiffness coefficients [m^{-1}]	200	[10 600]
$l_{p,slack,tri,}$	Slack length of connective tissue [m]	0.05	[0.01 0.09]
$l_{p,slack,tib}$		0.05	[0.01 0.11]
G_{tri},(3x) G_{tib}	EMG weighting factors [-]	$1*10^4$	[0 10^{10}] (all muscles)
f_0	Activation cutoff frequency [Hz]	2	[0.5 4]
Beta	Relative damping [-]	1	[0.5 1.25]
$L_{opt,tri}$	Optimal muscle lengths [m]	0.048	[0.02 0.09]
$l_{opt,tib}$		0.068	[0.02 0.11]
tau_{rel}	Tissue relaxation time constant [s]	2	[0.1 6]
k_{rel}	Tissue relaxation factor [-]	0.1	[0.05 1]

Table 3C: *Estimated values (median (1st- 3rd quartile) for model parameters for extended knee and flexed knee.*

Parameter	Healthy		Stroke	
	Extended knee	**Flexed knee**	**Extended knee**	**Flexed knee**
m [kg]	1.20 (1.20-1.85)	1.20 (1.20-1.28)	1.20(1.20-1.92)	1.20 (1.20-1.21)
k_{tri} [m^{-1}]	264 (225-295)	279 (250-306)	319(260-359)	325 (270-363)
k_{tib} [m^{-1}]	191 (166-222)	195 (160-234)	172(126-208)	161 (114-208)
$l_{p,slack,tri,}$ [m]	0.020 (0.018-0.024)	0.023 (0.020-0.026)	0.023(0.020-0.026)	0.024 (0.021-0.026)
$l_{p,slack,tib}$ [m]	0.066 (0.062-0.069)	0.065 (0.060-0.072)	0.061(0.052-0.067)	0.060 (0.046-0.067)
$l_{tri,opt}$ [m]	0.046 (0.042-0.051)	0.047 (0.044-0.055)	0.043 (0.037-0.048)	0.045 (0.039-0.051)
$l_{tib,opt}$ [m]	0.068 (0.061-0.075)	0.073 (0.060-0.085)	0.085 (0.076-0.093)	0.082 (0.066-0.088)
Tau_{rel} [s]	1.6 (0.84-2.3)	1.6 (0.86-2.5)	1.8(1.0-2.5)	2.1 (1.3-2.9)
k_{rel} [-]	0.27 (0.19-0.46)	0.26 (0.19-0.35)	0.31(0.21-0.53)	0.26 (0.20-0.46)
G_{tri} [-]	$6.0*10^6$ (33-$3.1*10^7$), $7.6*10^6$ (82-$3.8*10^7$), $8.3*10^6$ (58-$3.6*10^7$)	$8.0*10^6$ (46-$3.1*10^7$), $1.1*10^7$ (546-$4.9*10^7$), $1.1*10^7$(961-$5.0*10^7$)	$1.5*10^7$($1.7*10^4$-$3.7*10^7$), $7.2*10^6$(2842-$2.7*10^7$), $1.1*10^7$($4.9*10^5$-$3.6*10^7$)	1.3*107 (2257-$3.9*10^7$), $1.1*10^7$ (1055-$3.6*10^7$),$9.3*10^6$(367-$3.3*10^7$)
G_{tib} [-]	$2.3*10^6$ ($1.2*10^6$-$4.0*10^7$)	$8.9*10^6$ ($1.6*10^6$-$8.1*10^7$)	$1.4*10^7$($3.7*10^6$-$1.2*10^8$)	$5.6*10^6$($1.9*10^6$-$5.4*10^7$)
f_0 [Hz]	0.65 (0.5-1.2)	0.50 (0.50-1.0)	0.94(0.50-1.4)	0.89 (0.50-1.4)
beta [-]	1.25 (1.22-1.25)	1.25 (1.23-1.25)	1.25(0.80-1.25)	1.25 (0.79-1.25)

Table 3D: *SEM values (median (1st- 3rd quartile) for model parameters for extended knee and flexed knee.*

Parameter	Healthy		Stroke	
	Extended knee	**Flexed knee**	**Extended knee**	**Flexed knee**
m [kg]	0.073(0.051-0.10)	0.052 (0.041-0.066)	0.082(0.061-0.13)	0.068 (0.050-0.096)
k_{tri} [m^{-1}]	0.013(0.0097-0.017)	0.015 (0.012-0.019)	0.022(0.014-0.037)	0.022 (0.015-0.032)
k_{tib} [m^{-1}]	0.015(0.012-0.020)	0.015 (0.012-0.018)	0.015(0.011-0.021)	0.016 (0.011-0.020)
$l_{p,slack,tri,}$ [m]	0.0047(0.0036-0.0067)	0.0049 (0.0040-0.0064)	0.0053(0.0039-0.0076)	0.0054 (0.0039-0.0075)
$l_{p,slack,tib}$ [m]	0.012(0.0085-0.016)	0.010 (0.0077-0.014)	0.015(0.011-0.025)	0.016 (0.0093-0.028)
$l_{tri,opt}$ [m]	0.047 (0.020-0.39)	0.049 (0.022-0.23)	0.023 (0.0072-0.064)	0.030 (0.013-0.072)
$l_{tib,opt}$ [m]	0.019 (0.011-0.041)	0.031-0.016-0.081)	0.031 (0.015-0.16)	0.032 (0.013-0.17)
Tau_{rel} [s]	0.019(0.0081-0.038)	0.020 (0.0097-0.045)	0.023(0.012-0.044)	0.029 (0.013-0.060)
k_{rel} [-]	0.056(0.040-0.11)	0.053 (0.038-0.086)	0.071(0.047-0.14)	0.067 (0.044-0.13)
G_{tri} [-]	375(141-1759), 557(220-2260), 481 (197-1568)	648 (203-3093), 988 (320-3874), 764 (282-3340)	285(114-1337),274(100-1513),313(101-1661)	576 (182-2357), 572 (204-2705), 516 (169-2943)
G_{tib} [-]	51 (5-1670)	527 (82-91547)	417(38-3.0*10^5)	264 (29-2515)
f_0 [Hz]	0.018(0.013-0.031)	0.021 (0.013-0.041)	0.014(0.0096-0.026)	0.018 (0.011-0.033)
beta [-]	0.082(0.053-0.12)	0.10 (0.072-0.16)	0.063(0.023-0.11)	0.064 (0.031-0.12)

Appendix 3B: Ankle model

The model structure was based on the ankle model from de Vlugt et al.[1] with the following adaptations:

a) the model is able to describe plantar- and dorsiflexion forces during both dorsi-flexion and plantar flexion motions[2] estimating parameters that model the relaxation effects during the hold phase where Sloot et al.[2] used an offset torque constant to account for the relaxation effect.
b) Optimal muscle length parameters, i.e. the length at which the muscle can generate its maximum force, of the contractile element of the Hill-models were estimated
c) Other equations were used for the moment arm and muscle length to better resemble literature

The total ankle reaction torque, T_{mod} [Nm], applied by the ankle to the manipulator was modeled and described by:

$$T_{mod}(t) = I\ddot{\theta}(t) + T_{tri}(t) - T_{tib}(t) + T_{grav}(\theta) \quad \text{(A3.1)}$$

where t is the independent time variable [s], $I\ddot{\theta}(t)$ the ankle angular acceleration [rad/s^2], I the inertia of ankle plus footplate [kg.m^2], T_{tri} the torque generated by the plantar flexion muscles (*tri:* SL, GL, GM) or triceps surae [Nm], T_{tib} the torque generated by the dorsiflexion muscle (*tib:* TA) [Nm], and T_{grav} the torque due to gravity [Nm].

Muscle torques for *tri* and *tib* muscle were described by:

$$T_m(\theta,t) = (F_{elas,m}(l) + F_{act,m}(v,l,\alpha))r_m(\theta) \quad \text{(A3.2)}$$

with $F_{elas,m}$ the elastic force of the parallel connective tissues [N/m], $F_{act,m}$ the active or "reflexive" muscle forces and $r_m(\theta)$ the angle dependent moment arm [m] of the tendon:

$$r_{tri}(\theta) = -0.0104 * \theta + 0.0480 \quad \text{(A3.3)}$$

$$r_{tib}(\theta) = 0.0171 * \theta + 0.0393 \quad \text{(A3.4)}$$

Muscle length (l_m) was obtained from its muscle moment arm (r_m) from *tri* and *tib* using data from literature[3;4]

$$l_{tri} = -1.67 * r_{tri}(\theta) + 0.118 \quad \text{(A3.5)}$$

$$l_{tib} = -1.56 * r_{tib}(\theta) + 0.136 \quad \text{(A3.6)}$$

Inertia of ankle plus footplate was modeled as a point mass m [kg] at distance l_a (fixed at 0.10 m) from the center of rotation, i.e. $I = ml_a^2$ [kg.m^2]. Torque due to gravity equals:

$$T_{grav} = mgl_a \cos(\theta - \theta_{fgnd}) \quad \text{(A3.7)}$$

Where g is the gravitational acceleration (g = 9.8 m/s^2). θ_{fgnd} represents the angle of the foot with respect to the horizontal (ground) at zero degrees ankle angle [rad] using the anatomical reference angle.

The elastic components were modeled as follows:

$$F_{elas,m}(t) = e^{k_m(l_m(t) - l_{p,slack,m})} \quad \text{(A3.8)}$$

Where k_m is the stiffness coefficient of the muscle and $l_{p,slack,m}$ the slack length of the connective tissue. Muscle connective tissue under tension exhibits relaxation or force decrease[5-7], which is modeled by a first order filter, according to:

$$F_{elas,m}(s) = \frac{\tau_{rel}s+1}{\tau_{rel}s+1+k_{rel}} F_{elas,m}(s) \quad \text{(A3.9)}$$

with τ_{rel} the tissue relaxation time constant and k_{rel} the tissue relaxation factor. In the previous version of the ankle model by de Vlugt et al.[1] tissue relaxation was approximated by a viscous damper.

For clinical comparison between subjects, peripheral tissue stiffness, K_{joint}, was calculated at a unique joint angle (θ_{comp}) for all subjects and patients. This angle was set at zero degrees (foot perpendicular to the lower leg).

$$K_{\text{joint,m}} = k_m e^{k_m(l_{m,comp} - l_{p,slack})} r_m^2(\theta_{comp}) \quad \text{for } \theta_{\text{comp}} = 0° \quad \text{(A3.10)}$$

where $l_{m,comp}$ is the muscle length at θ_{comp}. Eq. (A3.10) was obtained by differentiation of Eq. (A3.8) with respect to muscle length and multiplied by the squared moment arm. The total tissue stiffness was derived by summation of the stiffness from both muscles:

$$K_{jo\,\mathrm{int}} = K_{jo\,\mathrm{int},tri} + K_{jo\,\mathrm{int},tib} \tag{A3.11}$$

Neural muscle activity for *tri* and *tib* due to stretch reflexes was estimated from corresponding EMG signals according to:

$$U_{tri}(t) = G_{SOL} EMG_{SOL}(t) + G_{GL} EMG_{GL}(t) + G_{GM} EMG_{GM}(t) \tag{A3.12}$$

$$U_{tib}(t) = G_{TA} EMG_{TA}(t) \tag{A3.13}$$

with U the excitation input to the muscle model (1/Volt) of the muscle serving as input to the Hill-type muscle model; G the dimensionless EMG weight scaling factors and EMG the activity of each muscle.

The neural excitations of both muscles were filtered with a linear second order filter to describe the activation process of a contracted muscle[1]:

$$\alpha_m(s) = \frac{\omega_0^2}{s^2 + 2\beta_m\omega_0 s + \omega_0^2} U_m(s) \tag{A3.14}$$

α_m is the dimensionless active state of the muscle m, $\omega_0 = 2\pi f_{0,m}$ the cut off frequency of the activation filter, s the Laplace operator denoting the first time derivative, β_m the relative damping and $U_m(s)$ the modeled neural muscle activity.

The Hill-type muscle model was used to compute the muscle force from the active state and the muscle length and velocity according to:

$$F_{act,m} = f_v(v_m) f_l(l, l_{opt,m}) \alpha_m \tag{A3.15}$$

with f_v the force-velocity relationship and f_l the force-length relationship. The optimal muscle lengths ($l_{opt,m}$) were estimated by the model and used to derive the force-length relationships by

$$f_l = e^{-\left(l_m - l_{opt,m}\right)^2 / wfl,m} \quad \text{(A3.16)}$$

With $w_{fl,m}$ a shape factor defined as:

$$w_{fl,m} = cf * l_{opt,m}{}^2 \quad \text{(A3.17)}$$

with *cf* the shape parameter of the force-length relationship with value 0.1 to resemble the force-generating range of the muscles.

By introducing the optimal muscle length, the active component was uncoupled from the passive component, i.e. the slack length of the muscle which is often assumed to be equal to the optimal muscle length[8-10].

References

(1) de Vlugt E, de Groot JH, Schenkeveld KE, Arendzen JH, van der Helm FC, Meskers CG. The relation between neuromechanical parameters and Ashworth score in stroke patients. *J Neuroeng Rehabil* 2010;7:35.

(2) Sloot LH, van der Krogt MM, de Gooijer-van de Groep KL, Van Eesbeek S, de Groot JH, Buizer AI et al. The validity and reliability of modelled neural and tissue properties of the ankle muscles in children with cerebral palsy. Gait Posture . 2015.

(3) Maganaris CN, Baltzopoulos V, Sargeant AJ. Changes in Achilles tendon moment arm from rest to maximum isometric plantarflexion: in vivo observations in man. *J Physiol* 1998;510 (Pt 3):977-985.

(4) Maganaris CN. Imaging-based estimates of moment arm length in intact human muscle-tendons. *Eur J Appl Physiol* 2004;91:130-139.

(5) Magnusson SP, Simonsen EB, Dyhre-Poulsen P, Aagaard P, Mohr T, Kjaer M. Viscoelastic stress relaxation during static stretch in human skeletal muscle in the absence of EMG activity. *Scand J Med Sci Sports* 1996;6:323-328.

(6) McNair PJ, Dombroski EW, Hewson DJ, Stanley SN. Stretching at the ankle joint: viscoelastic responses to holds and continuous passive motion. *Med Sci Sports Exerc* 2001;33:354-358.

(7) Bressel E, McNair PJ. The effect of prolonged static and cyclic stretching on ankle joint stiffness, torque relaxation, and gait in people with stroke. *Phys Ther* 2002;82:880-887.

(8) Winters JM. An improved muscle-reflex actuator for use in large-scale neuro-musculoskeletal models. *Ann Biomed Eng* 1995;23:359-374.

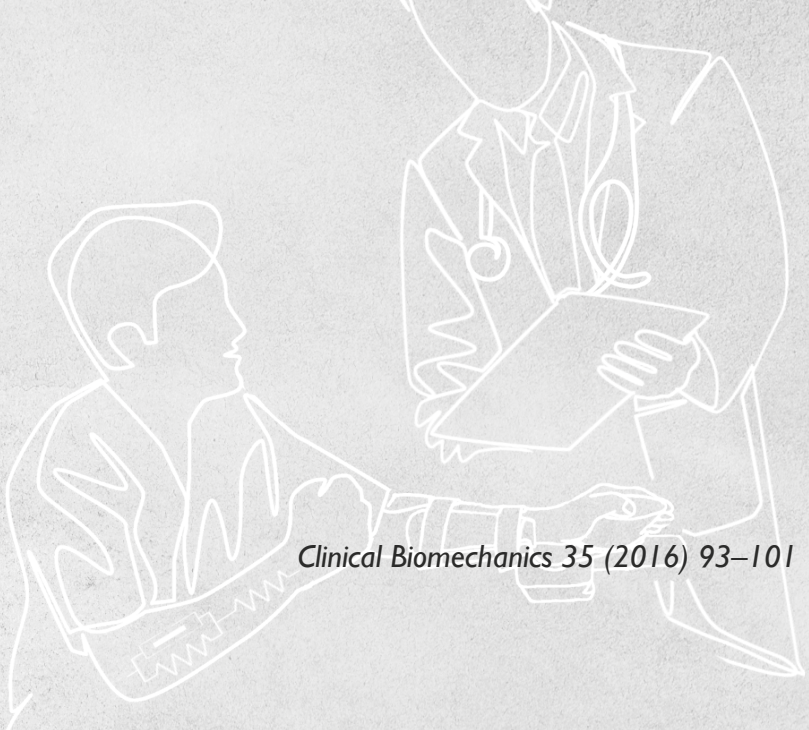
(9) Thelen DG. Adjustment of muscle mechanics model parameters to simulate dynamic contractions in older adults. *J Biomech Eng* 2003;125:70-77.

(10) de Vlugt E, de Groot JH, Wisman WH, Meskers CG. Clonus is explained from increased reflex gain and enlarged tissue viscoelasticity. *J Biomech* 2011.

CHAPTER 4

Estimation of tissue stiffness, reflex activity, optimal muscle length and slack length in stroke patients using an electromyography driven antagonistic wrist model

Authors:
Karin L. de Gooijer-van de Groep, Erwin de Vlugt,
Hanneke J. van der Krogt, Áróra Helgadóttir, J. Hans Arendzen,
Carel G.M. Meskers, Jurriaan H. de Groot



Clinical Biomechanics 35 (2016) 93–101

Abstract

About half of all chronic stroke patients experience loss of arm function coinciding with increased stiffness, reduced range of motion and a flexed wrist due to a change in neural and/or structural tissue properties. Quantitative assessment of these changes is of clinical importance, yet not trivial. The goal of this study was to quantify the neural and structural properties contributing to wrist joint stiffness and to compare these properties between healthy subjects and stroke patients.

Stroke patients (n=32) and healthy volunteers (n=14) were measured using ramp-and-hold rotations applied to the wrist joint by a haptic manipulator. Neural (reflexive torque) and structural (connective tissue stiffness, optimal muscle lengths and slack lengths of connective tissue) parameters were estimated using an electromyography driven antagonistic wrist model. Kruskal-Wallis analysis with multiple comparisons was used to compare results between healthy subjects, stroke patients with modified Ashworth score of zero and stroke patients with modified Ashworth score of one or more.

Stroke patients with modified Ashworth score of one or more differed from healthy controls (P<0.05) by increased tissue stiffness, increased reflexive torque, decreased optimal muscle length and decreased slack length of connective tissue of the flexor muscles.

Non-invasive quantitative analysis, including estimation of optimal muscle lengths, enables to identify neural and non-neural changes in chronic stroke patients. Monitoring these changes in time is important to understand the recovery process and to optimize treatment.

Introduction

Movement disorders of central neurological origin, like stroke and cerebral palsy, are characterized by increased resistance to imposed movement in the relaxed condition. Increased joint stiffness can be of neural origin (hyperreflexia, "spasticity") and/or non-neural, structural origin (altered tissue viscoelastic properties, "contracture")[1;2]. Separation of joint stiffness into neural and non-neural contributions has gained much attention recently, both from technical and clinical research, resulting in new and promising instrumented methods[2;3]. The separation of joint stiffness into different components is important for treatment selection aiming to improve joint dexterity. In case of suspected neural origin, botulinum toxin may be administered[4;5], while in case of suspected non-neural origin patients may benefit from corrective casting, splinting or surgical lengthening[6-8]. The use of an instrumented joint manipulator and an electromyography driven biomechanical model was successfully used previously to quantitatively discriminate joint stiffness into contributions from connective tissue viscoelasticity and stretch reflex activity in the ankle of patients with stroke[9] and cerebral palsy[10;11].

About half of all stroke survivors experience loss of arm function[12;13] often due to a flexed position of the wrist at the affected side due to developing contractures at about 0.5 degrees per week in the first 8 months post-stroke[14]. The origin of these contractures is not fully clear, but may be the result of reduced number of sarcomeres in series[15-18] and/or shortened optimal sarcomere length[17], increased stiffness of the extracellular matrix[18], functional immobilization[14;19] and co-activation synergies[20]. Biomechanically, these tissue changes mean a shift in slack length of the connective tissues and/or shift of the muscle force-length curve and a reduction of the optimal muscle length of the flexor muscles, i.e. the length of the muscle where it generates highest forces.

In the acute and sub-acute phase post-stroke, quantification of neural and non-neural contributors to joint stiffness, including optimal muscle length and slack length of connective tissue, could help understanding the mechanism of (poor) recovery after stroke and characterization of changes over time using longitudinal observations[21;22]. Also the effect of therapies, like botulinum toxin, on the neural and non-neural parameters is not yet understood and should be measured to evaluate and optimize treatment[23].

The goal of this study was to quantify the neural and non-neural contributions to wrist joint stiffness from both flexor and extensor muscles in a cohort of chronic stroke patients. The current model is an extended version of a previous ankle model[9] now including an antagonistic pair of muscle elements to allow for property analysis of both wrist flexor and extensor muscle groups. Three demands were imposed to the model: The structure of the model should represent the (non-linear) joint physiology, the predicted torques should resemble the measured torques and the parameters should be sensitive to discriminate clinical different patients from healthy subjects. Optimal muscle lengths, slack muscle lengths, tissue stiffness and reflexive torques from both flexor and extensor muscles were estimated by model optimization and compared between healthy subjects, stroke patients with a modified Ashworth score of 0 (MAS = 0) and stroke patients with modified Ashworth score of one or more (MAS ≥ 1). We hypothesized an increase in tissue stiffness and reflexive torque and decrease of optimal muscle length and slack length of connective tissue of the flexor muscles in chronic stroke patients with modified Ashworth score of one or more (MAS ≥ 1). We addressed the validity and agreement of the method.

Methods

Subjects

Instrumented ramp-and-hold (RaH) measurements at the wrist at rest were performed as part of the EXPLICIT-stroke study[21;24;25]. Exclusion criteria were neurological deficiencies additional to stroke, (prior) orthopedic problems in hand or shoulder and inability to comply with the protocol. Patients were measured on two occasions within a month. Healthy volunteers were measured as a reference group. The study was approved by the medical ethics committee of the Leiden University Medical Center. All participants gave their written informed consent prior to the experimental procedure. Measurements from fourteen healthy volunteers (mean age 49.4, SD 15.1 years), 21 chronic stroke patients with MAS = 0 (mean age 60.4, SD 13.1 years) and 11 chronic stroke patients with MAS ≥ 1 (mean age 54.4, SD 12.7 years) were analyzed in this study. Subject characteristics are provided in Table 4.1.

Table 4.1: *Subject characteristics*[25]

	Healthy volunteers	**Chronic patients MAS = 0**	**Chronic patients MAS ≥ 1**
	(n=14)	**(n = 21)**	**(n = 11)**
Age (years) (SD)	49.4 (15.1)	60.4 (13.1)	54.5 (12.7)
Men (n) (%)	9 (64%)	10 (48%)	3 (27%)
Right side dominant (n) (%)	13 (93%)	21 (100%)	8 (73%)
Measured side dominant (n) (%)	14 (100%)	10 (48%)	4 (36%)
Time between measurements (days) (SD)	27 (21)	18 (7)	29 (17)
Time after stroke (months) (SD)	-	30 (27.6)	53 (34.4)
Age at moment of stroke (years) (SD)	-	58 (13.1)	50 (14.5)
Passive range of motion deg,(median min;max)	138 (118; 148)	132 (100; 151)	100 (42; 133)

Instrumentation

The subjects were seated with their shoulder relaxed and elbow flexed in approximately 90°. A haptic wrist manipulator (Wristalyzer, 1 degree of freedom (dorsi- and plantar flexion), Moog, Nieuw Vennep, the Netherlands) was used (Figure 4.1). Forearm and hand were strapped to a cuff and handle respectively using Velcro straps. The rotation axis of the wrist joint was aligned visually to the rotation axis of the handle. Handle rotation was driven by a vertically positioned servo motor (Parker SMH100). Positive direction was assigned to flexion movement and extension torque. Muscle activation was recorded by bipolar surface electrodes (electromyography, EMG) using a Delsys Bagnoli 8 system (Delsys Inc., Boston MA, USA). Two bipolar electrodes were placed on the flexor carpi radialis (FCR) and two on the extensor carpi radialis (ECR) in order to have a good representation for the FCR and ECR activation[26;27]. EMG signals were sampled at 2048 Hz, online band pass filtered (20-450 Hz), rectified and low pass filtered (20 Hz, 3rd order Butterworth) to obtain the EMG envelope. The minimal EMG value (average of moving window of 0.06 sec) was subtracted from the total EMG to ensure

noise was minimal in the data. Wrist torque and joint angle were recorded at 2048 Hz and filtered with the same 20 Hz low pass 3rd order Butterworth filter.

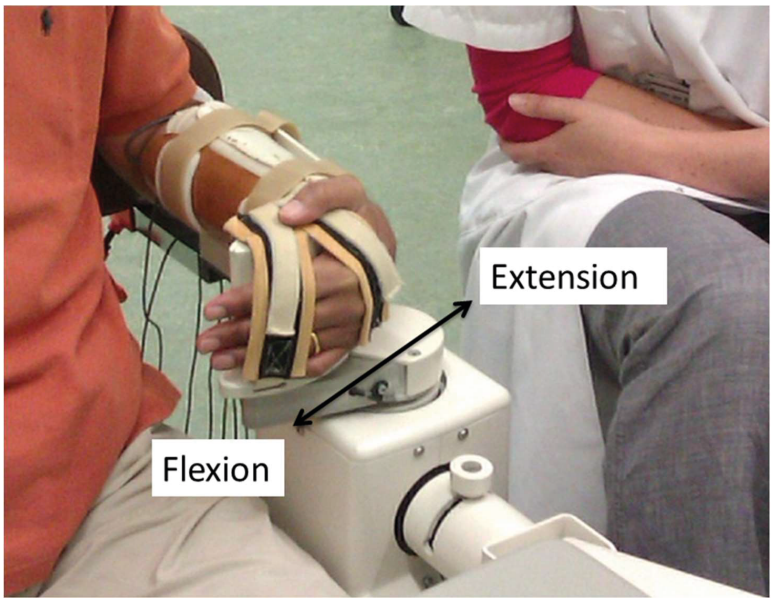


Figure 4.1: *Experimental setup. The forearm and hand of the subject were fixed to the manipulator (Wristalyzer® by MOOG, the Netherlands). Ramp-and-hold rotations in flexion and extension were imposed to the wrist while the subject was instructed to remain relaxed and not react to the rotations. Wrist joint torque, angle and EMG of the FRC and ECR muscles were recorded.*

Measurement protocol

Measurements were performed on the right wrist in healthy subjects and on the impaired wrist in patients. The range of motion (RoM) was determined as the difference between maximal flexion and extension angle resulting from an imposed slow changing torque ranging between 2 Nm (extension torque) and –2 Nm (flexion torque). Subsequently, RaH rotations were imposed onto the wrist at a constant velocity over the full RoM. Two RaH trials were imposed per measurement. Each trial contained a fast ramp in 1 second in extension or flexion direction (named “extension fast” or “flexion fast”), two slow ramps in the opposite direction and three hold periods in between the ramps in which the position of the wrist stayed the same (Figure 4.2). The directions of the ramps in the second trial were opposite to the first trial. The individually determined RoM in combination with the duration of the ramp (1 second)

determined the velocity of the imposed perturbations. Subjects were asked to remain relaxed during the entire experiment and not to react to the wrist movement.

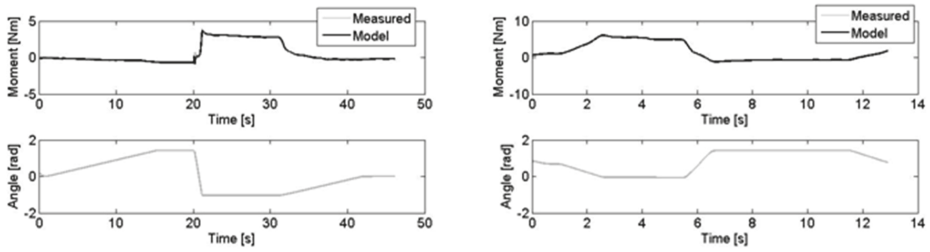


Figure 4.2: *Example of imposed angular rotation (bottom) and torque response with model fit (top row) for a healthy subject (left, "extension fast", VAF=99.6%) and stroke subject with MAS=3 (right, "flexion fast", VAF=99.8).*

Model description

A biomechanical EMG driven antagonistic muscle model was used to predict wrist torque from wrist angle and EMG. The model was based on the ankle model from de Vlugt et al.[9] and extended with a second Hill-type model to describe the passive and active force of the antagonist muscles.

Wrist joint stiffness is described by:

$$T_{mod}(t) = I\ddot{\theta}(t) + T_{ext}(t) - T_{flex}(t) \qquad (4.1)$$

where t is the independent time variable [s], T_{mod} the modeled wrist reaction torque [Nm], $\ddot{\theta}(t)$ the wrist angular acceleration [rad/s^2], I the inertia of wrist and handle [kg.m^2], T_{ext} the torque generated by the extensor muscles [Nm] and T_{flex} the torque generated by the flexor muscles [Nm].

Muscle torques (T_m) for extensor and flexor muscle are described by:

$$T_m(\theta,t) = (F_{elas,m}(l) + F_{act,m}(v_m, l_m, \alpha_m))r_m(\theta) \qquad (4.2)$$

with $F_{elas,m}$ the elastic force of the parallel connective tissues [N], $F_{act,m}$ the active or "reflexive" muscle forces [N] according to the Hill-type model, v_m the muscle lengthening velocity [m/s], l_m the muscle length [m], α_m the active state [-] and $r_m(\theta)$ the angle dependent moment arm [m] of the tendon.

The elastic components for the extensor and flexor muscles were modeled as follows:

$$F_{elas,m}(t) = e^{k_m(l_m(\theta)-l_{p,slack,m})} \tag{4.3}$$

Where k_m is the estimated stiffness coefficient of the muscle and $l_{p,slack,m}$ the estimated slack length of the connective tissue. Muscle length l_m for FCR and ECR equals:

$$l_{FCR} = l_{FCR,0} - r_{FCR}(\theta) * \theta \tag{4.4}$$

$$l_{ECR} = l_{ECR,0} + r_{ECR}(\theta) * \theta \tag{4.5}$$

Where l_{FCR} and l_{ECR} are the lengths of the muscle at each position θ and $l_{FCR,0}$ and $l_{ECR,0}$ the muscle length at zero degrees wrist angle position (handle in line with forearm). r_m is the moment arm defined by Ramsay et al.[28].

The Hill-type muscle model was used to compute the muscle force from the active state and the muscle length and velocity according to:

$$F_{act,m} = f_v(v_m) f_l(l, l_{opt,m}) \alpha_m \tag{4.6}$$

with f_v the force-velocity relationship and f_l the force-length relationship.

The optimal muscle lengths ($l_{opt,m}$) were estimated using the model and used to derive the force-length relationships by

$$f_l = e^{-\left(l_m - l_{opt,m}\right)^2 / w_{fl,m}} \quad (4.7)$$

With $w_{fl,m}$ a shape factor.

The complete model is described in the Appendix 4.

The modeled force-length and force-velocity characteristics are shown in Figure 4.3 together with the modeled tissue and neural forces. In estimating the optimal muscle lengths, the active filament overlap component was decoupled from the passive component, i.e. the slack length of the muscle which is often assumed to be equal to the optimal muscle length[29-31] was decoupled. The parameters of the wrist model that were optimized including the initial values and constraints are listed in Table 4.2.

Table 4.2: *Estimated model parameters and optimization parameters.*

Model wrist	**Description**	**Initial value and [Min Max] of optimization**			
M	Mass (kg)	2	[0.5-5]		
k_{ext}, k_{flex}	Stiffness coefficients (1/m)	240	[10 800]	230	[10 800]
$l_{p,slack,ext}$, $l_{p,slack,flex}$	Slack lengths of connective tissue (m)	0.06	[-0.1 0.1]	0.04	[-0.1 0.1]
G_{ext}, G_{flex}	EMG weighting factors (-)	$1*10^4$	[$1*10^0$ $1*10^{11}$] (both muscles)		
f_0	Activation cutoff frequency (Hz)	0.2	[0.01 10]		
$l_{opt,ext}$, $l_{opt,flex}$	Optimal muscle lengths (m)	0.070	[0.04 0.11]	0.063	[0.04 0.11]
tau_{rel}	Tissue relaxation time constant (s)	0.9	[0 10]		
k_{rel}	Tissue relaxation factor (-)	1	[0 50]		
12	(Number of parameters)				

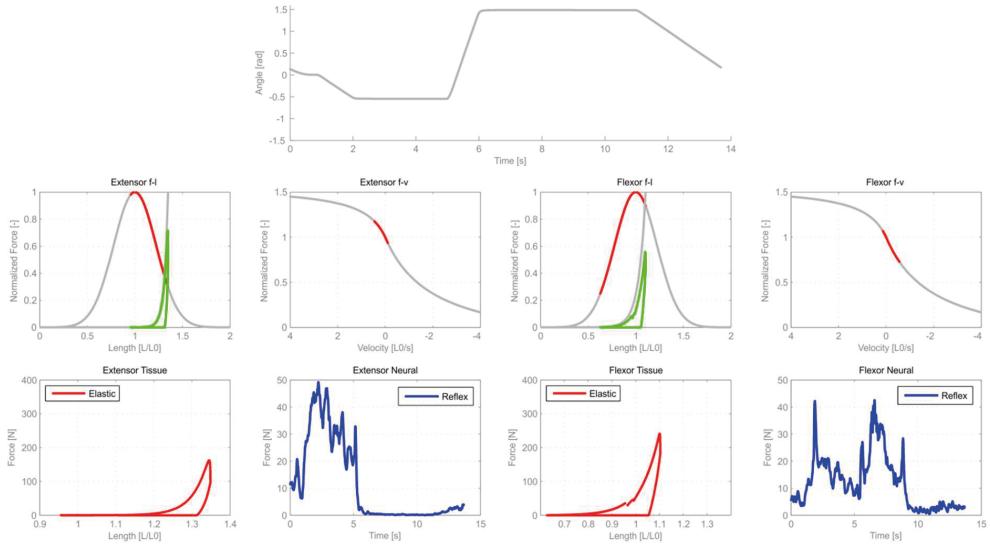


Figure 4.3: *Example of model characteristics of a stroke patient (MAS = 0). Top panel: applied movement, second row: normalized force-length and force-velocity curves of the extensor (left) and flexor (right) muscles (grey lines) including the perturbed length and velocity domains by the red and green intervals. Bottom row: Tissue and neural forces from the extensor (left) and flexor (right) muscles.*

The predicted model torque (T_{mod}) was fitted to the measured wrist torque (T_{meas}), except for the first second of the data to ensure data quality. Model parameters were estimated for the complete movement by minimizing the quadratic difference (error function) between the measured and predicted wrist torque using a non-linear least-square optimization algorithm (steepest descent, Matlab function lsqnonlin).

The main estimated outcome measures used to characterize subjects were tissue stiffness at joint level (K_{joint}), optimal muscle length ($l_{opt,m}$), slack muscle length ($l_{p,slack,m}$) and the reflexive torque (T_{reflex}) determined for both the extensor and flexor muscle groups. The estimated reflexive torque was calculated by using the root mean square of the active muscle torque[9]. Tissue stiffness at joint level (K_{joint}) was derived from the passive force-length relationship, see Appendix 4. For clinical comparison between subjects, K_{joint}, was compared at the same wrist

angle (θ_{comp}) for all subjects. This angle was chosen at zero degrees, i.e. where the handle is in line with the forearm.

Repeated measures were averaged for each subject in order to be able to compare groups of subjects.

Simulation and analysis was performed in Matlab (The Mathworks Inc., Natick MA).

Validity and agreement

Model validity was assessed using the standard error of the mean (SEM) and variance accounted for (VAF). Validity of the measurements was determined by systematic error assessment. Agreement of measurement[32] was determined by the minimal detectable change (MDC) and was used to assess clinical potential to discriminate pathological deviating parameters from normal values.

Model fit and parameter confidence

The standard error of the mean (SEM) represents the parameter confidence and is based on the sensitivity (first and second partial derivatives) of each parameter to the error function (Jacobian and Hessian respectively)[9;33]. High sensitivity, indicated by low SEM values, means that the parameter has substantial contribution to the error function. Model fit was indicated by the torque variance accounted for (VAF):

$$VAF = \left(1 - \frac{\sum\left((T_{meas}(t) - T_{mean}(t)) - (T_{\mathrm{mod}}(t) - T_{mean}(t))\right)^2}{\sum (T_{meas}(t) - T_{mean}(t))^2}\right) * 100\% \quad (4.8)$$

The VAF was estimated for each trial. Estimated torques with a VAF less than 98% were disregarded from group analysis.

Assessment of systematic error

A Wilcoxon signed rank test with significant level 0.05 was used to determine systematic errors between the measurements of two different visits.

Clinical potential

Using post-hoc analysis based on variance (Levene's test) we observed significant higher parameter variances in stroke patients compared to controls for the tissue stiffness and reflexive torque of the FCR. Conform the analysis of[25] we introduced an a priory subdivision of stroke patients based on MAS.

Kruskal-Wallis one-way analysis of variance with multiple comparisons was used to compare stroke patients with modified Ashworth scores of 0 (MAS = 0) and greater than 0 (MAS ≥ 1) respectively with healthy subjects. The minimal detectable change (MDC)[32;34] with confidence interval of 95% was calculated to identify deviated parameters i.e. parameters that are outside the range of mean value +/- MDC indicating that the observed value was not likely to be due to chance variation. Thus, values above the threshold of mean value +/- MDC were classified as "deviated" and can be used to identify pathological cases.

For statistical analysis IBM SPSS statistics 22 and GraphPad Prism 6 was used.

Results

One patient was unable to comply with the protocol. All other trials (93 in "extension fast" direction and 93 in "flexion fast" direction were used to estimate model parameters, VAF and SEM values (Table 4.3). Twenty trials (10%, 5 (5%) in "extension fast" and 15 (16%) in "flexion fast" direction) were excluded for further analysis based on VAF values below 98% and in one case (1 of 93, "extension fast") the input signal was corrupt. In only one (out of 45) subject, the parameters could not be estimated because the patient had low VAF values in both movement direction and for both trials. From all other subjects, through repeated trials in flexion and extension, data were available to estimate the relevant parameters. In total data from 14 healthy subjects and 30 stroke were used for further analysis. Low VAF values may have originated from experimental artefacts e.g. poor fixation or misalignment or voluntary interaction with the passive protocol.

Table 4.3: *Model parameters (estimated value and standard error of the mean (SEM)) for all healthy subjects (A), stroke patients with MAS = 0 (B) and stroke patients with MAS ≥ 1(C).*

A

Parameter	Estimated Value*		SEM*	
	Extension fast	Flexion fast	Extension fast	Flexion fast
m (kg)	0.89 (0.65-1.1)	0.96 (0.73-1.1)	0.012 (0.0094-0.016)	0.015 (0.010-0.019)
k_{ext} (1/m)	206 (164-313)	307 (227-441)	0.012 (0.0059-0.019)	0.023 (0.013-0.037)
k_{flex} (1/m)	211 (162-265)	218 (205-288)	0.0057 (0.0037-0.012)	0.0059 (0.0043-0.0097)
$l_{p,slack,ext,}$ (m)	0.066 (0.058-0.072)	0.072 (0.065-0.076)	0.0045 (0.0028-0.0066)	0.0047 (0.0027-0.0082)
$l_{p,slack,flex}$ (m)	0.048 (0.038-0.052)	0.047 (0.043-0.055)	0.0039 (0.0032-0.0072)	0.0044 (0.0026-0.0086)
$l_{opt,ext}$ (m)	0.057 (0.050-0.066)	0.064 (0.054-0.072)	0.0066 (0.0031-0.025)	0.017 (0.0054-0.38)
$l_{opt,flex}$ (m)	0.067 (0.051-0.078)	0.070 (0.060-0.090)	0.0083 (0.0050-0.020)	0.023 (0.0077-0.093)
Tau_{rel} (s)	2.1 (0.79-3.5)	1.6 (0.74-4.0)	0.028 (0.010-0.058)	0.052 (0.018-0.14)
k_{rel} (-)	0.65 (0.48-1.3)	1.1 (0.64-2.2)	0.0098 (0.0054-0.019)	0.022 (0.0086-0.050)
G_{ext} (-)	5676 (1858-17038)	1756 (201-8411)	0.019 (0.0070-0.22)	0.025 (0.0041-0.27)
G_{flex} (-)	15192 (5280-62793)	35866 (4764-112308)	0.071 (0.021-0.16)	0.22 (0.042-0.94)
f_0 (Hz)	0.19 (0.062-0.52)	0.19 (0.072-0.67)	0.012 (0.0039-0.028)	0.019 (0.0042-0.067)

* median, 25-75 percentile

B

Parameter	Estimated Value*		SEM*	
	Extension fast	Flexion fast	Extension fast	Flexion fast
m (kg)	1.4 (1.0-2.0)	1.1 (0.72-1.6)	0.040 (0.022-0.052)	0.034 (0.021-0.053)
k_{ext} (1/m)	207 (155-253)	244 (207-287)	0.019 (0.011-0.040)	0.025 (0.014-0.034)
k_{flex} (1/m)	204 (171-235)	215 (198-280)	0.010 (0.008-0.016)	0.011 (0.0076-0.019)
$l_{p,slack,ext,}$ (m)	0.065 (0.056-0.070)	0.067 (0.062-0.073)	0.0092 (0.0050-0.016)	0.0084 (0.0053-0.013)
$l_{p,slack,flex}$ (m)	0.046 (0.040-0.050)	0.048 (0.042-0.055)	0.0098 (0.0055-0.013)	0.0076 (0.0048-0.014)
$l_{opt,ext}$ (m)	0.064 (0.053-0.084)	0.068 (0.058-0.095)	0.026 (0.011-0.11)	0.024 (0.012-0.14)
$l_{opt,flex}$ (m)	0.059 (0.050-0.069)	0.064 (0.056-0.11)	0.0098 (0.0051-0.045)	0.022-0.0079-0.18)
Tau_{rel} (s)	0.87 (0.57-1.2)	0.69 (0.47-1.5)	0.026 (0.012-0.037)	0.019 (0.014-0.060)
k_{rel} (-)	0.95 (0.66-1.9)	1.3 (0.66-2.2)	0.025 (0.016-0.050)	0.037 (0.012-0.068)
G_{ext} (-)	3285 (550-11671)	2147 (668-8556)	0.031 (0.0080-0.23)	0.040 (0.0092-0.19)
G_{flex} (-)	12534 (5499-29479)	10440 (5908-32914)	0.050 (0.016-0.27)	0.087 (0.032-1.8)
f_0 (Hz)	0.68 (0.14-1.3)	0.83 (0.22-2.0)	0.080 (0.031-0.12)	0.084 (0.037-0.18)

* median, 25-75 percentile

C

Parameter	Estimated Value*		SEM*	
	Extension fast	Flexion fast	Extension fast	Flexion fast
m (kg)	0.50 (0.50-1.5)	0.97 (0.50-1.4)	0.069 (0.035-0.090)	0.037 (0.026-0.061)
k_{ext} (1/m)	253 (174-303)	220 (167-277)	0.028 (0.011-0.057)	0.023 (0.012-0.028)
k_{flex} (1/m)	167 (130-209)	178 (134-256)	0.0090 (0.0045-0.015)	0.0085 (0.0057-0.013)
$l_{p,slack,ext.}$ (m)	0.066 (0.058-0.073)	0.064 (0.059-0.069)	0.0084 (0.0050-0.016)	0.0085 (0.0049-0.016)
$l_{p,slack,flex}$ (m)	0.027 (0.012-0.035)	0.035 (0.019-0.044)	0.013 (0.0079-0.019)	0.0079 (0.0058-0.015)
$l_{opt,ext}$ (m)	0.059 (0.042-0.11)	0.066 (0.054-0.10)	0.038 (0.015-0.077)	0.045 (0.014-0.18)
$l_{opt,flex}$ (m)	0.054 (0.050-0.060)	0.057 (0.048-0.092)	0.0056 (0.0038-0.011)	0.0096 (0.0048-0.11)
Tau_{rel} (s)	1.1 (0.81-1.9)	1.3 (0.87-2.2)	0.020 (0.014-0.032)	0.030 (0.019-0.043)
k_{rel} (-)	2.2 (1.1-3.5)	1.4 (0.97-2.2)	0.031 (0.020-0.10)	0.029 (0.018-0.042)
G_{ext} (-)	50920 (13062-125798)	12023 (3627-36043)	1.6 (0.35-5.9)	0.42 (0.11-1.8)
G_{flex} (-)	15010 (7010-22856)	15134 (7540-26495)	0.045 (0.017-0.088)	0.044 (0.020-0.81)
f_0 (Hz)	0.72 (0.29-1.0)	0.33 (0.20-0.56)	0.043 (0.022-0.10)	0.042 (0.024-0.071)

* median, 25-75 percentile

Validity and agreement

Model fit and parameter confidence

Estimated values of model parameters and SEM values are presented in Table 4.3 for "extension fast" and "flexion fast" direction for all healthy subjects and stroke patients with MAS = 0 and MAS ≥ 1, i.e. without excluding data based on low VAF values. The median VAF for the "extension fast" were 99.6 (interquartile range (*IQR):* 99.4 - 99.7)%, 99.5 (*IQR:* 98.9-99.8)% and 99.8 (*IQR:* 99.6-99.9)% for healthy subjects, patients with MAS = 0 and patients with MAS ≥ 1 respectively and for "flexion fast" direction 99.3 (*IQR:* 98.1 - 99.7)%, 99.5 (*IQR:* 98.5-99.7)%.and 99.8 (*IQR:* 99.7-99.9)%. Median SEM values were lower than 0.1, except for G_{flex} for "flexion fast" (0.22) for healthy subjects and G_{ext} for both movement directions (1.6 and 0.42) for patients with MAS ≥ 1.

Assessment of systematic error

We observed no significant differences for almost all outcome parameters between the measurements of two different visits based on the Wilcoxon signed rank test, indicating that no systematic error between measurements was present for these parameters. One exception was observed for the reflexive torque T_{reflex} of the flexors in "flexion fast" direction (P=0.022).

Clinical potential

Figure 4.4 shows the results of the comparison between healthy controls and patients with MAS = 0 and MAS ≥ 1 score. Patients with MAS ≥ 1, MAS = 0 and healthy controls significantly differed for tissue stiffness, K_{joint} (P=0.0023 "extension fast"; P=0.0020 "flexion fast"), reflexive torque, T_{reflex} of the flexors (P=0.0011 "extension fast"; P=0.014 "flexion fast"), optimal muscle length, l_{opt} of the flexors (P=0.047 "extension fast") and slack muscle length, $l_{p,slack}$ of the flexors (P=0.0031 "extension fast"; P=0.0177 "flexion fast") and extensors (P=0.020 for "flexion fast"). Multiple comparison showed significant differences between patients with MAS ≥ 1 and healthy controls for K_{joint} (both movement directions), T_{reflex} of the flexors ("extension fast"), l_{opt} of the flexors and $l_{p,slack}$ of the flexors (both movement directions) and extensors. Between MAS = 0 and MAS ≥ 1 significant differences were found for K_{joint} (both movement directions), T_{reflex} of the flexors (both movement directions) and $l_{p,slack}$ of the flexors ("extension fast"). Healthy subjects and stroke patients with MAS = 0 did not differ.

When using the MDC, ten patients had a deviated K_{joint} value (≥3.13 Nm/rad, MDC=1.79 Nm/rad) in "extension fast" direction, eight patients a deviated K_{joint} (≥3.45 Nm/rad; MDC=2.34 Nm/rad) in the "flexion fast" direction and ten patients a deviated T_{reflex} of the flexor muscles (≥ 0.72 Nm; MDC=0.457 Nm) in "extension fast" direction. Almost all of these patients had a MAS ≥ 1: 9 out of 10 for K_{joint} in "extension fast" direction, 8 out of 8 for K_{joint} in "flexion fast" direction and 8 out of 10 for T_{reflex} of the flexors in "extension fast" direction. For the "extension fast" direction 9 out of 11 patients had an increased K_{joint} together with an increased T_{reflex} of the FCR. All patients that showed an increased K_{joint} in the "flexion fast" direction had an increased K_{joint} in the "extension fast" direction.

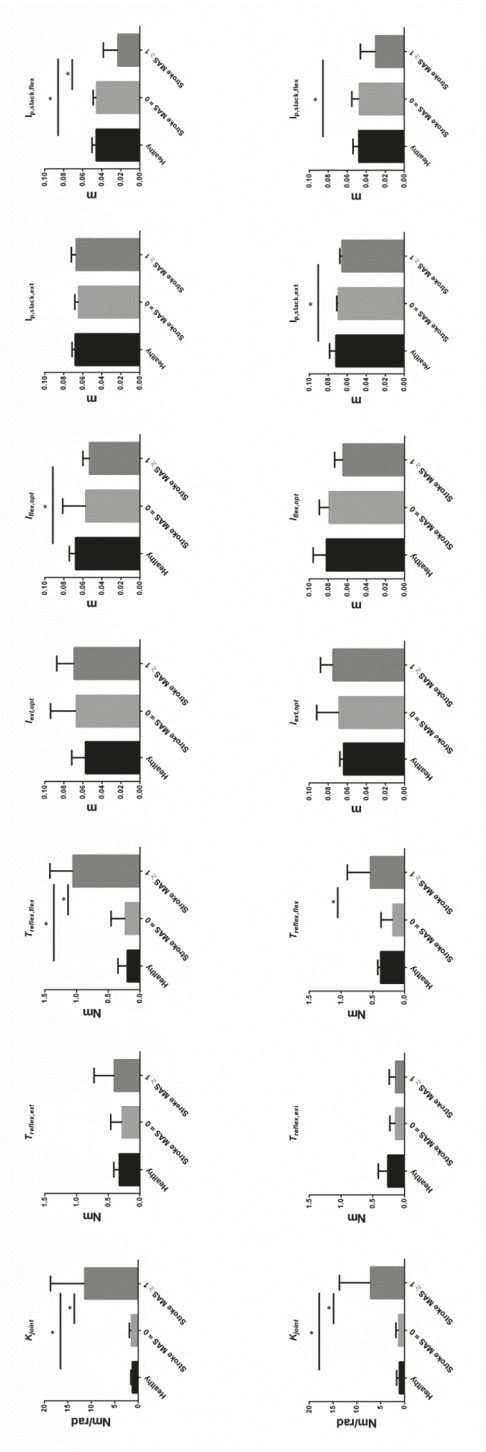


Figure 4.4: *Outcome measures (median with interquartile range) for "extension fast" (top) and "flexion fast" (bottom) direction for healthy subjects and patients with stroke with MAS = 0 and MAS ≥ 1. Asterisks denote significant differences between groups.*

Discussion

Neural and non-neural outcome parameters including optimal muscle length and slack length of connective tissue were quantitatively assessed for the wrist joint in a cohort of chronic stroke patients using an EMG driven antagonistic muscle model. High VAF values and low SEM illustrated the validity of the model approach. Differences in tissue stiffness, reflexive torque, optimal muscle length and slack length of connective tissues between patients with MAS score ≥ 1 and healthy controls demonstrated clinical potential of the method.

Validity and agreement

We advocate the use of an EMG driven model because non-invasive techniques to estimate the physiological parameters are yet lacking. This imposes both the quest for validation and the implicit inability to do so. Three demands were imposed to the model: The structure of the model should represent the (non-linear) joint physiology, the predicted torques should resemble the measured torques and the parameters should be sensitive to discriminate clinical different patients from healthy volunteers.

Model fit and parameter confidence

The model structure was able to describe the relation between joint position and EMG input and the torque output as indicated by the high variance accounted for (VAF) of 98% or higher in 90% of the cases) in the healthy group and both stroke groups.

The model contains 12 parameters. Sensitivity and the absence of parameter redundancy within the model were checked using the standard error of the mean (SEM). The estimation of the model parameters was sufficiently accurate indicated by the low SEM values (Table 4.3).

The SEM for the gain factor G_{flex} for “flexion fast” (0.22) in healthy subjects and the SEM for the gain factor G_{ext} in “extension fast” (1.6) and “flexion fast” (0.42) was largest. These scaling factors are essential in relating muscle activation with torque, but only relevant in case of sufficient (reflexive) activation, explaining the relatively high SEM for G_{flex} for the “flexion fast” direction and G_{ext} for the “extension fast” direction.

Assessment of systematic error

There was no systematic error between measurements at two different visits except for the the reflexive torque, T_{reflex} of the flexors in "flexion fast" direction, possibly due to varying muscle activity in stroke patients. This was confirmed by systematic error assessment between measurements of two different visits for T_{reflex} of the flexors for healthy subjects (P=0.314) and stroke patients (P=0.033) separately.

Clinical potential: Increased neural and structural contributors of joint stiffness in stroke

Patients with MAS ≥ 1 differed from healthy controls in neural (T_{reflex}) and non-neural or structural (K_{joint}, $l_{opt,m}$ and $l_{p,slack,m}$) parameters. The decrease in optimal muscle length (l_{opt}) and muscle slack length ($l_{p,slack}$) of the flexor muscles indicates a shift in the active and passive force-length relationship. Functionally, this structural change implies a flexed joint rest position with a smaller RoM for the impaired wrist, the latter confirmed by a previous study on the same cohort[25] where the authors found significant differences for the passive and active RoM between MAS ≥ 1 and both the MAS = 0 and healthy group. However, van der Krogt et al.[25] could not establish a significant change in the passive angle at rest (angle at zero torque), which could be explained by the influence of active components (e.g. muscle tone) which could have resulted in a rest angle comparable to healthy controls.

When using the MDC, ten patients had a deviating tissue stiffness, K_{joint} and ten patients had a deviating reflexive torque, T_{reflex} of the flexor muscles in "extension fast" direction. Nine of these eleven patients with deviated outcome measures had a MAS score ≥ 1. One patient with MAS ≥ 1 (for flexor muscles) score showed tissue stiffness and reflexive torque values within the range observed in healthy subjects. Differences between patients in outcome measures indicate that there may be a large variety in the neural and non-neural characteristics in stroke patients as also shown by the variation in the MAS.

Nine out of the eleven identified patients had an increased K_{joint} together with an increased T_{reflex} of the flexors. Increased values for both K_{joint} and T_{reflex} are comparable with results found for the ankle where K_{joint} and T_{reflex} were also both increased with elevated MAS[9]. This is in contrast with results in cerebral palsy where a large variation was found between the neural (reflexive torque of triceps surae) and structural (tissue stiffness of triceps surae) contributors of joint stiffness in the ankle[10;11]. This variation in the manifestation of neural and non-neural

contributors suggests a different mechanism in development of increased joint stiffness in stroke and cerebral palsy.

Estimation of optimal muscle length and slack muscle length

Parameters represent physiology of subjects but these in vivo estimated parameters for lumped muscle groups cannot directly be related to muscular parameter values as muscle activation dynamics (slow and fast fibre types) and muscle structure (e.g. pennation angle, muscle and tendon) is not exactly represented. The goal of this model is to systematically discriminate neural contributions from secondary structural changes in connective and contractile tissue observed in patients with upper neuron motor diseases like stroke. The exact value for the outcome measures can be different with literature, but the values and changes need to be of the same order of magnitude.

In literature an optimal fiber length of 0.064-0.099 m was reported for the ECR[35-41] and 0.081 m and 0.059 m for the ECR longus and brevis[42-44]. An optimal fiber length of 0.052-0.080 m was reported for the FCR[35-42;44]. A fiber length of 0.076 m and 0.048 m was reported for the ECRL and ECRB and 0.051 m for the FCR[42]. Our optimal length and slack length were in the same order of magnitude as the parameters in literature (median l_{opt} of 0.061 m and 0.071 m for extensor and flexor muscles respectively; median $l_{p,slack}$ of 0.069 m for the extensors and 0.047 m for the flexors).

The estimated l_{opt} and $l_{p,slack}$ of the flexors of the MAS $\geq$ 1 group were smaller compared to the values for healthy controls indicating that the range the flexor can generate force is reduced and connective tissue is stiffer and shortened. By uncoupling the slack muscle length and optimal muscle length we allow the model to estimate the passive and active characteristics of the muscle independently. Physiologically, the parameters may be related. E.g. longer sarcomeres, i.e. less sarcomeres in series, result in higher passive stiffness through the intrinsic fiber skeletal properties. However, an increase in extracellular matrix stiffness, described in children with cerebral palsy[18], results in a decoupled increase of passive stiffness: the slack muscle length becomes smaller while the optimal muscle length remains unchanged.

Clinical implication

Patients with MAS ≥ 1 can be discriminated from healthy controls and patients with MAS = 0 by neural and non-neural contributors of joint stiffness using the presented bidirectional EMG driven model describing the position and force signals including EMG obtained with a wrist manipulator at high temporal resolution. We now have a method to study longitudinal changes of the neuromuscular system and the effect of treatment, like botulinum toxin injections, on the different neural and non-neural contributors of joint stiffness. Individual stroke patients with deviated tissue stiffness and reflexive torque can be discriminated from healthy controls using the minimal detectable change (MDC). This method gives the clinician the opportunity to monitor the different components of joint stiffness in time and to adjust treatment in individual stroke patients.

The mechanism of muscle shortening after an upper motor neuron disease is not yet understood[16]. Longitudinal observation of the neural and non-neural contributors of joint stiffness, including the estimation of parameters representing the optimal muscle length and slack length of connective tissue, in the acute and sub-acute phase post-stroke and during ageing in children with cerebral palsy, could be of great value to e.g. better understand the mechanism of development of structural changes after a neural lesion.

Limitations

The wrist was rotated over its full RoM in one second to approximate the clinical Ashworth test. Because RoM in patients was generally reduced, movement velocity for the stroke patients was lower as compared to the healthy group. As stretch reflexes are velocity dependent reflexive muscle forces in the patients may even have been underestimated compared to the observations in the healthy group.

Optimal muscle length is a characteristic observable only in the active muscles, while the presented data are measured during a passive task. There was generally sufficient muscle activity present to estimate the optimal muscle length in a valid way as demonstrated by the SEM values (median SEM value <0.05 for optimal muscle length for all conditions). Additional active tasks should be considered to ensure sufficient muscle activation to estimate the optimal muscle length in all cases.

10% of the trials were rejected based on VAFs lower than 98%. In only one (out of 45) subject, the parameters could not be estimated because the patient had low VAF values in both movement direction and for both trials. From all other subjects, in repeated trials in flexion or extension, data became available to estimate the relevant parameters. Repetition of trials is therefore recommended. The constraint of VAF to be larger than 98% in order to approve trials was quite strict to ensure sufficient quality of the model fits. Low VAF values may have originated from experimental artefacts or voluntary interaction with the passive protocol.

In our model the moment arms and muscle lengths at zero degrees wrist angle position of the ECR longus and brevis are averaged which is a simplification of reality[45]. Furthermore, as the torque measured is the result of all extensor and flexor muscles, the modeled extensor and flexor muscle elements are lumped descriptions of the wrist muscles affecting the wrist flexion and extension torques (e.g. extensor carpi ulnaris, flexor carpi ulnaris). The characteristics of the ECR and FCR were used as initial parameter values for the corresponding muscle elements. Pennation angles were not included in the model, i.e. pennation angles were defined zero and consequently muscle and fiber length were defined to be equal. Since pennation angle changes the relationship between muscle length and force, the outcome parameters may be biased by this assumption. However, as this is the case in all subjects, differences in optimal muscle length and slack muscle length, parameterized by $l_{opt,m}$ and $l_{p,slack,m}$ are assumed to represent physiological adaptation of the neuromuscular system and although the model is a simplification of the wrist joint it appeared to be sensitive to evaluate changes after stroke.

Conclusions

The EMG driven model in combination with the applied ramp-and-hold movements in both patients and healthy controls enabled us to estimate parameters representing tissue stiffness, reflexive torques, optimal muscle lengths and slack muscle lengths of connective tissue at the wrist in rest. Patients with an elevated MAS (MAS $\geq$ 1) were distinguished from healthy controls and patients with MAS = 0. Patients with MAS $\geq$ 1 differed from healthy controls through increased tissue stiffness and reflexive torque and reduced optimal muscle length and slack length of flexor connective tissue. The differentiation of joint stiffness into different neural and structural components is essential for individualized treatment selection in patients with upper motor neuron diseases and will be of benefit to follow the disease in time in acute

and sub-acute stroke patients and during ageing in children with cerebral palsy. Validation remains a point of attention in future applications. Next studies will focus on the effect of botulinum toxin treatment in chronic stroke patients and the quantification of joint stiffness during the acute and sub-acute phase of stroke.

Acknowledgments

This research was funded by the Dutch Technology Foundation (STW) (ROBIN project, grant no. 10733), which is part of the Dutch National Organization for scientific research (NWO) and partly funded by the Ministry of Economic Affairs, Agriculture and Innovation, and the Dutch Organization for Health Research and Development ZonMW (Explicit Stroke project, grant no. 890000001).

References

(1) Dietz V, Sinkjaer T. Spastic movement disorder: impaired reflex function and altered muscle mechanics. *Lancet Neurol* 2007;6:725-733.

(2) van der Krogt HJ, Meskers CG, de Groot JH, Klomp A, Arendzen JH. The gap between clinical gaze and systematic assessment of movement disorders after stroke. *J Neuroeng Rehabil* 2012;9:61.

(3) Bar-On L, Molenaers G, Aertbelien E et al. Spasticity and its contribution to hypertonia in cerebral palsy. *Biomed Res Int* 2015;2015:317047.

(4) Sheean G. Botulinum toxin should be first-line treatment for poststroke spasticity. *J Neurol Neurosurg Psychiatry* 2009;80:359.

(5) Gracies JM, Singer BJ, Dunne JW. The role of botulinum toxin injections in the management of muscle overactivity of the lower limb. *Disabil Rehabil* 2007;29:1789-1805.

(6) Thompson AJ, Jarrett L, Lockley L, Marsden J, Stevenson VL. Clinical management of spasticity. *J Neurol Neurosurg Psychiatry* 2005;76:459-463.

(7) Mortenson PA, Eng JJ. The use of casts in the management of joint mobility and hypertonia following brain injury in adults: a systematic review. *Phys Ther* 2003;83:648-658.

(8) Renzenbrink GJ, Buurke JH, Nene AV, Geurts AC, Kwakkel G, Rietman JS. Improving walking capacity by surgical correction of equinovarus foot deformity in adult patients with stroke or traumatic brain injury: a systematic review. *J Rehabil Med* 2012;44:614-623.

(9) de Vlugt E, de Groot JH, Schenkeveld KE, Arendzen JH, van der Helm FC, Meskers CG. The relation between neuromechanical parameters and Ashworth score in stroke patients. *J Neuroeng Rehabil* 2010;7:35.

(10) de Gooijer-van de Groep KL, de Vlugt E, de Groot JH et al. Differentiation between non-neural and neural contributors to ankle joint stiffness in cerebral palsy. *J Neuroeng Rehabil* 2013;10:81.

(11) Sloot LH, van der Krogt MM, de Gooijer-van de Groep KL et al. The validity and reliability of modelled neural and tissue properties of the ankle muscles in children with cerebral palsy. *Gait Posture* 2015.

(12) Parker VM, Wade DT, Langton HR. Loss of arm function after stroke: measurement, frequency, and recovery. *Int Rehabil Med* 1986;8:69-73.

(13) Broeks JG, Lankhorst GJ, Rumping K, Prevo AJ. The long-term outcome of arm function after stroke: results of a follow-up study. *Disabil Rehabil* 1999;21:357-364.

(14) Malhotra S, Pandyan AD, Rosewilliam S, Roffe C, Hermens H. Spasticity and contractures at the wrist after stroke: time course of development and their association with functional recovery of the upper limb. *Clin Rehabil* 2011;25:184-191.

(15) Lieber RL, Friden J. Spasticity causes a fundamental rearrangement of muscle-joint interaction. *Muscle Nerve* 2002;25:265-270.

(16) Lieber RL, Steinman S, Barash IA, Chambers H. Structural and functional changes in spastic skeletal muscle. *Muscle Nerve* 2004;29:615-627.

(17) Gao F, Zhang LQ. Altered contractile properties of the gastrocnemius muscle poststroke. *J Appl Physiol (1985)* 2008;105:1802-1808.

(18) Smith LR, Lee KS, Ward SR, Chambers HG, Lieber RL. Hamstring contractures in children with spastic cerebral palsy result from a stiffer extracellular matrix and increased in vivo sarcomere length. *J Physiol* 2011;589:2625-2639.

(19) Ada L, Canning CG, Low SL. Stroke patients have selective muscle weakness in shortened range. *Brain* 2003;126:724-731.

(20) Hu X, Tong K, Tsang VS, Song R. Joint-angle-dependent neuromuscular dysfunctions at the wrist in persons after stroke. *Arch Phys Med Rehabil* 2006;87:671-679.

(21) Kwakkel G, Meskers CG, van Wegen EE et al. Impact of early applied upper limb stimulation: the EXPLICIT-stroke programme design. *BMC Neurol* 2008;8:49.

(22) Mirbagheri MM, Rymer WZ. Time-course of changes in arm impairment after stroke: variables predicting motor recovery over 12 months. *Arch Phys Med Rehabil* 2008;89:1507-1513.

(23) Kwakkel G, Meskers CG. Botulinum toxin A for upper limb spasticity. *Lancet Neurol* 2015.

(24) Klomp A, van der Krogt JM, Meskers CGM et al. Design of a concise and comprehensive protocol for post stroke neuromechanical assessment. *J Bioengineer & Biomedical Sci* 2012.

(25) van der Krogt HJ, Klomp A, de Groot JH et al. Comprehensive neuromechanical assessment in stroke patients: reliability and responsiveness of a protocol to measure neural and non-neural wrist properties. *J Neuroeng Rehabil* 2015;12.

(26) Instrumented Stretch Reflexes of Flexor Carpi Radialis and Flexor Carpi Ulnaris Muscle. XVIth ISEK Conference; 06 Jun 29; 2006.

(27) Hodson-Tole EF, Loram ID, Vieira TM. Myoelectric activity along human gastrocnemius medialis: different spatial distributions of postural and electrically elicited surface potentials. *J Electromyogr Kinesiol* 2013;23:43-50.

(28) Ramsay JW, Hunter BV, Gonzalez RV. Muscle moment arm and normalized moment contributions as reference data for musculoskeletal elbow and wrist joint models. *J Biomech* 2009;42:463-473.

(29) Winters JM. An improved muscle-reflex actuator for use in large-scale neuro-musculoskeletal models. *Ann Biomed Eng* 1995;23:359-374.

(30) Thelen DG. Adjustment of muscle mechanics model parameters to simulate dynamic contractions in older adults. *J Biomech Eng* 2003;125:70-77.

(31) de Vlugt E, de Groot JH, Wisman WH, Meskers CG. Clonus is explained from increased reflex gain and enlarged tissue viscoelasticity. *J Biomech* 2011.

(32) de Vet HC, Terwee CB, Knol DL, Bouter LM. When to use agreement versus reliability measures. *J Clin Epidemiol* 2006;59:1033-1039.

(33) Ljung L. *System identification - Theory for the user*. Prentice Hall, 1999.

(34) Haley SM, Fragala-Pinkham MA. Interpreting change scores of tests and measures used in physical therapy. *Phys Ther* 2006;86:735-743.

(35) Amis AA, Dowson D, Wright V. Muscle strengths and musculoskeletal geometry of the upper limb. *Eng Med (Berlin)* 1979;8:41-48.

(36) An KN, Hui FC, Morrey BF, Linscheid RL, Chao EY. Muscles across the elbow joint: a biomechanical analysis. *J Biomech* 1981;14:659-669.

(37) Brand PW, Beach RB, Thompson DE. Relative tension and potential excursion of muscles in the forearm and hand. *J Hand Surg Am* 1981;6:209-219.

(38) Winters JM, Stark L. Estimated mechanical properties of synergistic muscles involved in movements of a variety of human joints. *J Biomech* 1988;21:1027-1041.

(39) Cutts A, Alexander RM, Ker RF. Ratios of cross-sectional areas of muscles and their tendons in a healthy human forearm. *J Anat* 1991;176:133-137.

(40) Loren GJ, Shoemaker SD, Burkholder TJ, Jacobson MD, Friden J, Lieber RL. Human wrist motors: biomechanical design and application to tendon transfers. *J Biomech* 1996;29:331-342.

(41) Garner BA, Pandy MG. Estimation of musculotendon properties in the human upper limb. *Ann Biomed Eng* 2003;31:207-220.

(42) Lieber RL, Fazeli BM, Botte MJ. Architecture of selected wrist flexor and extensor muscles. *J Hand Surg Am* 1990;15:244-250.

(43) Murray WM, Buchanan TS, Delp SL. The isometric functional capacity of muscles that cross the elbow. *J Biomech* 2000;33:943-952.

(44) Holzbaur KR, Murray WM, Delp SL. A model of the upper extremity for simulating musculoskeletal surgery and analyzing neuromuscular control. *Ann Biomed Eng* 2005;33:829-840.

(45) Lieber RL, Ljung BO, Friden J. Intraoperative sarcomere length measurements reveal differential design of human wrist extensor muscles. *J Exp Biol* 1997;200:19-25.

Appendix 4: Wrist model

The model structure was based on the ankle model from de Vlugt et al.[1] and adapted to the neuromechanical characteristics of the wrist joint. The following structure aspects were added in the wrist model compared to the ankle model: Optimal muscle length parameters were estimated, the stiffness components were modeled for both flexor and extensor muscles making the model fully bi-directional and tissue relaxation was included. Model parameters are listed in Table 4.2.

Wrist joint stiffness is described by:

$$T_{mod}(t) = I\ddot{\theta}(t) + T_{ext}(t) - T_{flex}(t) \qquad \text{(A4.1)}$$

where t is the independent time variable [s], T_{mod} the modeled wrist reaction torque [Nm], $I\ddot{\theta}(t)$ the wrist angular acceleration [rad/s^2], I the inertia of wrist and handle [kg.m^2], T_{ext} the torque generated by the extensor muscles [Nm] and T_{flex} the torque generated by the flexor muscles [Nm].
Muscle torques (T_m) for extensor and flexor muscle are described by:

$$T_m(\theta,t) = (F_{elas,m}(l) + F_{act,m}(v_m, l_m, \alpha_m))r_m(\theta) \qquad \text{(A4.2)}$$

with $F_{elas,m}$ the elastic force of the parallel connective tissues [N], $F_{act,m}$ the active or "reflexive" muscle forces [N] according to the Hill-type model, v_m the muscle lengthening velocity [m/s], l_m the muscle length [m], α_m the active state [-] and $r_m(\theta)$ the angle dependent moment arm [m] of the tendon.

The ECR and FCR were used as representation of the extensor and flexor muscles. The moment arms [m] of the ECR and FCR muscles are dependent on the angular position of the joint and defined using the equations of Ramsay et al.[2]:

$$r_{FCR}(\theta) = 13.2040 + 1.5995\theta \quad \text{for} \quad \theta > -10^{\circ} \quad [\text{x}10^{-3} m] \qquad \text{(A4.3)}$$

$$r_{ECR,brevis}(\theta) = 13.4337 - 2.1411\theta \text{ for } \theta < 10^{o} \text{ [x10}^{-3} m\text{]} \quad \text{(A4.4)}$$

$$r_{ECR,longus}(\theta) = 11.7166 - 2.2850\theta \text{ for } \theta < 10^{o} \text{ [x10}^{-3} m\text{]} \quad \text{(A4.5)}$$

$$r_{ECR}(\theta) = (r_{ECR,brevis}(\theta) + r_{ECR,longus}(\theta))/2 \quad \text{(A4.6)}$$

The ECR is in fact two separate muscles: the extensor carpi radialis longus and brevis. Since only a combined EMG signal can be measured the extensor moment arm is assumed to be the average of the two separate moment arms. Muscle length equals:

$$l_{FCR} = l_{FCR,0} - r_{FCR}(\theta)\theta \quad \text{(A4.7)}$$

$$l_{ECR} = l_{ECR,0} + r_{ECR}(\theta)\theta \quad \text{(A4.8)}$$

Where l_{FCR} and l_{ECR} are the lengths of the muscle at each position θ and $l_{FCR,0}$ and $l_{ECR,0}$ the muscle length at zero degrees wrist angle position (handle in line with the forearm). The zero muscle lengths are $l_{FCR,0}$ = 6.3 cm and $l_{ECR,0}$ = 7.0 cm (average of ECR longus and brevis, optimal fiber lengths from[3-5]. $r_{FCR}(\theta)\theta$ and $r_{ECR}(\theta)\theta$ are the arc lengths of the tendon that stretches around the joint bone when the joint rotates about angle θ [6]. Positive angles represent flexion, thus the flexor muscles shorten during flexion and the extensor muscles lengthen during flexion, and vice versa for extension.

Inertia of hand and the handle is modeled as a point mass m [kg] at distance l_a (fixed at 0.1 m) from the axis of rotation:

$$I = ml_a^2 \text{ [kg.m}^2\text{]} \quad \text{(A4.9)}$$

The elastic components for the extensor and flexor muscles were modeled as follows:

$$F_{elas,m}(t) = e^{k_m(l_m(\theta) - l_{p,slack,m})} \quad \text{(A4.10)}$$

Where k_m is the estimated stiffness coefficient of the muscle and $l_{p,slack,m}$ the estimated slack length of the connective tissue. Muscle connective tissue under tension exhibits relaxation or force decrease[7-9], which is modeled by a first order filter, according to:

$$F_{elas,m}(s) = \frac{\tau_{rel}s + 1}{\tau_{rel}s + 1 + k_{rel}} F_{elas,m}(s) \qquad \text{(A4.11)}$$

with τ_{rel} the estimated tissue relaxation time constant and k_{rel} the estimated tissue relaxation factor. In the previous version of the model by de Vlugt et al.[1] tissue relaxation was approximated by a viscous damper.

For clinical comparison between subjects, tissue stiffness at joint level, K_{joint}, was compared at the same wrist angle (θ_{comp}) for all subjects. This angle was chosen at zero degrees, i.e. where the handle is in line with the forearm.

$$K_{joint,m} = k_m e^{k_m(l_{m,comp} - l_{p,slack,m})} r_m^2(\theta_{comp}) \quad \text{for } \theta_{comp} = 0 \text{ degrees} \qquad \text{(A4.12)}$$

where $l_{m,comp}$ is the muscle length at θ_{comp}. Eq. (A4.12) was obtained by differentiation of Eq. (A4.10) with respect to muscle length and multiplied by the squared moment arm. The total tissue stiffness at joint level was derived by summation of the stiffness from both muscles:

$$K_{joint} = K_{joint,ext} + K_{joint,flex} \qquad \text{(A4.13)}$$

Neural muscle activity for the extensors and flexors due to stretch reflexes was estimated from corresponding EMG signals according to:

$$U_m(t) = G_m EMG_m(t) \tag{A4.14}$$

with U the excitation input to the muscle model [1/Volt]; G_m the dimensionless EMG weight scaling factor and EMG_m the average of the recorded EMG signal values of both muscle electrodes.

The neural excitations of both muscles were filtered with a linear second order filter to describe the activation process of a contracted muscle[1]:

$$\alpha_m(s) = \frac{\omega_0^2}{s^2 + 2\beta_m\omega_0 s + \omega_0^2} U_m(s) \tag{A4.15}$$

α_m is the dimensionless active state of the muscle, $\omega_0 = 2\pi f_{0,m}$ the estimated cut off frequency of the activation filter, s the Laplace operator denoting the first time derivative and β_m the relative damping.

The Hill-type muscle model was used to compute the muscle force from the active state and the muscle length and velocity according to:

$$F_{act,m} = f_v(v_m) f_l(l, l_{opt,m}) \alpha_m \tag{A4.16}$$

with f_v the force-velocity relationship and f_l the force-length relationship. The optimal muscle lengths ($l_{opt,m}$) were estimated using the model and used to derive the force-length relationships by

$$f_l = e^{-\left(l_m - l_{opt,m}\right)^2 / w_{fl,m}} \quad \text{(A4.17)}$$

With $w_{fl,m}$ a shape factor defined as:

$$w_{fl,m} = cf\, l_{opt,m}^{\ 2} \quad \text{(A4.18)}$$

with *cf* the shape parameter of the force-length relationship with value 0.1 to resemble the force-generating range of the FCR and ECR[10;11]. The maximum shortening velocity was 8 times the optimal muscle length[12], the maximum eccentric force was 1.5 times the isometric force and the isometric force was normalized to 1 because the force had been scaled by the weighting factors G.

References

(1) de Vlugt E, de Groot JH, Schenkeveld KE, Arendzen JH, van der Helm FC, Meskers CG. The relation between neuromechanical parameters and Ashworth score in stroke patients. *J Neuroeng Rehabil* 2010;7:35.

(2) Ramsay JW, Hunter BV, Gonzalez RV. Muscle moment arm and normalized moment contributions as reference data for musculoskeletal elbow and wrist joint models. *J Biomech* 2009;42:463-473.

(3) Murray WM, Buchanan TS, Delp SL. The isometric functional capacity of muscles that cross the elbow. *J Biomech* 2000;33:943-952.

(4) Holzbaur KR, Murray WM, Delp SL. A model of the upper extremity for simulating musculoskeletal surgery and analyzing neuromuscular control. *Ann Biomed Eng* 2005;33:829-840.

(5) Lieber RL, Fazeli BM, Botte MJ. Architecture of selected wrist flexor and extensor muscles. *J Hand Surg Am* 1990;15:244-250.

(6) Lieber RL, Ljung BO, Friden J. Intraoperative sarcomere length measurements reveal differential design of human wrist extensor muscles. *J Exp Biol* 1997;200:19-25.

(7) Magnusson SP, Simonsen EB, Dyhre-Poulsen P, Aagaard P, Mohr T, Kjaer M. Viscoelastic stress relaxation during static stretch in human skeletal muscle in the absence of EMG activity. *Scand J Med Sci Sports* 1996;6:323-328.

(8) McNair PJ, Dombroski EW, Hewson DJ, Stanley SN. Stretching at the ankle joint: viscoelastic responses to holds and continuous passive motion. *Med Sci Sports Exerc* 2001;33:354-358.

(9) Bressel E, McNair PJ. The effect of prolonged static and cyclic stretching on ankle joint stiffness, torque relaxation, and gait in people with stroke. *Phys Ther* 2002;82:880-887.

(10) Garner BA, Pandy MG. Estimation of musculotendon properties in the human upper limb. *Ann Biomed Eng* 2003;31:207-220.

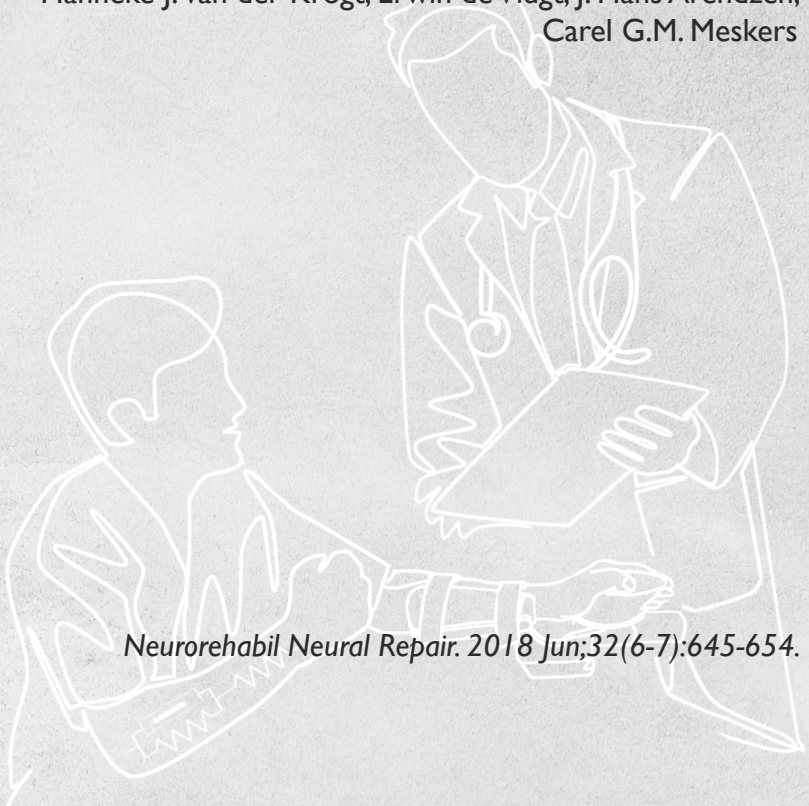
(11) Zajac FE. Muscle and tendon: properties, models, scaling, and application to biomechanics and motor control. *Crit Rev Biomed Eng* 1989;17:359-411.

(12) Thelen DG. Adjustment of muscle mechanics model parameters to simulate dynamic contractions in older adults. *J Biomech Eng* 2003;125:70-77.

CHAPTER 5

Early shortening of wrist flexor muscles coincides with poor recovery after stroke

Authors:
Karin L. de Gooijer-van de Groep, Jurriaan H. de Groot,
Hanneke J. van der Krogt, Erwin de Vlugt, J. Hans Arendzen,
Carel G.M. Meskers



Neurorehabil Neural Repair. 2018 Jun;32(6-7):645-654.

Abstract

The mechanism and time course of increased wrist joint stiffness post-stroke and clinically observed wrist flexion deformity is still not well understood. The components contributing to increased joint stiffness are of neural reflexive and peripheral tissue origin and quantified by reflexive torque and muscle slack length and stiffness coefficient parameters.

To investigate the time course of the components contributing to wrist joint stiffness during the first twenty-six weeks post-stroke in a group of patients, stratified by prognosis and functional recovery of the upper extremity.

36 stroke patients were measured on eight occasions within the first twenty-six weeks post-stroke using ramp-and-hold rotations applied to the wrist joint by a robot manipulator. Neural reflexive and peripheral tissue components were estimated using an electromyography driven antagonistic wrist model. Outcome was compared between groups cross-sectionally at twenty-six weeks post-stroke and development over time was analyzed longitudinally.

At twenty-six weeks post-stroke, patients with poor recovery (ARAT≤9 points) showed a higher predicted reflexive torque of the flexors ($P<.001$) and reduced predicted slack length ($P<.001$) indicating shortened muscles contributing to higher peripheral tissue stiffness ($P<.001$), compared to patients with good recovery (ARAT≥10 points). Significant differences in peripheral tissue stiffness between groups could be identified around week four and five; for neural reflexive stiffness this was the case around week twelve.

We found onset of peripheral tissue stiffness to precede neural reflexive stiffness. Temporal identification of components contributing to joint stiffness after stroke may prompt longitudinal interventional studies to further evaluate and eventually prevent these phenomena.

Introduction

Recovery of motor function of the upper limb after stroke mainly adheres to the first eight weeks post-stroke[1;2]. These early changes are related to underlying mechanisms of spontaneous neurologic repair[3], which is still poorly understood. Most patients with a poor recovery of motor function show increased joint stiffness. The components contributing to increased joint stiffness are of neural reflexive and peripheral tissue origin and quantified by reflexive torque and muscle slack length and tissue stiffness coefficient[4-6], determined by e.g. sarcomere length and collagen composition. The timing of developing increased joint stiffness and contribution of its underlying components post-stroke is not clear[7].

The goal of the current study was to investigate the time course of neural reflexive and peripheral tissue changes in the wrist joint during the first twenty-six weeks post-stroke in three groups of patients, stratified by prognosis and functional recovery of the upper extremity. With a recently developed and validated technique we were able to simulate the wrist torques using muscle activation (electromyography, EMG) and wrist position as input[8;9]. The time course of the contribution of estimated neural reflexes to wrist joint stiffness and the value of the estimated peripheral tissue parameters (muscle slack length and tissue stiffness coefficient) may ultimately explain the development of wrist joint stiffness over time[7;8;10;11]. We hypothesize that stroke patients with poor recovery of motor function of the arm have increased reflexive torque and shortened muscles of the flexor muscles at twenty-six weeks resulting in increased joint stiffness and wrist flexion deformity compared to patients with good recovery. As stroke primarily results in a neural paresis and muscle tissue may respond to muscle state changes caused by altered neural input[4] we presume that neural reflexive changes precede the peripheral tissue changes in the patients with poor recovery.

Knowledge about the time course of changes in the contributors of joint stiffness, i.e. neural reflexes and peripheral tissue stiffness, may significantly contribute to the choice of treatment during the early phase post-stroke and may hand us a key to understand underlying mechanisms of functional recovery.

Methods

Study design

In the multicenter randomized clinical EXPLICIT-stroke trial, the effects of early applied constrained induced movement therapy (CIMT) or EMG triggered neuromuscular stimulation of the finger extensors (EMG-NMS) were compared to usual care on recovery of arm-hand function after stroke[7;12;13]. A cohort of 36 acute patients was recruited within this EXPLICIT-stroke trial[7;12;13] (Dutch Trial register NTR1424, part B3). Inclusion criteria comprised first-ever ischemic stroke in the area of middle cerebral artery, impairment of the arm, age 18-80 year and able to travel to the Leiden University Medical Center (LUMC) or University Medical Center Utrecht (UMCU). Exclusion criteria were previous upper extremity orthopedic limitations on the affected side and insufficient communication.

Patients were assessed for eligibility within a week after stroke. Depending on the prognostic presence of finger extension post-stroke and the National Institutes of Health Stroke Score (NIHSS) item 5a or 5b[7;14;15], patients were initially stratified in two groups. In the first stratum (finger extension ten degrees or larger at the end of the first week post-stroke and a NIHSS score of 1 or 2 on item 5, good prognosis) patients were randomized to receive constrained-induced movement therapy within their usual care programs[16]. In the second stratum (finger extension less than 10 degrees and NIHSS score 3 or 4 on item 5, poor prognosis) patients were randomized to receive electromyography-triggered neuromuscular stimulation of the finger extensors[17] within their usual care programs[16].

Within the measurement framework of EXPLICIT-stroke, patients were measured on eight occasions, i.e. at 1–5, 8, 12, 26 weeks post-stroke. We applied stratification based on the Explicit-stroke study. Therefore, based on both the initial prognosis for functional recovery, i.e. good and poor, and functional outcome at 26 weeks post-stroke, three groups were identified: 1) a GG group of 15 patients with an initially good prognosis for upper extremity motor recovery and showing good recovery at 26 weeks post-stroke, i.e. a score of 10 points or more on the ARAT; 2) a PG group of 12 patients with poor prognosis and good recovery; 3) a PP group of 9 patients with poor prognosis and poor recovery, i.e. a score of 9 points or less on the ARAT at 26 weeks post-stroke.

The study was approved by the medical ethics committee of the LUMC and UMCU. All participants gave their written informed consent prior to the experimental procedure.

Instrumentation and protocol

Subjects were seated upright with the affected arm slightly abducted in the frontal plane. The lower arm was fixed in an arm rest with the elbow at approximately 90 degrees of flexion and the shoulder comfortably relaxed. The hand was fixed into a custom-made handle (Meester Techniek, Leiden, the Netherlands). The wrist joint was aligned to the motor axis of a robot manipulator (Wristalyzer, Moog, Nieuw Vennep, the Netherlands). The robot manipulator delivered precise angular position (rotation) perturbations to the handle via a vertically positioned servomotor (Parker SMH100 series, Parker Hannifin, Charlotte NC, USA) and synchronously recorded the angular position of the handle and torque at the vertical motor axis of the handle, representing the wrist angular position and wrist torque respectively (Figure 5.1)[9:13:14].

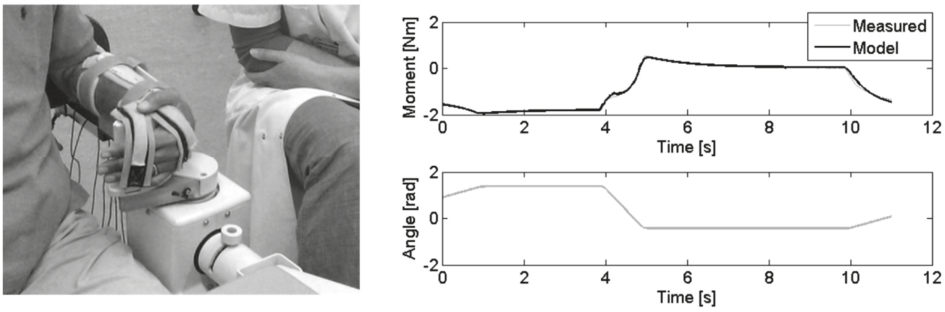


Figure 5.1: *Left: Experimental setup. The forearm and hand of the subject were fixed to the manipulator (Wristalyzer® by MOOG, the Netherlands). Ramp-and-hold rotations in flexion and extension direction (right) were imposed to the wrist while the subject was instructed to remain relaxed and not react to the rotations. Top right: measured torque and model fit; bottom right measured angle.*

Muscle activation was recorded by means of EMG with bipolar surface electrodes using a Delsys Bagnoli 8 system (Delsys Inc., Boston MA, USA). Electrodes were placed on the flexor carpi radialis (FCR) and on the extensor carpi radialis (ECR) muscles respectively. For the FCR, electrodes were placed on the muscle belly at one third of the line originating from the medial epicondyle of the humerus to the radial styloid process and for the ECR, electrodes were placed on the muscle belly at one third of the line originating from the lateral epicondyle of the humerus to the ulnar styloid process. The EMG signals were sampled at 2048 Hz, online band

pass filtered (20–450 Hz), rectified and low pass filtered (20 Hz, 3rd order Butterworth) to obtain the EMG envelope. EMG at rest was subtracted from the total EMG in order to reduce noise. The filtered and rectified EMG was input for the model. The range of motion (RoM) was determined as the difference between maximal wrist flexion and wrist extension angle resulting from an imposed sinusoidal varying wrist torque starting from 0 Nm and ranging between 2 Nm (extension torque) and –2 Nm (flexion torque) with a duration of about 80-100 seconds. Subsequently, ramp-and-hold (RaH) rotations were imposed onto the wrist over the full (individual) RoM within 1 second. Two RaH trials were imposed per measurement. Each trial encompassed a one second ramp in either extension or in flexion direction, two slow ramps in the opposite direction and three "hold" periods in between the ramps in which the position of the wrist did not change (Figure 5.1). Subjects were asked to remain relaxed during the entire experiment and not to voluntary react to the imposed wrist movements.

Data analysis

A validated biomechanical EMG driven antagonistic muscle model was used to predict wrist torque from the imposed wrist angle and recorded EMG[8]. The following twelve parameters of the model were predicted through least squares optimization by fitting the predicted torque derived from the model onto the experimentally recorded torque: of both flexor and extensor muscles: the stiffness coefficient, muscle slack length, optimal muscle length, EMG weighting factors and further: mass of the hand and the handle, activation cut-off frequency and parameters related to tissue relaxation, i.e. the tissue relaxation time constant and tissue relaxation factor[8]. The present study focused on four main outcome parameters: 1) The slack muscle length ($l_{p,slack,m}$), which is the minimal muscle (m) length at which passive forces are generated and where m either represents the lumped system of wrist flexors or wrist extensors. 2) The stiffness coefficient (k_m) representing the shape of the force-length curvature of the muscle tissue at lengths exceeding the slack muscle length: the higher the coefficient, the steeper the force-length curvature and the stiffer the muscle; the shorter the slack length, the higher the force at any given length exceeding the slack length. The force-length characteristics of the flexor and extensor muscle models were used to determine 3) the peripheral tissue dependent joint stiffness (peripheral tissue stiffness, K_{joint}) which is both joint angle, i.e. muscle

length, and direction dependent (described for the present study from neutral position towards wrist extension)[8;9].

For clinical comparison between subjects, the peripheral tissue stiffness was compared at an identical wrist angle for all subjects. This angle was chosen at zero degrees, i.e. where the robot manipulator handle is in line with the forearm. Besides the peripheral tissue stiffness component of wrist joint stiffness also the neural reflexive stiffness was predicted. As a measure of the amount of reflex activity, the root mean square reflex torques from the flexor and extensor muscles were derived by calculating the integral of the squared instantaneous measurements over the full observation period resulting in the reflexive torque[8;9] ($T_{reflex,m}$) (4). Trials were excluded from further analysis when the model was not able to predict the measured torque adequately, i.e. variance accounted for (VAF) below 98%. Calculated model parameters were discarded when identified as outlier based on standard deviation when compared to the values at adjacent time points or extraordinary parameter value.

Statistical analysis

A linear mixed model was used to assess the difference in outcome measures at twenty-six weeks post-stroke and each of the other consecutive measured time points between PP, PG and GG groups. A linear model was used to model the within subject correlation structure of the time points as auto-regressive order 1 (AR(1)). There were no random factors in the model. Fixed effects were modelled for the group factor indicating the PP, PG and GG groups, for the time points and for the interaction between the time and group. Alpha was set at .05. For statistical analysis IBM SPSS statistics 22 and GraphPad Prism 6 were used.

Results

The characteristics of the 36 included patients are illustrated in Table 5.1. On average, a patient had 4.6 visits with a total of 163 measurements. Each measurement resulted in a ramp-and-hold trial in flexion direction and a trial in extension direction. Each set of flexion and extension trials resulted in 7 outcome measures. Twenty trials (of 326) were excluded due to poor model

fit (VAF < 98%) and four trials (two measurements) due to corrupt measurement files. For the remaining trials in total 22 outlier outcome measures (~2%) in 11 subjects were identified and excluded for further analysis. Missing measurements exceeded 70% in the first three weeks due e.g. to late enrolment in this part of the EXPLICIT-stroke protocol, medical factors associated with stroke and logistic difficulties. Therefore we focused our statistical analysis on week four and onwards.

Table 5.1: *Patient characteristics for patients with good prognosis and good recovery (GG), patients with poor prognosis and good recovery (PG) and patients with poor prognosis and poor recovery (PP).*

	GG	PG	PP
Number of patients	15	12	9
Age, years (SD)	6.7 (8.2)	59.6 (14.6)	58.6 (8.6)
Male gender, n (%)	12 (80)	8 (67)	7 (78)
Preferred hand, right, n (%)	13 (87)	11 (91)	7 (78)
Affected hand, right, n (%)	3 (20)	5 (42)	4 (44)
Affected = preferred, n (%)	4 (27)	4 (33)	2 (22)

Cross-sectional group comparison at 26 weeks post-stroke

The PP patient group with poor prognosis and poor recovery of motor function had a significant higher reflexive torque of the flexors ($T_{reflex,flexor}$), a higher peripheral tissue stiffness (K_{joint}) and a smaller slack length of the flexors ($l_{p,slack,flexor}$) compared to patient with good prognosis and good recovery (GG) and patients with poor prognosis and good recovery (PG) (Figure 5.2). The stiffness coefficient of the flexors (k_{flexor}) was lower in the PP group compared to PG group (P=.029) and higher in the extensor muscles ($k_{extensor}$) in the PP patient group compared to the PG patient group (P=.028). No other differences were observed for the wrist extensor muscles.

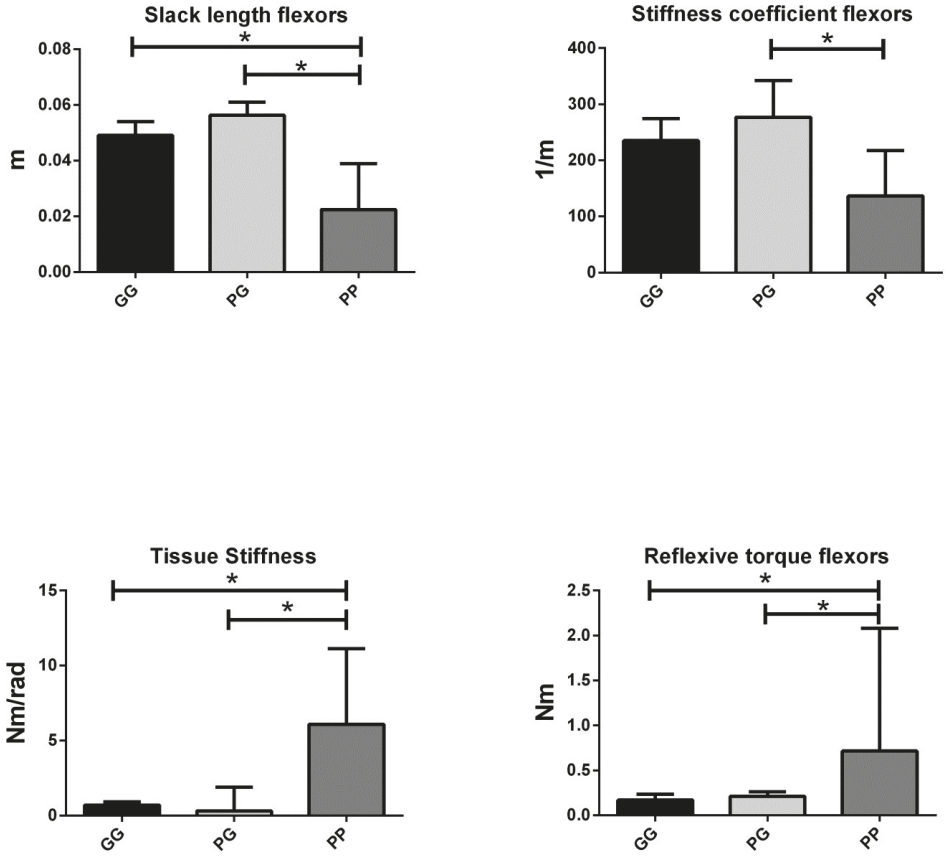


Figure 5.2: *Predicted outcome measures for the patients with good prognosis and good recovery (GG), patients with poor prognosis and good recovery (PG) and patients with poor prognosis and poor recovery (PP) at twenty-six weeks post-stroke. Significant differences between groups are indicated with asterisks.*

Table 5.2: *Median and interquartile range for the predicted stiffness coefficient (k_m), slack length ($l_{p,slack,m}$), reflexive torque ($T_{reflex,m}$) and peripheral tissue stiffness (K_{joint}) for patients with good prognosis and good recovery (GG), patients with poor prognosis and good recovery (PG) and patients with poor prognosis and poor recovery (PP). In the first three weeks most missing occasions are found. Therefore week four and onwards are shown. Numbers of patients per group and week are shown (n) for parameters related to flexor and extensor muscles. Differences between the two are due to bad model fits (variance accounted for < 98%)*

	k_{flex}	$l_{p,slack,flex}$	K_{ext}	$l_{p,slack,ext}$	$T_{Reflex,flex}$	$T_{Reflex,ext}$	K_{joint}	*n (flex)*	*n (ext)*
GG									
Week 4	268 (236-391)	.055 (.054-.057)	210 (175-282)	.070 (.061-.075)	.27 (.07-.48)	.066 (.001-.25)	.73 (.30-1.1)	5	6
Week 5	260 (234-329)	.054 (.050-.059)	345 (202-388)	.074 (.064-.078)	.15 (.009-.55)	.088 (.027-.25)	.70 (.26-1.2)	12	11
Week 8	268 (213-321)	.054 (.047-.059)	242 (205-303)	.067 (.058-.070)	.14 (.033-.29)	.16 (.013-.22)	.59 (.33-.84)	10	10
Week 12	244 (174-266)	.052 (.048-.054)	214 (167-319)	.068 (.063-.076)	.085 (.043-.29)	.17 (.083-.35)	.78 (.57-1.3)	12	9
Week 26	235 (196-275)	.049 (.045-.054)	185 (111-290)	.064 (.053-.070)	.17 (.030-.24)	.014 (.000-.089)	.69 (.54-.91)	11	10
PG									
Week 4	251 (239-263)	.054 (.051-.065)	256 (179-382)	.070 (.062-.078)	.23 (.028-.45)	.15 (.000-.36)	.62 (.052-1.0)	3	3
Week 5	217 (187-244)	.053 (.042-.056)	227 (167-279)	.065 (.060-.070)	.19 (.073-.41)	.15 (.052-.41)	.67 (.36-1.8)	12	12
Week 8	244 (234-247)	.052 (.045-.055)	218 (154-239)	.063 (.056-.070)	.20 (.039-.57)	.17 (.13-.33)	1.2 (.57-2.2)	8	8
Week 12	252 (168-385)	.056 (.037-.058)	253 (149-343)	.065 (.051-.074)	.037 (.000-.70)	.20 (.027-.95)	.81 (.36-2.3)	6	6
Week 26	277 (227-342)	.056 (.047-.061)	148 (76-192)	.063 (.052-.071)	.21 (.18-.26)	.078 (.006-.34)	.30 (.28-1.9)	8	8
PP									
Week 4	197 (159-295)	.042 (.036-.056)	242 (189-400)	.072 (.067-.076)	.27 (.14-.39)	.26 (.098-.62)	1.4 (.52-2.5)	5	5
Week 5	187 (132-255)	.042 (.025-.050)	249 (234-320)	.069 (.065-.074)	.34 (.18-.66)	.027 (.003-.40)	2.8 (.82-4.5)	9	9
Week 8	192 (166-267)	.036 (.031-.046)	252 (225-290)	.070 (.062-.072)	.54 (.16-.71)	.015 (.001-.21)	5.8 (4.4-6.9)	6	5
Week 12	152 (121-307)	.029 (.014-.047)	253 (198-330)	.066 (.065-.072)	.71 (.43-1.4)	.14 (.001-.18)	5.0 (2.6-9.0)	5	7
Week 26	137 (119-217)	.023 (.010-.039)	231 (171-340)	.066 (.059-.074)	.71 (.51-2.1)	.027 (.000-.085)	6.1 (4.3-11)	7	7

Longitudinal group comparisons (repeated measures)

Table 5.2 shows the medians with interquartile range (IQR) for the predicted outcome measures. Significant differences initiating at different moments of measurement between the different groups were observed for the reflexive torque of the flexors, the peripheral tissue stiffness (K_{joint}) and the slack length of the flexors (Table 5.3, Figure 5.3).

Table 5.3: *Significant differences between patients with good prognosis and good recovery (GG), patients with poor prognosis and good recovery (PG) and patients with poor prognosis and poor recovery (PP) for the predicted slack length of the flexors ($l_{p,slack,flex}$), reflexive torque of the flexors ($T_{reflex,flex}$) and peripheral tissue stiffness (K_{joint}). In the first three weeks most missing occasions are found. Therefore week four and onwards are shown.*

	$l_{p,slack,flex}$			$T_{Reflex,flex}$			K_{joint}		
	PP vs GG	***PP vs PG***	***GG vs PG***	***PP vs GG***	***PP vs PG***	***GG vs PG***	***PP vs GG***	***PP vs PG***	***GG vs PG***
Week 4	*P*=.025	*P*=.005	*P*=.37	*P*=.94	*P*=.94	*P*=.89	*P*=.577	*P*=.335	*P*=.69
Week 5	*P*<.001	*P*=.013	*P*=.21	*P*=.30	*P*=.35	*P*=.91	*P*=.002	*P*=.069	*P*=.23
Week 8	*P*=.002	*P*=.010	*P*=.72	*P*=.21	*P*=.36	*P*=.74	*P*<.001	*P*<.001	*P*=.51
Week 12	*P*<.001	*P*<.001	*P*=.83	*P*=.001	*P*=.006	*P*=.73	*P*<.001	*P*<.001	*P*=.52
Week 26	*P*<.001	*P*<.001	*P*=.42	*P*<.001	*P*<.001	*P*=.29	*P*<.001	*P*<.001	*P*=.60

Overall effect of time and group and the interaction effect are shown in Appendix 5. At week four and onwards the slack length of the flexors was significantly smaller in the PP group compared to the GG and PG groups. The peripheral tissue stiffness was increased from week five to week twenty-six for the PP group compared to the GG and PG groups. At week twelve and twenty six the reflexive torque of the flexors was increased in the PP compared to GG and PG.

Extensor reflexive torque differed at week twelve (*P*=.019) between the PG and the PP groups. The extensor slack length was smaller in PG compared to GG (*P*=.032) at week five.

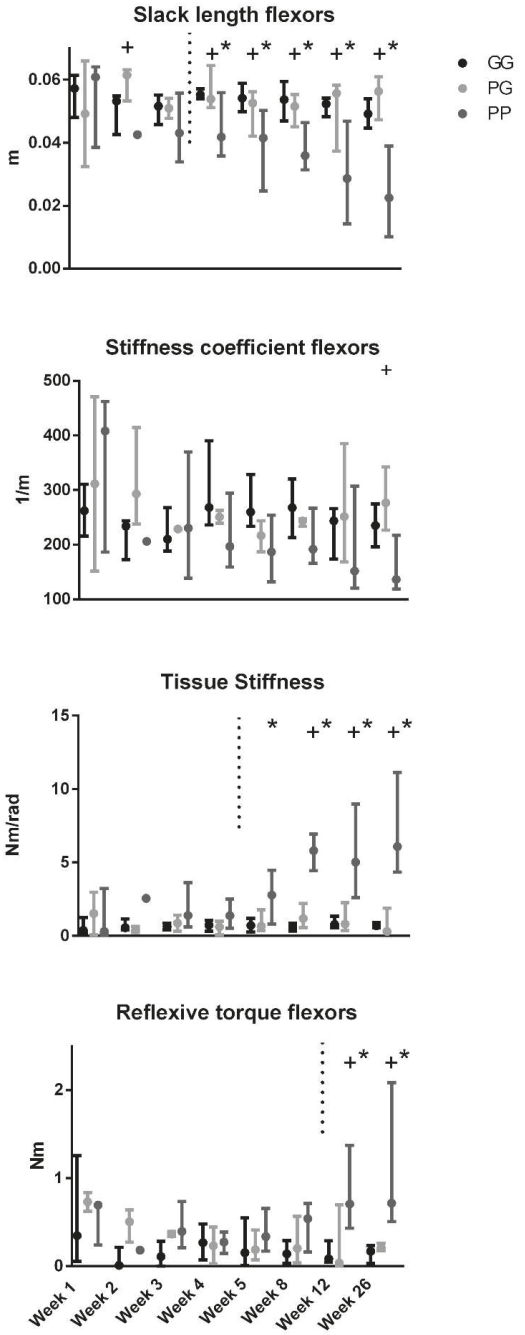


Figure 5.3: *Longitudinal observations for the predicted outcome measures for the patients with good prognosis and good recovery (GG), patients with poor prognosis and good recovery (PG) and patients with poor prognosis and poor recovery (PP). Significant differences between the GG and PP groups are indicated with an asterisk (*) and significant differences between the PG and PP group are indicated with a cross ($^{+}$). The dashed line denotes the onset of changes between the poor recovery and good recovery groups.*

Discussion

Increased reflexive torque of the flexor muscles and shortened flexor muscles were predicted in patients with poor prognosis and poor recovery of the upper limb (PP, ARAT≤9 points) compared to patients with good prognosis and good recovery (GG, ARAT≥10 points) and patients with poor prognosis and good recovery (PG, ARAT≥10 points) using a validated electromyography driven modeling in 36 stroke patients at twenty-six weeks post-stroke[8;9]. As expected, patients with an initial poor prognosis and poor recovery showed increased reflexive torque of the flexor muscles ($T_{reflex,flex}$), increased peripheral tissue stiffness (K_{joint}) and shortened flexor muscles, indicated by smaller flexor slack length ($l_{p,slack,flex}$) compared to patients with good recovery, at twenty-six weeks post-stroke. The current study suggests that peripheral tissue changes, i.e. slack length, around week four and five in the PP group preceded the neural reflexive stiffness, i.e. reflexive torque, changes observed around week twelve (Table 5.3).

Cross-sectional group comparison at 26 weeks post-stroke

The PP patient group with poor prognosis and poor recovery had shortened flexor muscles at twenty-six weeks post-stroke, indicated by the smaller slack length of the modelled flexor muscles compared to the good recovery groups (PG and GG). The shortening of the muscle in the PP group is in concordance with the flexion deformity found by van der Krogt et al. (unpublished results), i.e. a marked shift of the wrist rest angle towards flexion, observed in these patients. Note that in the present study the peripheral tissue stiffness (K_{joint}) was measured at a fixed angle of zero degrees. Peripheral tissue stiffness determined at the individual rest angles of patients may reveal a difference with the current study as was previously observed (unpublished results, van der Krogt et al.). This illustrates that peripheral tissue stiffness depends on the angle of observation. Additionally, at the rest position of the wrist (zero torque)[3], the stiffness is lowest and contrast between the different groups is minimal. The stiffness coefficient was lower in the PP group compared to the PG group. This could be due to structural changes in the muscle or because of and interaction of the contractile state of passive tissue with the active state of the muscle, e.g. background activation[18] which we currently do not

account for. However, without further substantiating data these physiological explanations are speculative and obviously additional research endeavors and validation are warranted.

The exact mechanism of muscle shortening after an upper motor neuron disease is still unclear[19]. A diminished neural input might results in disuse or immobilization and therefore muscle atrophy. Immobilized muscles in a shortened position adapt to their resting length and lose sarcomeres to develop maximal force at their shortened length[5;20-23] . When stretching the shortened muscles, the diminished number of sarcomeres in series results in a higher tissue stiffness compared to normal muscles. Our data suggest that muscle shortening occurs soon (around week 4) after stroke. Immobilization and muscle over-activity in the sub-acute phase post-stroke may worsen shortening[5;24].

Peripheral tissue changes precede neural reflexes changes

The current study suggests that tissue changes in the flexor muscles around week four and five in the poor recovery group (PP) preceded the neural reflexive changes observed around week twelve. The progressive increase in peripheral tissue stiffness and neural reflexive stiffness around the wrist in stroke patients is in accordance with results found by Mirbagheri et al.[25] in the elbow joint.

Movement disorders after stroke are the result of a complex interplay between tissue and neural properties[4;26]. After stroke, central neural drive changes with excessive responses to muscle stretch via several proposed mechanisms which encompass alpha motor neuron hyper excitability, changes in recruitment gain and plateau potentials of motor neurons, loss of presynaptic inhibition and changes in gamma- motor- neuron excitability[24]. Altered neural input may also comprise increased background muscle activation which may also explain hyper excitability of reflexes[18;27]. Loss of neural drive also results in flexion synergies at the wrist due to neural coupling with the shoulder and elbow[28] which may worsen immobilization of the flexors in a short position. Increased muscle strain in shortened muscles may potentially result in increased spindle responses and subsequent increased spinal reflex activity[5;29]. This may offer an alternative yet interesting explanation of the temporal delay between tissue changes and reflexive responses. We suppose that tissue changes occur within the first weeks after

stroke. This was confirmed by the large differences between the groups at week four. The onset of shortening within the poor recovery group (PP) is likely to start in the weeks before.

Changes were mainly observed in the flexor muscles. Changes in the extensor muscle were only found for the stiffness coefficient at twenty-six weeks: the stiffness coefficient of the extensors was higher for the PP group compared to the PG group meaning that the extensor muscle was stiffer in the PP group. The different adaptation of the extensor muscle in recovery is not yet clear. At week twenty-six, no differences were found in outcome measures between the GG patients and PG patients. Differences between these groups could arise earlier after stroke. Increased resolution of measurements by increasing the number of observations within these first weeks may reveal differences especially between the PG and PP and GG groups.

Limitations

For this study a validated EMG driven wrist model[8] was used to predict the peripheral tissue stiffness and neural reflexive components of wrist joint stiffness. Using this method allows us to predict lumped parameters of the flexor and extensor muscle groups. The method can be useful in decisions for treatment and may hand us a key to understand underlying mechanisms of functional recovery[9;30-34]. However, the method has also some limitations. During the processing of EMG input data, background muscle activation, which is assumed to be noise, was removed from the EMG signal and only the variances in EMG amplitude were used to estimate the reflexive torque. As in stroke patients the rest level EMG may be elevated[18] this elevated additional input is discarded and therefore not included in the active (contractile) contribution to torque. The background activation could not be identified by the model but might be traced back in the overall peripheral tissue stiffness meaning that the peripheral tissue stiffness might have been overestimated in patients with increased background activation. However, analysis of the EMG levels at rest showed no difference between the three groups which made it less likely that differences in background activation explain the observed elevated reflex activity and flexor muscle shortening.

In the EMG driven wrist model[8] the muscle length at which the highest forces are generated was also included. In the current study this optimal muscle length (i.e. due to the maximal

overlap between contractile filaments) was not presented as reflexive muscle activation in these patients was low in most patients and estimation of contractile muscle properties was therefore unreliable.

The model is a lumped representation of all flexor and extensor muscles. The differences between individual muscles (e.g. flexor carpi radialis and flexor carpi ulnaris) after stroke were therefore not identified.

Most drop-outs were found in the first three weeks. Additional observations, thus increasing statistical power, are needed to obtain reliable information about the neural reflexes and peripheral tissue changes in the first weeks post-stroke for patients with different recovery patterns. Small sample size also prevented further substantiation of the additional effects of treatment. However, subgroup analysis in the present sample showed no substantial differences between intervention and control groups. We chose to use an interaction term in our statistical model, because of plausibility of group and time interaction. Small sample size prevented that this interaction term was significant in all cases.

Clinical implications

Clinically observed changes post-stroke, e.g. the altered wrist flexion deformity, were now further specified by predicting its components explaining increased joint stiffness, i.e. neural reflexive and peripheral tissue stiffness, and characterized over time. Around 4-5 weeks post-stroke significant peripheral tissue changes were observed in a group of patients with initially poor prognosis for functional recovery and a poor recover (i,e, ARAT≤9 points) at 26 weeks; changes in reflex torque were only observed after 12 weeks. The exact interplay of properties of neural reflexive stiffness, i.e. reflexive torque and peripheral tissue stiffness, i.e. slack length and stiffness coefficient, background muscle activation and the interplay of both muscle groups need to be studied further to pinpoint the cause-and-effect of increased joint stiffness and whether it can be influenced by therapy shortly after stroke.

Preventing immobilization in a shortening position early after stroke should be an important focus in clinical practice. The effect of therapies on neural reflexive and peripheral tissue stiffness in the acute and sub-acute stroke patients, e.g. neuromuscular electrical stimulation of the wrist extensors (suggested to enhance motor recovery)[35], the best timing of physical

therapy[36] or the effect of splinting of the wrist[37], needs to be studied using longitudinal observations at fixed time points post-stroke.

Acknowledgements

This research was funded by the Dutch Technology Foundation STW (ROBIN project, grant nr. 10733), which is part of the Dutch national organization for scientific research (NWO) and partly funded by the Ministry of Economic Affairs, Agriculture and Innovation, and the Dutch organization for Health Research and Development ZonMW (Explicit Stroke project, grant nr. 890000001). CM is supported by a grant from the Dutch Brain foundation. We thank the Department of Medical Statistics at the LUMC for assistance in statistical analysis.

References

(1) Kwakkel G, Kollen B. Predicting improvement in the upper paretic limb after stroke: a longitudinal prospective study. *Restor Neurol Neurosci* 2007;25:453-460.

(2) van Kordelaar J, van Wegen E, Kwakkel G. Impact of time on quality of motor control of the paretic upper limb after stroke. *Arch Phys Med Rehabil* 2014;95:338-344.

(3) Kwakkel G, Kollen B, Lindeman E. Understanding the pattern of functional recovery after stroke: facts and theories. *Restor Neurol Neurosci* 2004;22:281-299.

(4) Dietz V, Sinkjaer T. Spastic movement disorder: impaired reflex function and altered muscle mechanics. *Lancet Neurol* 2007;6:725-733.

(5) Gracies JM. Pathophysiology of spastic paresis. I: Paresis and soft tissue changes. *Muscle Nerve* 2005;31:535-551.

(6) Diong J, Harvey LA, Kwah LK et al. Gastrocnemius muscle contracture after spinal cord injury: a longitudinal study. *Am J Phys Med Rehabil* 2013;92:565-574.

(7) Kwakkel G, Meskers CG, van Wegen EE et al. Impact of early applied upper limb stimulation: the EXPLICIT-stroke programme design. *BMC Neurol* 2008;8:49.

(8) de Gooijer-van de Groep K, de Vlugt E., van der Krogt HJ et al. Estimation of tissue stiffness, reflex activity, optimal muscle length and slack length in stroke patients using an electromyography driven antagonistic wrist model. *Clin Biomech* 2016;35:93-101.

(9) de Vlugt E, de Groot JH, Schenkeveld KE, Arendzen JH, van der Helm FC, Meskers CG. The relation between neuromechanical parameters and Ashworth score in stroke patients. *J Neuroeng Rehabil* 2010;7:35.

(10) Mirbagheri MM, Rymer WZ. Time-course of changes in arm impairment after stroke: variables predicting motor recovery over 12 months. *Arch Phys Med Rehabil* 2008;89:1507-1513.

(11) Buma F, Kwakkel G, Ramsey N. Understanding upper limb recovery after stroke. *Restor Neurol Neurosci* 2013;31:707-722.

(12) Klomp A, van der Krogt JM, Meskers CGM et al. Design of a concise and comprehensive protocol for post stroke neuromechanical assessment. *J Bioengineer & Biomedical Sci* 2012.

(13) van der Krogt HJ, Klomp A, de Groot JH et al. Comprehensive neuromechanical assessment in stroke patients: reliability and responsiveness of a protocol to measure neural and non-neural wrist properties. *J Neuroeng Rehabil* 2015;12.

(14) Nijland RH, van Wegen EE, Harmeling-van der Wel BC, Kwakkel G. Presence of finger extension and shoulder abduction within 72 hours after stroke predicts functional recovery: early prediction of functional outcome after stroke: the EPOS cohort study. *Stroke* 2010;41:745-750.

(15) Stinear C. Prediction of recovery of motor function after stroke. *Lancet Neurol* 2010;9:1228-1232.

(16) Van Peppen RP, Kwakkel G, Wood-Dauphinee S, Hendriks HJ, van der Wees PJ, Dekker J. The impact of physical therapy on functional outcomes after stroke: what's the evidence? *Clin Rehabil* 2004;18:833-862.

(17) Kwakkel G, Winters C, van Wegen EE et al. Effects of Unilateral Upper Limb Training in Two Distinct Prognostic Groups Early After Stroke: The EXPLICIT-Stroke Randomized Clinical Trial. *Neurorehabil Neural Repair* 2016;30:804-816.

(18) Burne JA, Carleton VL, O'Dwyer NJ. The spasticity paradox: movement disorder or disorder of resting limbs? *J Neurol Neurosurg Psychiatry* 2005;76:47-54.

(19) Lieber RL, Steinman S, Barash IA, Chambers H. Structural and functional changes in spastic skeletal muscle. *Muscle Nerve* 2004;29:615-627.

(20) Tabary JC, Tabary C, Tardieu C, Tardieu G, Goldspink G. Physiological and structural changes in the cat's soleus muscle due to immobilization at different lengths by plaster casts. *J Physiol* 1972;224:231-244.

(21) Williams PE, Goldspink G. Changes in sarcomere length and physiological properties in immobilized muscle. *J Anat* 1978;127:459-468.

(22) Wisdom KM, Delp SL, Kuhl E. Use it or lose it: multiscale skeletal muscle adaptation to mechanical stimuli. *Biomech Model Mechanobiol* 2015;14:195-215.

(23) Kelleher AR, Gordon BS, Kimball SR, Jefferson LS. Changes in REDD1, REDD2, and atrogene mRNA expression are prevented in skeletal muscle fixed in a stretched position during hindlimb immobilization. *Physiol Rep* 2014;2:e00246.

(24) Gracies JM. Pathophysiology of spastic paresis. II: Emergence of muscle overactivity. *Muscle Nerve* 2005;31:552-571.

(25) Mirbagheri MM, Tsao C, Rymer WZ. Natural history of neuromuscular properties after stroke: a longitudinal study. *J Neurol Neurosurg Psychiatry* 2009;80:1212-1217.

(26) Meskers CG, Schouten AC, de Groot JH et al. Muscle weakness and lack of reflex gain adaptation predominate during post-stroke posture control of the wrist. *J Neuroeng Rehabil* 2009;6:29.

(27) Denny-Brown D. Chapter XII. The extrapyramidal cortical system. *The Cerebral Control of Movement*. Liverpool: University Press; 1966;173.

(28) Miller LC, Dewald JP. Involuntary paretic wrist/finger flexion forces and EMG increase with shoulder abduction load in individuals with chronic stroke. *Clin Neurophysiol* 2012;123:1216-1225.

(29) Gioux M, Petit J. Effects of immobilizing the cat peroneus longus muscle on the activity of its own spindles. *J Appl Physiol (1985)* 1993;75:2629-2635.

(30) de Gooijer-van de Groep KL, de Vlugt E, de Groot JH et al. Differentiation between non-neural and neural contributors to ankle joint stiffness in cerebral palsy. *J Neuroeng Rehabil* 2013;10:81.

(31) Gaverth J, Eliasson AC, Kullander K, Borg J, Lindberg PG, Forssberg H. Sensitivity of the NeuroFlexor method to measure change in spasticity after treatment with botulinum toxin A in wrist and finger muscles. *J Rehabil Med* 2014;46:629-634.

(32) Lindberg PG, Gaverth J, Islam M, Fagergren A, Borg J, Forssberg H. Validation of a new biomechanical model to measure muscle tone in spastic muscles. *Neurorehabil Neural Repair* 2011;25:617-625.

(33) Sloot LH, van der Krogt MM, de Gooijer-van de Groep KL et al. The validity and reliability of modelled neural and tissue properties of the ankle muscles in children with cerebral palsy. *Gait Posture* 2015.

(34) van der Krogt HJ, Meskers CG, de Groot JH, Klomp A, Arendzen JH. The gap between clinical gaze and systematic assessment of movement disorders after stroke. *J Neuroeng Rehabil* 2012;9:61.

(35) Powell J, Pandyan AD, Granat M, Cameron M, Stott DJ. Electrical stimulation of wrist extensors in poststroke hemiplegia. *Stroke* 1999;30:1384-1389.

(36) Veerbeek JM, van Wegen E, van Peppen R et al. What is the evidence for physical therapy poststroke? A systematic review and meta-analysis. *PLoS One* 2014;9:e87987.

(37) Lannin NA, Cusick A, McCluskey A, Herbert RD. Effects of splinting on wrist contracture after stroke: a randomized controlled trial. *Stroke* 2007;38:111-116.

Appendix 5: Supplementary Table

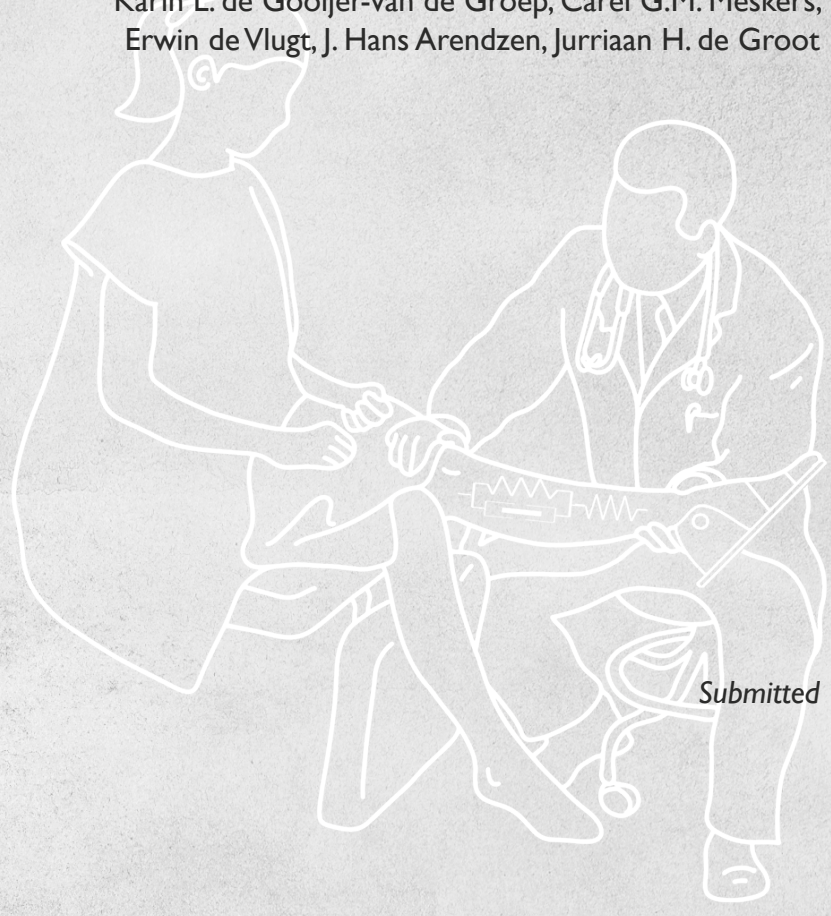
Table 5A: *Overall effect of time (weeks), overall effect of group (PP, PG, GG) and effect of interaction between group and time for patients with poor prognosis and poor recovery (PP) compared to the good recovery groups for the predicted slack length of the flexors ($l_{p,slack,flex}$), reflexive torque of the flexors ($T_{reflex,flex}$) and peripheral tissue stiffness (K_{joint}). In the first three weeks most missing occasions are found. Therefore week four and onwards are shown.*

	$l_{p,slack,flex}$			$T_{Reflex,flex}$			K_{joint}		
	Overall effect of time	*Overall effect of group*	*Interaction effect*	*Overall effect of time*	*Overall effect of group*	*Interaction effect*	*Overall effect of time*	*Overall effect of group*	*Interaction effect*
Week 4	F=2.4 (P=0.026)	F=11.9 (P<0.001)	F=1.4 (P=0.17)	F=1.9 (P=0.079)	F=6.2 (P=0.003)	F=1.8 (P=0.043)	F=7.7 (P<0.001)	F=13.7 (P<0.001)	F=5.2 (P<0.001)
Week 5	F=3.5 (P=0.002)	F=10.5 (P<0.001)	F=1.9 (P=0.034)	F=1.9 (P=0.077)	F=6.2 (P=0.003)	F=1.8 (P=0.043)	F=7.1 (P<0.001)	F=13.9 (P<0.001)	F=5.4 (P<0.001)
Week 8	F=3.3 (P=0.004)	F=11.2 (P<0.001)	F=1.9 (P=0.041)	F=1.9 (P=0.079)	F= 6.2 (P=0.003)	F=1.8 (P=0.045)	F=5.3 (P<0.001)	F=14.5 (P<0.001)	F=3.8 (P<0.001)
Week 12	F=1.8 (P=0.098)	F=9.8 (P<0.001)	F=1.5 (P=0.13)	F=1.9 (P=0.070)	F=6.4 (P=0.003)	F=1.9 (P=0.038)	F=4.1 (P=0.001)	F=11.6 (P<0.001)	F=3.2 (P=0.001)
Week 26	F=1.7 (P=0.13)	F=10.0 (P<0.001)	F=1.3 (P=0.22)	F=1.8 (P=0.090)	F=5.5 (P=0.006)	F=1.7 (P=0.06)	F=4.5 (P<0.001)	F=10.2 (P<0.001)	F=3.2 (P<0.001)

CHAPTER 6

Estimating the effects of botulinum toxin A therapy post-stroke: evidence for reduction of background muscle activation

Authors:
Karin L. de Gooijer-van de Groep, Carel G.M. Meskers,
Erwin de Vlugt, J. Hans Arendzen, Jurriaan H. de Groot



Submitted

Abstract

Clinical application of botulinum toxin (BoNT) will benefit from a better understanding and quantitative assessment of the underlying neural and non-neural properties of spasticity related joint stiffness increase and their response to BoNT treatment.

The effect of BoNT on underlying ankle joint stiffness properties was estimated using an EMG-driven ankle model in 15 chronic stroke patients who underwent instrumented passive ankle rotations before and after BoNT injections in the calf muscles.

Dorsal range of motion (dRoM) increased after BoNT. Baseline values of and changes in non-neural joint stiffness, triceps surae slack length and recorded soleus EMG rest activation were associated with changes in dRoM and neutral rest angle. No associations were found for reflex activity.

Observed and estimated responses are in line with an effect of BoNT on background muscle activity. The instrumented approach may assist to identify those patients who will likely benefit from BoNT therapy.

Introduction

Botulinum neurotoxin-A (BoNT) is recommended for treatment of post-stroke spasticity[1-8]. BoNT blocks the release of acetylcholine from the nerve terminal, thereby uncoupling the excitation-contraction mechanism and thus reducing muscle (hyper)activity[3]. This results in a reduction of muscle tone and joint stiffness and a subsequent decrease in resistance to passive joint manipulation as clinically assessed by the (modified) Ashworth Score (mAS)[9]. Clinical application of BoNT for spasticity treatment post-stroke may benefit from a better understanding and quantitative assessment of the underlying properties of spasticity related joint stiffness increase and their response to BoNT treatment. Is spasticity defined by a velocity dependent resistance to passive stretch according to the concept of Lance[10] or is it better explained by an increased muscle activation at rest, i.e. background muscle activation, according to the Burne concept[11]?

Evaluation of BoNT treatment is hampered by e.g. differences in dosing regimens, injection sites, heterogeneity in patients, concurrent treatment, outcomes selected, and the poor methodological quality of insufficiently powered, placebo-controlled trials[12-15]. Furthermore, assessment of the effects of BoNT by clinical semi-quantitative scaling like the mAS is problematic as the mAS has a questionable reliability and a low responsiveness to change[9;16]. We recognize an urgent need for alternative, high-resolution assessment that enables us to understand the concept of spasticity and its response to BoNT in upper motor neuron diseases like stroke[14].

Neuromuscular modeling in combination with joint manipulation paradigms using high precision robotics is promising in terms of reliable and valid identification of the underlying contributors of joint stiffness[17-23]. An instrumented electromyography (EMG)-driven modeling approach would allow for quantitative estimation of the neural reflexive and non-neural tissue properties to joint stiffness, i.e. muscle shortening and muscle stiffening[18;19;24]. This method should potentially be able to identify (stroke) patient characteristics at baseline prior to BoNT treatment and assess the effects of BoNT post treatment.

The aim of the present study was therefore to estimate the effect of BoNT on underlying neural reflexive and non-neural tissue properties of increased ankle joint stiffness in chronic stroke patients.

Methods

Subjects

Fifteen stroke patients participated in the study. Patients were included following ischemic or hemorrhagic stroke over 6 months at inclusion and were clinically referred for BoNT treatment (Botox, Allergan, Inc., Irvine, CA) in the soleus (SOL), gastrocnemius medialis (GM), gastrocnemius lateralis (GL) and/or tibialis posterior (TP). Patients were recruited from the outpatient clinic of the Leiden University Medical Center between January 2013 and June 2015. The indication for treatment was based on clinical arguments and independent of the present study. Exclusion criteria comprised (other) concomitant neurological and/or orthopedic disorders, treatment within the last 4 months that could interfere with a stable ankle joint stiffness, surgery of leg/foot within last 12 months and inability to participate in the experiment, either physically (i.e. inability to be mounted in the experimental set-up), cognitively (i.e. unable to understand test instructions or to give informed consent). Participants were measured prior to BoNT treatment (baseline T0) and 6-8 weeks (T1) and 12-16 weeks (T2) after BoNT treatment. Written informed consent was obtained from the participants. The study was approved by the medical ethics committee of the Leiden University Medical Center.

Instrumentation

Subjects were seated with their foot fixated onto an electrically powered single axis footplate (Achilles, MOOG FCS Inc., Nieuw-Vennep) with their knee positioned at 70 degrees of flexion (Figure 6.1). The axis of rotation of the ankle and footplate were aligned by visually minimizing knee translation in the sagittal plane during manual rotation of the footplate. For safety reasons and to avoid pain, the maximum tolerated dorsal- and plantar flexion of the ankle were restricted by hard- and software stops of the manipulator and determined by manually moving the ankle through its RoM by a trained operator before starting the measurements. The footplate was aligned visually at 25° plantar flexion with respect to the line connecting the head of the fibula and the lateral malleolus. During robotic movements, EMG, torque and angle were simultaneously recorded.



Figure 6.1: *Measurement set-up.*

EMG assessment

Muscle activation of the tibialis anterior (TA) and triceps surae (TS) was recorded using surface EMG (Porti, TMSi B.V. Oldenzaal, The Netherlands) according to the SENIAM guidelines[25] (supplementary table). EMG signals were sampled at 1000 Hz, offline high pass filtered (20Hz, 3th-order Butterworth), rectified and low pass filtered (20 Hz zero overshoot filter). Rest EMG, i.e. the minimal EMG determined for each muscle by applying a moving window of 8 ms, was subtracted from the total EMG because assumed not to contribute to ankle torque. Rest EMG of the TA, SOL, GL and GM were also used as outcome measure. Torque and ankle angle were sampled at 1024 Hz and low pass filtered (20 Hz zero overshoot filter) and resampled to 1000 Hz.

Range of motion and ramp and hold measurements

Maximum dorsal and plantar flexion angles were assessed by gradually increasing flexion torque from 0 to 15 Nm in dorsal flexion direction and subsequently to -7.5 Nm in plantar flexion direction and back to zero torque in dorsal flexion direction. From this measurement the

following outcome measures were determined: 1) dorsal range of motion (dRoM), i.e. the maximum ankle angle at 15 Nm or, in case the patients did not tolerate 15 Nm, at the highest common torque measured over all three measurements (T0,T1,T2) and 2) the neutral angle (NA) which is the ankle angle at zero torque, i.e. the ankle at rest. The zero torque angle is ankle flexion direction dependent (hysteresis) and the NA was defined as the average 0-Nm crossing angle determined for the plantar flexion and dorsiflexion movement.

The instrumented RoM was used as boundary for the subsequent ramp-and-hold (RaH) trials. During the RaH measurements the ankle was rotated at two different angular velocities (15 and 100 deg/sec), starting in maximal plantar flexion and ending in maximum dorsiflexion angle (first ramp). After an approximate 10 seconds hold phase, the ankle was moved back to the maximal plantar flexion angle (second ramp). The subjects were instructed to relax during the RaH trials. Each velocity was repeated, which resulted in four RaH trials and one RoM trial per measurement.

Neuromuscular modeling

A validated neuromuscular model was used to predict ankle torque from measured ankle angle and EMG and subsequently estimating neural reflexive and non-neural tissue properties of ankle joint stiffness[26]. The model encompassed in total 15 parameters, i.e. of both TS and TA: the stiffness coefficient, muscle slack length, optimal muscle length, EMG weighting factors (three for TS and one for TA) and further: mass of the foot and footplate, activation cut-off frequency, relative damping and parameters related to tissue relaxation, i.e. tissue relaxation time constant and tissue relaxation factor. The present study focused on the following properties: 1) The estimated non-neural muscle slack length of TS and TA; 2) The estimated non-neural stiffness coefficient of TS and TA and which is an indicator of muscle stiffness; 3) the estimated non-neural peripheral tissue stiffness, a function of joint angle determined by the combination of slack length and stiffness coefficient of both TA and TS muscles. For comparison purposes, the peripheral tissue stiffness was assessed at an ankle angle of 0 degrees over all subjects and trials, i.e. foot (plate) perpendicular to the lower leg; 4) the estimated neural reflexive torque of TS and TA. The estimated reflexive torque was calculated by the root

mean square of the involuntary active muscle torque during the observed trial. Slack muscle length, stiffness coefficient and peripheral tissue stiffness were determined at an ankle rotation speed of 15 deg/sec; the reflexive torque was determined at an ankle rotation speed of 100 deg/sec. Outcome parameters were averaged over two trials (repetitions), unless trials were excluded due to low variance accounted for (VAF<99%).

Statistical analysis

A linear mixed model was used to compare outcome measures between the different measurement time points. Secondly, a linear regression analysis was performed addressing the association between changes in outcome measures, i.e. estimated neural reflexive and non-neural tissue properties and measured EMG rest activity, as independent variables and respectively changes in measured dRoM and NA as dependent variables. Thirdly, the same procedure was repeated for the baseline values (T0) of the outcome measures, i.e. estimated neural reflexive and non-neural tissue properties and EMG rest activity, as independent variables and changes in measured dRoM and NA as dependent variables to address the predictive value of aforementioned baseline parameters for the outcome after BoNT treatment. Significance level was set at 0.05. Statistical analysis was performed using IBM SPSS statistics 22.

Results

One patient quitted the study after the first measurement due to various reasons leaving 14 stroke patients for further analysis, encompassing a total of 42 measurements. Thus, 42 RoM trials were available, and due to lack of valid RaH data in 2 patients, 144 RaH trials. In 2 patients over 2 trials, the maximum dorsal flexion torque of 15 Nm exceeded the patient's tolerance and thus hardware restricted dRoM was determined at a lower torque level. Of the 144 RaH trials, 3 trials were excluded due to low VAF values (<99%). 9 out of 14 patients were injected in the soleus muscle. Patient characteristics are shown in Table 6.1.

Table 6.1: *Patient characteristics.*

Patient	Age	Gender	Affected side	Years post-stroke	Stroke type	Injected muscles (dose)[+]	Ashworth score	Splint[**]
1	55	M	R	2.6	Ischemic	SOL (100), GM (50), GL (50)	4	1
2	46	M	L	3.0	Ischemic	SOL (50), GM (50)	4	0
3	46	F	R	21.4	Ischemic	SOL (50), TP (100), TA (100)	3	1
4	52	F	L	2.0	Hemorrhagic	GM (25), GL (25), TP (50)	2	1
5	61	M	R	10.4	Ischemic	SOL (100)	3	0
6	41	M	R	16.1	Hemorrhagic	SOL (100)	3	0
7	64	M	R	5.6	Ischemic	SOL (50)	2	1
8	65	M	L	2.5	Hemorrhagic	SOL (100)	2	1
9	68	M	R	3.1	Ischemic	TP (50)	1	1
10	48	F	L	1.6	Ischemic	SOL (100), GM (50), GL (50)	1	1
11	58	M	R	-	-	SOL (100), GM (50), GL (50)	3	1
12	55	F	R	-	Hemorrhagic	GM (100), TP (50)	3	0
13	54	M	L	2.8	Ischemic	GM (50), GL (50)	1	1
14	69	F	L	~4	Hemorrhagic	GM (50), GL (50)	1	0

[+]*SOL: soleus, GM: gastrocnemius medialis, GL: gastrocnemius lateralis, TP: tibialis posterior, TA: tibialis anterior*

*** unspecified, 1=yes; 0=no.*

Measured and estimated parameters before and after BoNT injection

Measured and estimated parameters before and after BoNT injections are presented in Table 6.2. The dRoM improved on average with 4.1 (SD 6.7) degrees from T0 to T1 and the NA shifted from plantar flexion to the (neutral) anatomical ankle angle by 4.6 (SD 7.7) degrees. Significant changes between T0 and either T1 or T2 after BoNT injection were only observed for dRoM and NA (Table 6.2). Estimated neural reflexive and non-neural tissue properties showed no significant change after BoNT injections.

Table 6.2: *Overview of outcome measures before (T0) and after (6-8 weeks: T1 and 12-16 weeks: T2) BoNT injections. P-values for comparison between measurement moments.*

	Measurement moment					
Outcome measure	T0	T1	T2	N	**T0 vs T1 P-value**	**T0 vs T2 P-value**
Dorsal RoM (deg)	5.5 (8.6)	9.5 (5.5)	8.6 (6.7)	14	**.032**	.093
Neutral angle (deg)	-30.1 (10.5)	-25.5 (6.7)	-23.6 (5.4)*	14	.052	**.010***
Peripheral tissue stiffness (Nm/rad)	245 (351)	132 (61)	125 (73)	12	.39	.21
Slack length TS (mm)	22.8 (2.6)	23.2 (2.6)	23.6 (3.8)	12	.60	.38
Slack length TA (mm)	63.6 (11)	60.2 (17)	58.5 (12)	12	.39	.10
Stiffness coefficient TS (1/m)	346 (43)	343 (48)	360 (98)	12	.79	.58
Stiffness coefficient TA (1/m)	186 (54)	192 (62)	185 (42)	12	.57	.96
Reflexive torque TS (Nm)	2.9 (2.1)	3.0 (2.2)	2.7 (2.0)	12	.89	.49
Reflexive torque TA (Nm)	.25 (.20)	.48 (.37)	.31 (.48)	12	.052	.69
Rest EMG SOL (μV)	2.3 (1.6)	2.3 (1.8)	2.3 (1.7)	12	.97	.99
Rest EMG GM (μV)	1.3 (.50)	1.3 (.30)	1.6 (0.92)	12	.50	.21
Rest EMG GL (μV)	1.2 (.24)	1.2 (.37)	1.3 (0.25)	12	.90	.69
Rest EMG TA (μV)	1.5 (.87)	1.5 (.99)	1.5 (.60)	12	.75	.98

**based on 13 stroke patients*

Associations between baseline values and changes in measured and estimated parameters with changes in dRoM and NA

A decrease in estimated peripheral tissue stiffness, an increase in estimated TS slack length and a decrease in measured rest EMG of soleus significantly associated with an increase of measured dRoM and/or a shift in NA towards anatomical ankle angle after BoNT, while no significant changes of reflex torques were observed (Table 6.3). A high estimated peripheral tissue stiffness and a small estimated TS slack length appeared to be predictive for a respectively increase in measured dRoM and NA shift towards anatomical ankle angle. Again, no significant associations between estimated baseline reflex torque and measured dROM and NA were observed (Table 6.4).

Table 6.3: *Association between changes estimated neural reflexive and non-neural tissue properties and measured EMG rest activity and changes in measured dorsal RoM and neutral angle before (T0) and 6-8 weeks after BoNT injections (T1). Unstandardized effects and 95% confidence interval.*

	Dorsal RoM			**Neutral angle**		
	Unstandardized			**Unstandardized**		
	β	**95% CI**	**P-value**	**β**	**95% CI**	**P-value**
Peripheral tissue stiffness (Nm/rad)	-.014	-.023; -.005	**.006**	-.016	-.027; -.005	**.009**
Slack length TS (mm)	1.8	.54; 3.0	**.010**	2.1	.69; 3.5	**.008**
Slack length TA (mm)	-.15	-.60; .31	.49	-.40	-.85; .059	.081
Stiffness coefficient TS (1/m)	-.040	-.19; .11	.55	-.002	-.175; .171	.98
Stiffness coefficient TA (1/m)	-.005	-.12; .11	.93	-.054	-.18; 0.69	.35
Reflexive torque TS (Nm)	.35	-4.1; 4.8	.86	2.9	-1.8; 7.6	.20
Reflexive torque TA (Nm)	.56	-11.5; 12.6	.92	-1.1	-15.0; 12.8	.87
Rest EMG SOL (μV)	-1.5	-3.07;.005	.051	-1.9	-3.6; -.2	**.032**
Rest EMG GM (μV)	-.51	-14.5;13.5	.94	1.2	-15.0; 17.3	.88
Rest EMG GL (μV)	3.7	-11.3;18.8	.59	8.1	-8.6; 24.8	.31
Rest EMG TA (μV)	-10.1	-22.1; 1.9	.090	-10.2	-24.6; 4.1	.14

Table 6.4: *Association between estimated neural and non-neural tisseu properties and measured EMG rest activity at baseline (T0) and changes in measured dorsal RoM and neutral angle between T0 and 6-8 weeks after BoNT injections (T1). Unstandardized effects and 95% confidence interval.*

	Dorsal RoM			**Neutral angle**		
	Unstandardized			**Unstandardized**		
	β	**95% CI**	**P-value**	**β**	**95% CI**	**P-value**
Peripheral tissue stiffness (Nm/rad)	.013	.004; .022	**.010**	.015	.004; .025	**.010**
Slack length TS (mm)	-1.5	-2.9; -0.084	**.040**	-1.6	-3.3; .070	.058
Slack length TA (mm)	.18	-.22; .58	.35	.016	-.47; .50	.94
Stiffness coefficient TS (1/m)	.056	-.040; .15	.23	.071	-.072; .21	.30
Stiffness coefficient TA (1/m)	.008	-.099; .12	.87	-.049	-.17; .070	.38
Reflexive torque TS (Nm)	-.45	-2.6; 1.7	.66	-.94	-3.4; 1.5	.41
Reflexive torque TA (Nm)	-7.7	-30.2; 14.8	.46	2.5	-24.1; 29.1	.84
Rest EMG SOL (μV)	1.6	-.90; 4.1	.18	-2.0	-.90; 4.8	.16
Rest EMG GM (μV)	-2.2	-11.1; 6.8	.60	-1.8	-12.2; 8.6	.71
Rest EMG GL (μV)	-8.4	-26.6; 9.9	.33	-10.3	-31.2; 10.7	.30
Rest EMG TA (μV)	.042	-5.1; 5.2	.99	-.36	-6.3; 6.0	.90

Discussion

Significant improvements in measured dRoM and NA that coincided with an estimated lengthening of the musculo-tendon complex of the TS were observed using an instrumented EMG-driven model approach to evaluate the effect of BoNT injections in the calf muscles in chronic stroke patients on neural reflexive and non-neural tissue properties of ankle joint stiffness. Baseline values and changes of the estimated non-neural tissue parameters peripheral tissue stiffness and the slack length of triceps surae were associated with improvements of dRoM and the NA. The estimated neural and velocity dependent parameter reflexive torque did not associate.

Applicability of the instrumented EMG-driven model approach

With VAF values over 99% and only a few trials being discarded because of low VAF values (2%) the developed model approach seems well applicable to the present clinical case. Previous research showed that the internal model validity was good, test-retest reliability fair to good and that the method has clinical potential[26].

Measured and estimated parameters before and after BoNT injection

The effect of BoNT treatment was reflected by the increase in dRoM and the shift of NA towards the anatomical ankle angle. This is assumed to originate from an increased length of the musculo-tendon complex of the TS muscle during rest conditions and may thus be regarded a main effect of BoNT treatment[27;28]. The other parameters did not show changes as a function of BoNT treatment, which might be due to a large variability within the included cohort and the current lack of means to discriminate potential responders from non-responders in combination with a small sample size. The estimated observations cannot be compared to a gold standard that measures the effect of BoNT treatment because yet lacking. Clinically, we have to do with scales like the mAS with its acknowledged problems of sensitivity and reliability[16]. Significant effects of BoNT on the mAS may only be found in large study samples[29], averaging the large variation in e.g. doses, injection sites and techniques into account[14]. Changes in dRoM and shift of NA to the anatomical ankle angle may be an alternative clinical outcome parameter for

treatment evaluation. Further studies on validity and sensitivity to e.g. variations in dose, are needed in order to fully judge the merits of RoM measurements.

Associations between baseline values and changes in measured and estimated parameters

Changes in measured ankle dRoM and NA were associated with baseline values and changes of the estimated non-neural tissue parameters slack length of TS and peripheral tissue stiffness and estimated EMG rest activity of soleus. Non-neural tissue parameters are assumed to relate to changes in length of musculo-tendon structures thus explaining dRoM and NA more than the neural reflexive torque. Relating the changes in ankle dRoM and NA to the estimated neural reflexive and non-neural tissue properties to joint stiffness and measured rest EMG at baseline provided for the opportunity to predict the effects of BoNT in a heterogeneous group of responders and non-responders to BoNT.

BoNT may decrease background muscle activation: evidence for the "Burne" over the "Lance" concept of spasticity.

Improvement of dRoM and NA following BoNT treatment can potentially be explained by a decrease in background activation of the TS muscle. BoNT results in the relaxation (i.e. lengthening) of the contractile element and thus a shortening and relaxation of the serial elastic length (Figure 6.2). This concept is substantiated by an increase in estimated slack length. Slack length is assumed to reflect the muscle fiber slack length in combination with the muscle fiber pennation angle.

Additional evidence for background activation reduction is provided by the decrease in measured EMG rest activity of soleus, which is associated with the shift of the NA towards anatomical ankle angle. Also the absence of associations of BoNT treatment with reflexive torque suggests the evidence for background muscle activation reduction. The background muscle activation was not accounted for in the model and may therefore also affect the non-neural tissue parameters.

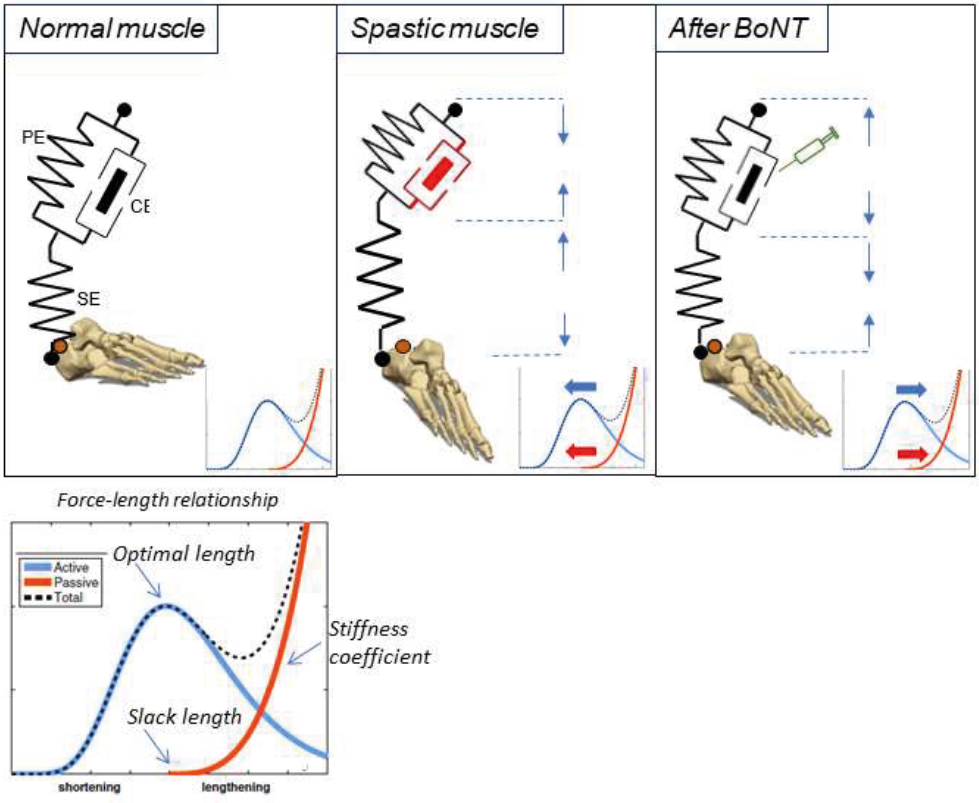


Figure 6.2: *Schematic illustration of a Hill type triceps surae and Achilles tendon (top) with the contractile element (CE), the parallel element (PE) and the serial elastic component (SE) and the muscle force-length relationship (bottom). Left: in the "normal" relaxed condition the foot is in a neutral position, with the SE and PE in 'slack length'. Middle: In the spastic/contractile condition, the CE is activated and the PE is shortened, while the SE length is increased, the foot rotated in equines position. The passive force-length relation and the working point (state) at the active force-length relationships are shifted to the left, meaning that in the neutral position of the ankle, the joint stiffness is increased, resulting in decreased dorsal RoM. Right: BoNT results in the relaxation (i.e. lengthening) of the CE and thus a shortening and relaxation of the SE length. The triceps surae muscle slack length changes/normalizes: the passive force-length relationship and the contractile state of the active force-length relationship are shifted to the right, i.e. towards "normal".*

Note: The shortened triceps surae in the contractile state is a combination of a shortening of the CE in combination with an increase of the muscle fiber pennation angle.

The combination of aforementioned findings is in favor of the "Burne" hypothesis of increased background activation as the underlying pathophysiological mechanism for spasticity[11] and the observed clinical effects of BoNT treatment. The potential mechanism of BoNT treatment may be to reduce background muscle activity so that the contractile muscle tissue relaxes and dorsal RoM increases (Figure 6.2).

All noticed effects are observed under resting task conditions. The higher contractile state of the resting muscle may have an indirect effect on the (increased) sensitivity of muscle spindles and Golgi tendon organs and the spinal reflex thresholds related to the "Lance" hypothesis as neural and non-neural tissue components are in tight interaction[30].

Strength, limitations and clinical implications

This study shows the applicability and merits of high resolution clinimetrics by using a robotic manipulator in combination with an EMG-driven neuromuscular model approach that allows for estimation of underlying properties to joint stiffness, in order to understand the pathophysiological effects of BoNT treatment in stroke patients. Patients were instructed to relaxed and do therefore not require the ability to selectively and voluntary activate muscles, making the method applicable in clinical practice. Addressing effects of dose, injection site and technique and the potential to discriminate responders from non-responders may be important topics for further study considering the costs and the wide spread use of BoNT treatment[14].

There are a number of limitations to the present study. First, the study sample was small, especially considering the expected underlying heterogeneity in patients, history of treatment, dose, selected muscles, injection site etc. Also, the current choice for outcome stratification based on increase of dRoM and NA shift needs further investigation. As background activity cannot be estimated directly yet from the current models, evidence of influence on this component was circumstantial as is the relation of background activity to slack length. Slack length is assumed to reflect both the contractile state of the muscle fibers and the muscle fiber pennation angle. Pennation angles were not in the model nor were measured separately. Therefore the increase of estimated slack length could be indicative for a decrease in pennation angle[27;28]. Ultrasound recordings can strengthen the assumption of changed pennation angles.

Conclusion

We used an instrumented EMG-driven modeling approach to address the effects of BoNT treatment on underlying neural reflexive and non-neural tissue properties of ankle joint stiffness in chronic stroke patients. Significant improvement of measured dorsal range of motion and neutral angle following BoNT treatment were associated with baseline values and changes of estimated peripheral tissue stiffness, estimated triceps surae slack muscle length and measured EMG rest activity of soleus and can potentially be explained by a decrease in background activation of the triceps surae muscle. The approach may be a promising solution in treatment selection, quantifying the effect of treatment and exploring the pathophysiology of spasticity.

Acknowledgements

We would like to thank all patients who participated in the study; all rehabilitation specialists of the Leiden University Medical Center for referral of patients and clinical assessment; Chantal Hofman and Jasper Mulder for conducting the experiment; Stijn Van Eesbeek for technical assistance. This research is supported by the Dutch Technology Foundation (STW), which is part of the Dutch National Organization for scientific research (NWO) and partly funded by the Ministry of Economic Affairs, Agriculture and Innovation (ROBIN project, grant nr. 10733).

References

(1) Ward AB. Spasticity treatment with botulinum toxins. *J Neural Transm (Vienna)* 2008;115:607-616.

(2) Brashear A, Gordon MF, Elovic E et al. Intramuscular injection of botulinum toxin for the treatment of wrist and finger spasticity after a stroke. *N Engl J Med* 2002;347:395-400.

(3) Simpson DM, Gracies JM, Graham HK et al. Assessment: Botulinum neurotoxin for the treatment of spasticity (an evidence-based review): report of the Therapeutics and Technology Assessment Subcommittee of the American Academy of Neurology. *Neurology* 2008;70:1691-1698.

(4) Rosales RL, Chua-Yap AS. Evidence-based systematic review on the efficacy and safety of botulinum toxin-A therapy in post-stroke spasticity. *J Neural Transm (Vienna)* 2008;115:617-623.

(5) Rosales RL, Efendy F, Teleg ES et al. Botulinum toxin as early intervention for spasticity after stroke or non-progressive brain lesion: A meta-analysis. *J Neurol Sci* 2016;371:6-14.

(6) Sheean G. Botulinum toxin treatment of adult spasticity. *Expert Rev Neurother* 2003;3:773-785.

(7) Sheean G. Botulinum toxin should be first-line treatment for poststroke spasticity. *J Neurol Neurosurg Psychiatry* 2009;80:359.

(8) Wu T, Li JH, Song HX, Dong Y. Effectiveness of Botulinum Toxin for Lower Limbs Spasticity after Stroke: A Systematic Review and Meta-Analysis. *Top Stroke Rehabil* 2016;23:217-223.

(9) Pandyan AD, Johnson GR, Price CI, Curless RH, Barnes MP, Rodgers H. A review of the properties and limitations of the Ashworth and modified Ashworth Scales as measures of spasticity. *Clin Rehabil* 1999;13:373-383.

(10) Lance JW. Spasticity: Disordered Motor Control. In: Feldman R, Young R, Koella W, eds. *Symposium Synopsis*. C: Year Book Medical Publishers; 1980;485-495.

(11) Burne JA, Carleton VL, O'Dwyer NJ. The spasticity paradox: movement disorder or disorder of resting limbs? *J Neurol Neurosurg Psychiatry* 2005;76:47-54.

(12) Childers MK, Brashear A, Jozefczyk P et al. Dose-dependent response to intramuscular botulinum toxin type A for upper-limb spasticity in patients after a stroke. *Arch Phys Med Rehabil* 2004;85:1063-1069.

(13) Foley N, Pereira S, Salter K et al. Treatment with botulinum toxin improves upper-extremity function post stroke: a systematic review and meta-analysis. *Arch Phys Med Rehabil* 2013;94:977-989.

(14) Kwakkel G, Meskers CG. Botulinum toxin A for upper limb spasticity. *Lancet Neurol* 2015.

(15) Gupta AD, Chu WH, Howell S et al. A systematic review: efficacy of botulinum toxin in walking and quality of life in post-stroke lower limb spasticity. *Syst Rev* 2018;7:1.

(16) Fleuren JF, Voerman GE, Erren-Wolters CV et al. Stop using the Ashworth Scale for the assessment of spasticity. *J Neurol Neurosurg Psychiatry* 2010;81:46-52.

(17) de Vlugt E, de Groot JH, Schenkeveld KE, Arendzen JH, van der Helm FC, Meskers CG. The relation between neuromechanical parameters and Ashworth score in stroke patients. *J Neuroeng Rehabil* 2010;7:35.

(18) de Gooijer-van de Groep KL, de Vlugt E, de Groot JH et al. Differentiation between non-neural and neural contributors to ankle joint stiffness in cerebral palsy. *J Neuroeng Rehabil* 2013;10:81.

(19) de Gooijer-van de Groep K, de Vlugt E., van der Krogt HJ et al. Estimation of tissue stiffness, reflex activity, optimal muscle length and slack length in stroke patients using an electromyography driven antagonistic wrist model. *Clin Biomech* 2016;35:93-101.

(20) Sloot LH, van der Krogt MM, de Gooijer-van de Groep KL et al. The validity and reliability of modelled neural and tissue properties of the ankle muscles in children with cerebral palsy. *Gait Posture* 2015.

(21) Lindberg PG, Gaverth J, Islam M, Fagergren A, Borg J, Forssberg H. Validation of a new biomechanical model to measure muscle tone in spastic muscles. *Neurorehabil Neural Repair* 2011;25:617-625.

(22) Lorentzen J, Grey MJ, Crone C, Mazevet D, Biering-Sorensen F, Nielsen JB. Distinguishing active from passive components of ankle plantar flexor stiffness in stroke, spinal cord injury and multiple sclerosis. *Clin Neurophysiol* 2010;121:1939-1951.

(23) Wang R, Herman P, Ekeberg O, Gaverth J, Fagergren A, Forssberg H. Neural and non-neural related properties in the spastic wrist flexors: An optimization study. *Med Eng Phys* 2017;47:198-209.

(24) de Gooijer-van de Groep KL, de Groot JH, van der Krogt H, de Vlugt E, Arendzen JH, Meskers CGM. Early Shortening of Wrist Flexor Muscles Coincides With Poor Recovery After Stroke. *Neurorehabil Neural Repair* 2018;1545968318779731.

(25) Hermens HJ, Freriks B, Disselhorst-Klug C, Rau G. Development of recommendations for SEMG sensors and sensor placement procedures. *J Electromyogr Kinesiol* 2000;10:361-374.

(26) de Gooijer-van de Groep KL, de Vlugt E, Arendzen JH, Meskers CGM, de Groot JH. Non-invasive assessment of ankle muscle force-length characteristics post-stroke. 2018.

(27) Kawano A, Yanagizono T, Kadouchi I, Umezaki T, Chosa E. Ultrasonographic evaluation of changes in the muscle architecture of the gastrocnemius with botulinum toxin treatment for lower extremity spasticity in children with cerebral palsy. *J Orthop Sci* 2018;23:389-393.

(28) Tok F, Ozcakar L, Safaz I, Alaca R. Effects of botulinum toxin-A on the muscle architecture of stroke patients: the first ultrasonographic study. *J Rehabil Med* 2011;43:1016-1019.

(29) Gracies JM, Brashear A, Jech R et al. Safety and efficacy of abobotulinumtoxinA for hemiparesis in adults with upper limb spasticity after stroke or traumatic brain injury: a double-blind randomised controlled trial. *Lancet Neurol* 2015;14:992-1001.

(30) de Vlugt E, de Groot JH, Wisman WH, Meskers CG. Clonus is explained from increased reflex gain and enlarged tissue viscoelasticity. *J Biomech* 2011.

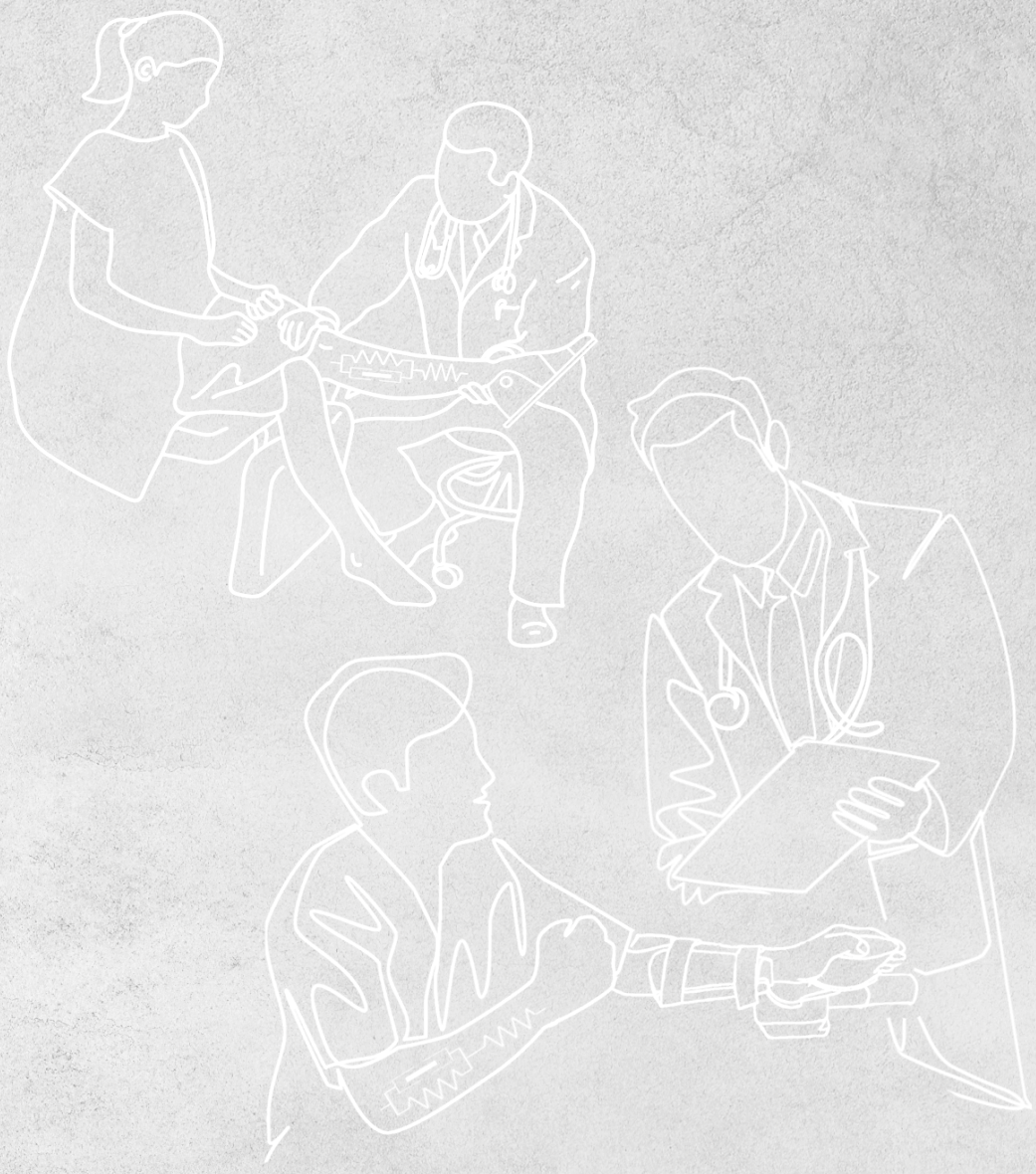
Appendix 6: Supplementary table

***Table 6A*:** *Electrode placement according to seniam guidelines (www.seniam.org)*

Muscle	**Location**
Tibialis anterior	At 1/3 on the line between the tip of the fibula and the tip of the medial malleolus.
Soleus	At 2/3 of the line between the medial condylis of the femur to the medial malleolus.
Gastrocnemius medialis	On the most prominent bulge of the muscle.
Gastrocnemius lateralis	At 1/3 of the line between the head of the fibula and the heel.

CHAPTER 7

Summary and general discussion



The aim of the studies in this thesis was to quantify neural reflexive and non-neural tissue contributors of ankle and wrist joint stiffness in patients with stroke and cerebral palsy using an instrumented electromyography (EMG) driven non-linear neuromuscular modeling approach. Underlying contributors of clinically observed increased joint stiffness, diminished range of motion and flexion deformity, i.e. a shift of joint rest angle, cannot be distinguished by current clinical tests like the Ashworth[1] and Tardieu scale[2;3], which are ordinal, subjective and of low resolution[4-6]. Quantification of underlying contributors is however important for understanding of underlying mechanisms of functional recovery and the effect of therapy on neural and non-neural components to diminish or eventually prevent these motor disorders. The clinical potential of the neuromuscular modeling approach was illustrated by the development over time of neural and non-neural contributors in the sub-acute phase post-stroke and by the effect of botulinum toxin A treatment on these contributors in chronic stroke patients.

Main findings

In chapter 2 neural reflexive and non-neural tissue contributors of ankle joint stiffness were identified in patients with CP using an instrumented non-linear EMG-driven modeling approach[7]. Patients with CP showed a higher neural reflexive stiffness and peripheral tissue stiffness compared to healthy subjects. A large inter-subject variation was found for the ratio between reflexive stiffness and peripheral tissue stiffness showing the heterogeneity of the CP group. In patients with diminished range of motion, a high peripheral tissue stiffness was observed. The non-linear model[7] was refined and extended with parameters describing the passive and active force-length relationships such to estimate the optimal muscle length, slack muscle length and muscle stiffness, of the triceps surae and tibialis anterior (chapter 3). The added parameters enabled to identify muscle shortening and stiffening in patients with stroke. It was demonstrated that the model was internally valid and sensitive for knee angles. In chapter 4 the ankle model was translated to a wrist model. The model included an antagonistic pair of muscle elements reflecting the wrist flexor and extensor muscle groups. The model was valid and sensitive to demonstrate increased reflexive stiffness and peripheral tissue stiffness in chronic stroke patients compared to healthy controls and based on the smaller slack muscle length and smaller optimal muscle length it was suggested that flexor muscles were shortened

in patients with stroke[8]. Development of contributors over time was shown in a longitudinal study in the first 26 weeks post-stroke in chapter 5. Shortening of the wrist flexor muscles was demonstrated to occur as early as 4 to 5 weeks in a group of patients with poor prognosis for functional outcome at 26 weeks post-stroke and poor functional recovery of the upper extremity that clinically showed increased joint stiffness and wrist flexion deformity compared to patients with good recovery. Onset of neural reflexive stiffness in the poor recovery group occurred around week 12[9]. Temporal identification of components contributing to joint stiffness and flexion deformity post-stroke may prompt longitudinal interventional studies to further evaluate and eventually prevent the development of tissue shortening.

The effect of a common clinical intervention to reduce stiffness, increase dorsiflexion range of motion and counteract undesirable rest angle shifts, i.e. botulinum toxin A injection, on the neural reflexive and non-neural tissue contributors was observed in a longitudinal study in chronic stroke patients (chapter 6). Significant improvements in dorsal range of motion and shift of neutral angle, i.e. the rest angle of the joint at zero torque, were observed, which coincided with an estimated lengthening of the musculo-tendon complex of the triceps surae after botulinum toxin A treatment. Aforementioned improvements could be related to peripheral tissue stiffness, muscle slack length and soleus rest activity and could not be related to reflex activity. The results found in this study support evidence of the effect of botulinum toxin A on background muscle activity, i.e. muscle activation at rest, in post-stroke spasticity. These findings show the possibility to relate clinical observed changes, i.e. diminished range of motion and shift of rest angle, to its underlying neural and non-neural contributors and further in its pathophysiological changes which is required for understanding, diagnosis and follow-up. As the outcome parameters proved to be sensitive for treatment, these findings indicate that the modeling approach may be a powerful tool in treatment selection and quantifying the effect of treatment.

Reflection

Non-neural tissue changes precede neural reflexes changes

In the EXPLICIT-trial (chapter 5) patients were followed 6 months post-stroke and stratified by prognosis for functional outcome at 26 weeks post-stroke, based on presence of finger extension and NIHSS, and recovery, based on ARAT[10]. This resulted in three groups: patients with good prognosis for functional recovery and good recovery, patients with poor prognosis and good recovery and patients with poor prognosis and poor recovery. In the group with poor recovery smaller wrist flexor slack lengths, representing muscle shortening, and increased peripheral tissue stiffness were observed to occur within 4-5 weeks after stroke followed by increased neural reflexive stiffness starting around 3 months.

Recovery after stroke varies with the nature and severity of the initial deficit after a cerebrovascular accident and is determined by unknown biological processes[11]. The mechanism of recovery of motor function on one side and development of shifted rest angle of the wrist on the other side are still poorly understood and mainly adhere to the first 8 weeks post-stroke[12;13]. A diminished neural input might result in disuse or immobilization; immobilized muscles in a shortened position adapt to their resting length and lose sarcomeres to develop force at their shortened length[14-18]. At comparable joint angles and compared to healthy muscles, the strain in spastic muscles is higher resulting in higher resistive muscle forces and a consequently higher joint stiffness due to the diminished number of sarcomeres in series[19]. Increased muscle strain in shortened muscle may potentially result in increased spindle response and consequently increased spinal reflex activity[16]. The development of increased background activation as a consequence of altered neural input may also result in hyperexcitability of reflexes[20;21]. There were no differences between the different groups in EMG magnitudes at rest suggesting that there was no difference in background muscle activation between the groups[9]. However, further substantiation requires a model that enables estimation of this neural contributor.

Non-neural tissue changes between the different recovery groups were observed within four weeks. An important focus in these first weeks might be to prevent the development of tissue changes in the acute and sub-acute phase post-stroke. Avoiding immobilization in a shortened position early after stroke might be an important aspect to prevent tissue changes. Possible treatments in the poor prognosis group may be to start immediately with physical therapy,

neuromuscular stimulation or splinting and casting to prevent flexion deformity. The instrumented non-linear neuromuscular modeling approach is a useful tool for follow-up to observe the neural and non-neural changes in time that correlate with the clinical observed changes, e.g. wrist flexion deformity, and it may be a useful tool to guide intervention at the right moment and at the right neuromuscular property.

Botulinum toxin A lowers background muscle activation

At 26 weeks post-stroke, patients with poor recovery showed increased neural reflexive torque and shortened and stiffened wrist flexor muscles resulting in increased peripheral tissue stiffness compared to stroke patients with good recovery[9]. This was in accordance with the results found in chronic stroke patients with an average of 30 (SD 27.6) months post-stroke (chapter 4). Here was found that patients with a modified Ashworth score of 1 or higher had increased reflexive stiffness of flexors, shortened flexor muscles and increased peripheral tissue stiffness compared to healthy subjects and patients with a modified Ashworth score of 0[8].

Botulinum toxin A treatment is a common clinical procedure to reduce joint stiffness, to increase dorsal range of motion and to correct shifted joint resting positions[22-29]. Botulinum toxin A blocks the release of acetylcholine from the nerve terminal, thereby uncoupling the excitation- contraction mechanism and thus reducing muscle (hyper)activity[26]. A lack of understanding the concept of spasticity in stroke may prevent optimal use of botulinum toxin A. It is important to know what the effect is of botulinum toxin A on the neural and non-neural components of joint stiffness and what the effect is on the association between these components, e.g. how will changes in the neural component interact with the changes of the non-neural components after stroke?[30]

After botulinum toxin A treatment, the dorsal range of motion increased and the neutral rest angle shifted (chapter 6). Baseline values and changes in peripheral tissue stiffness and triceps slack length were associated with the changes in dorsal range of motion and neutral angle and change in soleus EMG rest activity was associated with change in neutral angle. There were no associations found for changes in dorsal range of motion and neutral angle and changes in reflex activity. Large variation between patients was observed; not all of the patients showed improvements in outcome measures suggesting that there were responders and non-responders

to botulinum toxin A. Patients with high baseline peripheral tissue stiffness and/or small slack triceps muscle length seemed to benefit from botulinum toxin A. By examining patients on these properties, it may be possible to predict which patients might benefit from botulinum toxin A. Long term administration of botulinum toxin creates weakness and atrophy which may worsen motor function. Identifying the non-responders by low/normal peripheral tissue stiffness and/or normal slack length may help to prevent these undesirable effects and lowers medical expenses.

Following the administration of botulinum toxin A we were able to identify changes in the neural and non-neural contributors that were associated to increased dorsal range of motion and shifted neutral rest angle. This offers opportunities for further research: e.g. to study the effect of botulinum toxin A at an early stage after brain injury or to study the dose-response in botulinum toxin treatment[30].

Botulinum toxin is generally administered to reduce the neural reflexive component as spasticity is often defined according to the concept of Lance as a velocity dependent resistance to passive stretch[31]. In the current study, spasticity was explained by increased muscle activation at rest, i.e. background muscle activation[21]. Improvement in dorsal range of motion and neutral rest angle after botulinum toxin A can be explained by a decrease in an active contributor under rest conditions of the triceps surae muscles: botulinum toxin A may reduce background muscle activity so that the muscle relaxes and muscle length and range of motion increases. No associations in changes in dorsal range of motion and neutral angle were found for the neural reflexive components. Lowering background muscle activation by botulinum toxin might lower the increased reflex activity in contracted muscles[21], but this could not be confirmed in chapter 6 as the study was under passive conditions.

Background muscle activation could not be identified directly but may affect other parameters resulting in e.g. increased peripheral tissue stiffness and decreased slack muscle length, indicative for a decrease in pennation angle due to relaxation of muscle[32;33]. Considering the importance of background muscle activation as a neural contributor of joint stiffness, future model developments should be aimed at quantification of aforementioned contributor.

Development of joint stiffness in stroke and cerebral palsy

This thesis mainly focuses on stroke but application of the neuromuscular modeling approach was also shown in a group of patients with cerebral palsy. Both stroke and cerebral palsy are upper motor neuron diseases. Stroke appears mostly in adults in the developed brain; Cerebral palsy occurs in the fetal or neonatal developing brain[34]. Consequently, the posture and movement disorders may have a different sequel between the groups, which might be reflected in the neural and non-neural tissue distribution of joint stiffness. In patients with stroke we observed shortening of wrist flexor muscles around week 4 to 5 post-stroke and reflexive stiffness around week 12[9]. The development of contributors of joint stiffness over time in patients with cerebral palsy is not yet well described. From literature we learn that in cerebral palsy passive stiffness may increase over reflex activity with age[35] and that the range of dorsiflexion of the ankle joint decreased on average 19 degrees during the first 18 years of life[36]. From these two studies it is suggested that contribution of underlying components of joint stiffness in cerebral palsy changes over time and that variability in a group of adolescents is expected to be high. This latter was confirmed in our study in cerebral palsy by a large inter-subject variation for the ratio between triceps reflexive torque and peripheral tissue stiffness as we measured adolescents in a wide age range[37]. It would be interesting to study the change of underlying neural reflexive and non-neural tissue contributors of joint stiffness over time to learn more about the development of spasticity in cerebral palsy. As the contribution of neural reflexive and non-neural tissue stiffness might change over time, therapy in children with cerebral palsy needs to be evaluated whenever a new treatment strategy is considered.

Future directions

Assessment in clinical practice

The presented instrumented EMG-driven non-linear neuromuscular modeling approach is applicable in patients showing a variable degree of flexion deformity, diminished range of motion and increased joint stiffness. Applicability was demonstrated in patients with stroke and cerebral palsy. The method is safe, as the range of motion is prevented by hard- and software stops, comfortable for the patient and does not require voluntary contraction. The method

resembles clinical tests, like the Ashworth and Tardieu tests, by the movement over the full range of motion. In contrast to linear system identification methods that apply small deviations of e.g. joint angle, performing movement over the full range of motion resembles functional movement more closely. Awareness is needed in patients with small range of motion: the movement velocity needs to be high enough to induce reflexes.

Assessment under passive conditions, as in the current study, does not resemble functional tasks that need voluntary muscle contraction, like walking. This requires assessment under active conditions.

Clinical applicability could be enhanced by reducing the preparation time which is two to three times longer than the measurements time, e.g. due to placing EMG electrodes on the muscles which is a precise task and necessary to quantify the neural and non-neural tissue parameters. Methods without EMG were developed, like the NeuroFlexor method, which showed good agreement with EMG-driven optimization on the overall neural and non-neural components[38;39], but lack the ability of precise quantification of parameters, e.g. slack muscle lengths, optimal muscle lengths and stiffness coefficients. This precise information is essential for insight in pathological mechanism in e.g. the sub-acute phase post-stroke and whether the muscle is shortened and/or stiffened which is of value in treatment selection. In case of e.g. a first exploration of overall joint stiffness in a patient, devices like the NeuroFlexor may be a good alternative.

Neuromuscular model

For administration of botulinum toxin A in e.g. the triceps surae, it can be of benefit to know whether the gastrocnemii are most affected or the soleus muscle. With the neuromuscular modeling approach it was possible to discriminate between groups of lumped muscle, e.g. plantar flexors and dorsiflexors, but not between individual muscles. An alternative method was presented for the ankle in chapter 3: by changing the knee angle, the contribution of the gastrocnemii muscles and soleus muscle was varying.

Muscle relaxation and activation, background muscle activation and muscle atrophy interfere with the muscle pennation angle[32;33;40]. This parameter was not included in the present model. Also, the elastic muscle tendon was not included. Including the Achilles tendon in the ankle

model did not significantly affect the model parameters in healthy subjects[41], but could be of value in patients with different phenotypes as Achilles tendon mechanical properties might be altered post-stroke[42]. Changes in pennation angle affect the passive and active force-length curves and thus interfere with the model parameters slack length, stiffness and optimal length. Thus it was not possible to determine whether an increased slack length in patients post-stroke may be caused by a reduced pennation angle due to muscle atrophy[40]. Additional measurements, like ultrasound, are required to study pennation angles as an additional input to the model.

Clinical implications and recommendations

The results in this thesis are a step forward in answering "when" to treat stroke patients by performing longitudinal assessments. The EMG-driven neuromuscular modeling approach offers opportunity to gain more insight in the development of increased joint stiffness, diminished range of motion and rest angle shifts. This information is of value to prevent motor disorder developments in future.

The results in this thesis also gives direction to the question "how" to treat stroke patients, i.e. which treatment option is most effective in each individual patient, and is a step forward towards personalized treatment. Addressing effects of dose, injection site and technique and the potential to discriminate responders from non-responders are important subjects for further study considering the costs and the wide spread use of botulinum toxin A treatment. Quantification of neural and non-neural components is essential to diminish and eventually prevent motor disorders thereby improving activity of daily live and also quality of live in patients with stroke.

References

(1) Ashworth B. Preliminary trial of carisoprodol in multiple sclerosis. *Practitioner* 1964;192:540-542.

(2) Tardieu C, Huet dlT, Bret MD, Tardieu G. Muscle hypoextensibility in children with cerebral palsy: I. Clinical and experimental observations. *Arch Phys Med Rehabil* 1982;63:97-102.

(3) Haugh AB, Pandyan AD, Johnson GR. A systematic review of the Tardieu Scale for the measurement of spasticity. *Disabil Rehabil* 2006;28:899-907.

(4) Lorentzen J, Grey MJ, Crone C, Mazevet D, Biering-Sorensen F, Nielsen JB. Distinguishing active from passive components of ankle plantar flexor stiffness in stroke, spinal cord injury and multiple sclerosis. *Clin Neurophysiol* 2010;121:1939-1951.

(5) Fleuren JF, Voerman GE, Erren-Wolters CV et al. Stop using the Ashworth Scale for the assessment of spasticity. *J Neurol Neurosurg Psychiatry* 2010;81:46-52.

(6) Meskers CG, de Groot JH, de Vlugt E, Schouten AC. NeuroControl of movement: system identification approach for clinical benefit. *Front Integr Neurosci* 2015;9:48.

(7) de Vlugt E, de Groot JH, Schenkeveld KE, Arendzen JH, van der Helm FC, Meskers CG. The relation between neuromechanical parameters and Ashworth score in stroke patients. *J Neuroeng Rehabil* 2010;7:35.

(8) de Gooijer-van de Groep K, de Vlugt E., van der Krogt HJ et al. Estimation of tissue stiffness, reflex activity, optimal muscle length and slack length in stroke patients using an electromyography driven antagonistic wrist model. *Clin Biomech* 2016;35:93-101.

(9) de Gooijer-van de Groep KL, de Groot JH, van der Krogt H, de Vlugt E, Arendzen JH, Meskers CGM. Early Shortening of Wrist Flexor Muscles Coincides With Poor Recovery After Stroke. *Neurorehabil Neural Repair* 2018;1545968318779731.

(10) Kwakkel G, Meskers CG, van Wegen EE et al. Impact of early applied upper limb stimulation: the EXPLICIT-stroke programme design. *BMC Neurol* 2008;8:49.

(11) Dobkin BH. Clinical practice. Rehabilitation after stroke. *N Engl J Med* 2005;352:1677-1684.

(12) Kwakkel G, Kollen B. Predicting improvement in the upper paretic limb after stroke: a longitudinal prospective study. *Restor Neurol Neurosci* 2007;25:453-460.

(13) van Kordelaar J, van Wegen E, Kwakkel G. Impact of time on quality of motor control of the paretic upper limb after stroke. *Arch Phys Med Rehabil* 2014;95:338-344.

(14) Tabary JC, Tabary C, Tardieu C, Tardieu G, Goldspink G. Physiological and structural changes in the cat's soleus muscle due to immobilization at different lengths by plaster casts. *J Physiol* 1972;224:231-244.

(15) Williams PE, Goldspink G. Changes in sarcomere length and physiological properties in immobilized muscle. *J Anat* 1978;127:459-468.

(16) Gracies JM. Pathophysiology of spastic paresis. I: Paresis and soft tissue changes. *Muscle Nerve* 2005;31:535-551.

(17) Kelleher AR, Gordon BS, Kimball SR, Jefferson LS. Changes in REDD1, REDD2, and atrogene mRNA expression are prevented in skeletal muscle fixed in a stretched position during hindlimb immobilization. *Physiol Rep* 2014;2:e00246.

(18) Wisdom KM, Delp SL, Kuhl E. Use it or lose it: multiscale skeletal muscle adaptation to mechanical stimuli. *Biomech Model Mechanobiol* 2015;14:195-215.

(19) Lieber RL, Friden J. Spasticity causes a fundamental rearrangement of muscle-joint interaction. *Muscle Nerve* 2002;25:265-270.

(20) Denny-Brown D. Chapter XII. The extrapyramidal cortical system. *The Cerebral Control of Movement*. Liverpool: University Press; 1966;173.

(21) Burne JA, Carleton VL, O'Dwyer NJ. The spasticity paradox: movement disorder or disorder of resting limbs? *J Neurol Neurosurg Psychiatry* 2005;76:47-54.

(22) Brashear A, Gordon MF, Elovic E et al. Intramuscular injection of botulinum toxin for the treatment of wrist and finger spasticity after a stroke. *N Engl J Med* 2002;347:395-400.

(23) Sheean G. Botulinum toxin treatment of adult spasticity. *Expert Rev Neurother* 2003;3:773-785.

(24) Sheean G. Botulinum toxin should be first-line treatment for poststroke spasticity. *J Neurol Neurosurg Psychiatry* 2009;80:359.

(25) Ward AB. Spasticity treatment with botulinum toxins. *J Neural Transm (Vienna)* 2008;115:607-616.

(26) Simpson DM, Gracies JM, Graham HK et al. Assessment: Botulinum neurotoxin for the treatment of spasticity (an evidence-based review): report of the Therapeutics and Technology Assessment Subcommittee of the American Academy of Neurology. *Neurology* 2008;70:1691-1698.

(27) Rosales RL, Chua-Yap AS. Evidence-based systematic review on the efficacy and safety of botulinum toxin-A therapy in post-stroke spasticity. *J Neural Transm (Vienna)* 2008;115:617-623.

(28) Rosales RL, Efendy F, Teleg ES et al. Botulinum toxin as early intervention for spasticity after stroke or non-progressive brain lesion: A meta-analysis. *J Neurol Sci* 2016;371:6-14.

(29) Wu T, Li JH, Song HX, Dong Y. Effectiveness of Botulinum Toxin for Lower Limbs Spasticity after Stroke: A Systematic Review and Meta-Analysis. *Top Stroke Rehabil* 2016;23:217-223.

(30) Kwakkel G, Meskers CG. Botulinum toxin A for upper limb spasticity. *Lancet Neurol* 2015.

(31) Lance JW. Spasticity: Disordered Motor Control. In: Feldman R, Young R, Koella W, eds. *Symposium Synopsis*. C: Year Book Medical Publishers; 1980;485-495.

(32) Tok F, Ozcakar L, Safaz I, Alaca R. Effects of botulinum toxin-A on the muscle architecture of stroke patients: the first ultrasonographic study. *J Rehabil Med* 2011;43:1016-1019.

(33) Kawano A, Yanagizono T, Kadouchi I, Umezaki T, Chosa E. Ultrasonographic evaluation of changes in the muscle architecture of the gastrocnemius with botulinum toxin treatment for lower extremity spasticity in children with cerebral palsy. *J Orthop Sci* 2018;23:389-393.

(34) Stavsky M, Mor O, Mastrolia SA, Greenbaum S, Than NG, Erez O. Cerebral Palsy-Trends in Epidemiology and Recent Development in Prenatal Mechanisms of Disease, Treatment, and Prevention. *Front Pediatr* 2017;5:21.

(35) Pierce SR, Prosser LA, Lauer RT. Relationship between age and spasticity in children with diplegic cerebral palsy. *Arch Phys Med Rehabil* 2010;91:448-451.

(36) Hagglund G, Wagner P. Spasticity of the gastrosoleus muscle is related to the development of reduced passive dorsiflexion of the ankle in children with cerebral palsy. *Acta Orthop* 2011;82:744-748.

(37) de Gooijer-van de Groep KL, de Vlugt E, de Groot JH et al. Differentiation between non-neural and neural contributors to ankle joint stiffness in cerebral palsy. *J Neuroeng Rehabil* 2013;10:81.

(38) Gaverth J, Sandgren M, Lindberg PG, Forssberg H, Eliasson AC. Test-retest and inter-rater reliability of a method to measure wrist and finger spasticity. *J Rehabil Med* 2013;45:630-636.

(39) Scholte L. *Validation of the NeuroFlexor method for obtaining the neural and intrinsic component of wrist hyper-resistance post stroke*. TU Delft, The Netherlands; 2018.

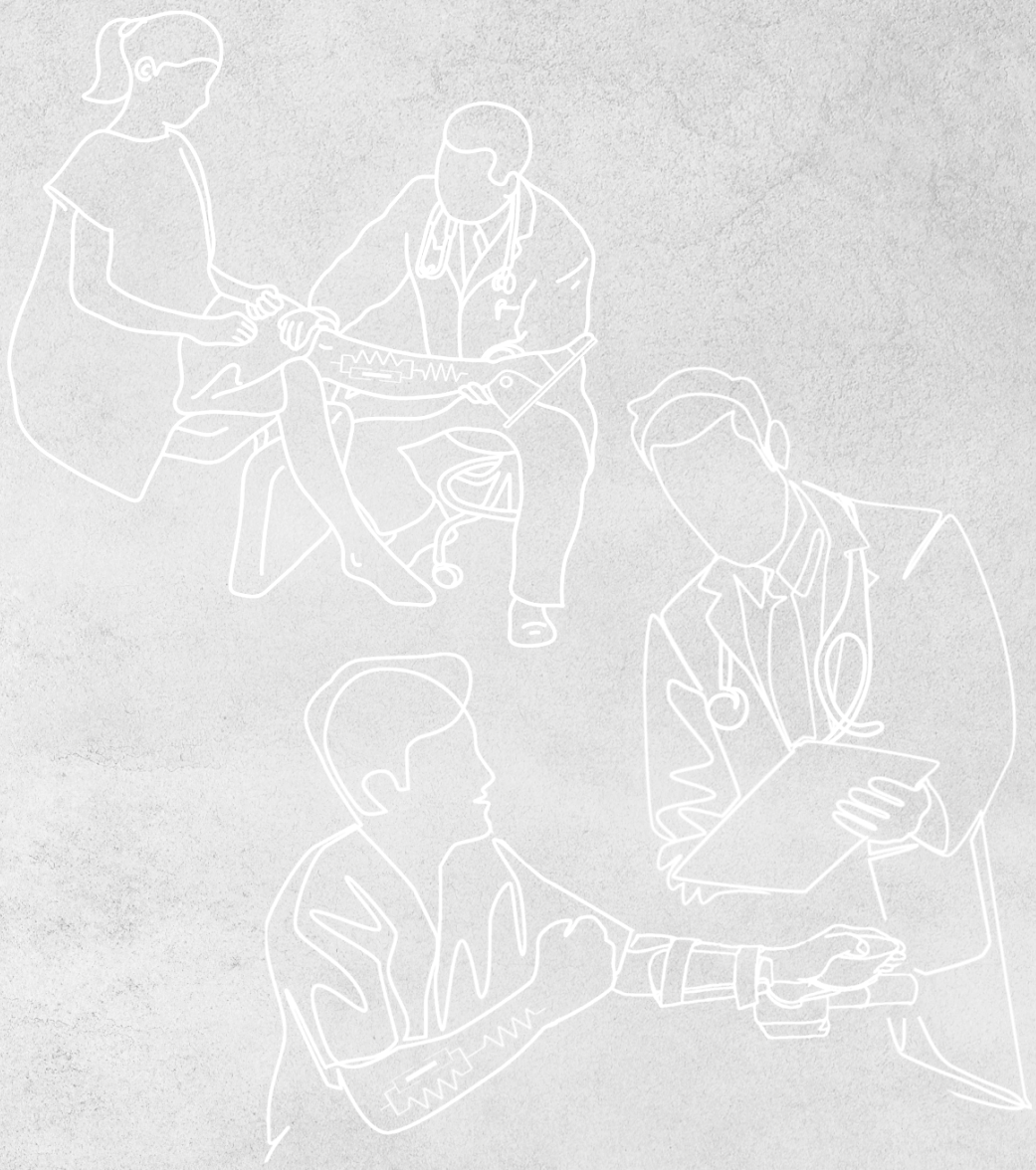
(40) Ramsay JW, Buchanan TS, Higginson JS. Differences in Plantar Flexor Fascicle Length and Pennation Angle between Healthy and Poststroke Individuals and Implications for Poststroke Plantar Flexor Force Contributions. *Stroke Res Treat* 2014;2014:919486.

(41) van de Poll KD. *Estimating ankle muscle parameters.* TU Delft, The Netherlands; 2016.

(42) Zhao H, Ren Y, Wu YN, Liu SQ, Zhang LQ. Ultrasonic evaluations of Achilles tendon mechanical properties poststroke. *J Appl Physiol* 2009;106:843-849.

CHAPTER 8

Nederlandse samenvatting - Summary in Dutch



Introductie

Dit proefschrift gaat over het meten van de gevolgen van een hersenbeschadiging op stijfheid van gewrichten en haar onderliggende factoren: neurale (reflexen) en niet-neurale (spier) weefsel eigenschappen. In het bijzonder wordt gekeken naar de gevolgen na cerebrale parese en cerebro vasculair accident (CVA). Cerebrale parese is een beschadiging van de hersenen die voor of tijdens de geboorte ontstaat, bijvoorbeeld door zuurstofgebrek, en wordt gezien bij 2 per 1000 levende geboortes[1;2]. Een CVA of beroerte is een hersenbeschadiging op latere leeftijd verkregen door een acute stoornis in de bloedvoorziening naar de hersenen, waardoor de hersenen te weinig zuurstof krijgen. In de meeste gevallen (80%) komt dit zuurstoftekort door een vernauwing of verstopping van een ader in de hersenen (herseninfarct); een andere oorzaak is een hersenbloeding[3]. Het merendeel van de mensen dat een CVA krijgt is ouder dan 65 jaar. Omdat onze samenleving vergrijst, zal daarom de mate waarin CVA voorkomt, toenemen. Op dit moment is het de tweede belangrijkste doodsoorzaak wereldwijd en staat het hoog op de ranglijst van ziekten die beperkingen met zich mee brengen[4-6].

De laatste decennia zijn verbeteringen doorgevoerd in de acute patiëntenzorg na een CVA wat resulteert in verhoogde overlevingskansen en vermindering van de initiële hersenschade. Dit laatste door toepassing van acute antistolling (trombolyse) en het verwijderen van het stolsel (trombectomie). Doordat de overleving beter is, moeten meer mensen leven met de gevolgen van een CVA. Dat kunnen problemen zijn met het bewegen, maar ook met taal, spraak en mentale en geestelijke gesteldheid[7;8]. Stoornissen in het bewegen gaan vaak gepaard met een verhoogde stijfheid van gewrichten, beperkingen in gewrichtsuitslagen, een abnormale buigstand (bijvoorbeeld een spitsvoet) en parese: een verminderde kracht en selectief kunnen aansturen van een spier[9].

De revalidatiegeneeskunde maakt in het handelen gebruik van instrumenten en terminologie die passen binnen het ICF model (International Classification of Functioning, Disability and Health)[10;11]. In het ICF model staat het functioneren van de patiënt in zijn omgeving centraal. Het menselijk functioneren en de factoren die daarop van invloed zijn, worden benaderd vanuit de wisselwerking tussen de verschillende aspecten van de gezondheidstoestand en de externe en persoonlijke factoren[10]. Op het ICF niveau “functies en anatomische eigenschappen” richten behandelingen zich onder andere op het verminderen van stijfheid, het stabiel houden of

verbeteren van het bewegingsbereik van gewrichten en het corrigeren van de abnormale rusthoek.

De combinatie van stijfheid en overactiviteit van spieren wordt klinisch vaak “spasticiteit” genoemd. Echter, de definitie van spasticiteit is nog steeds een punt van discussie[9;12]. Spasticiteit komt in 20-30% van de CVA patiënten voor[13]. Bij spasticiteit gaat men uit van een neuraal (uit de hersenen of ruggenmerg) geïnduceerde reflexstijfheid of anders gezegd een snelheidsafhankelijke weerstand van het gewricht bij passief bewegen (definitie van Lance)[14]. Het wordt echter steeds meer duidelijk dat bij gewrichtsstijfheid sprake is van een combinatie en/of interactie van neurale (reflexieve) en niet-neurale (spier) weefsel eigenschappen[15-18]. In de klinische praktijk is niet altijd duidelijk of de gewrichtsstijfheid het gevolg is van neurale over-activatie van spieren of door niet-neurale verstijving en/of verkorting van (spier) weefsel of een combinatie van beide[15;19]. Het onderscheid is van belang voor het juist toepassen van therapie, bijvoorbeeld botuline toxine bij gewrichtsstijfheid van neurale origine en spalk/gips of chirurgie bij gewrichtsstijfheid van niet-neurale origine.

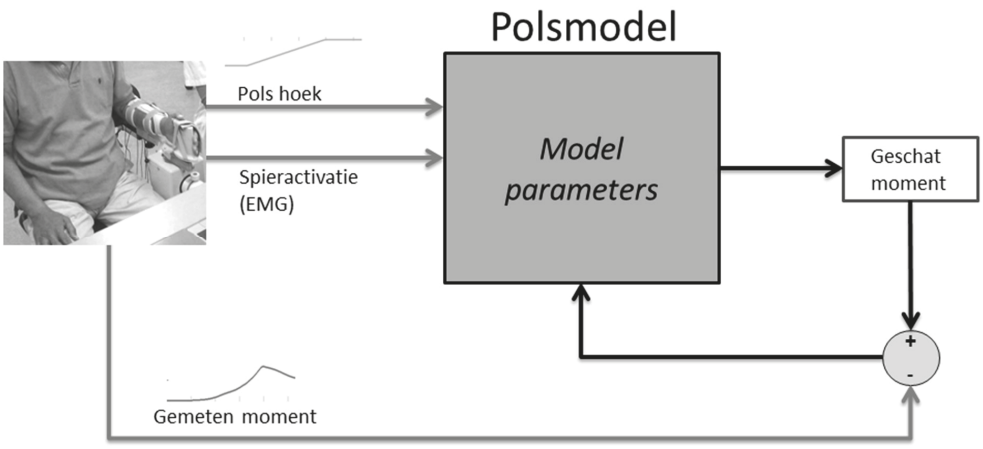
Bij klinische testen, zoals de Ashworth en Tardieu[20-22], wordt het gewricht met een bepaalde snelheid handmatig bewogen (Figuur 8.1) en de weerstand als maat voor gewrichtsstijfheid bepaald. Door dit bij verschillende snelheden te doen wordt getracht de neurale en niet-neurale component te onderscheiden. Helaas zijn deze testen weinig gevoelig en onvoldoende betrouwbaar voor het meten van onderliggende componenten van toegenomen gewrichtsstijfheid. De testen zijn daarnaast subjectief en niet goed reproduceerbaar[16;23;24].



Figuur 8.1*: Demonstratie van de klinische Ashworth test. De voet wordt bewogen richting dorsaalflexie (pijl) om de mate van weerstand bij beweging te bepalen.*

De neurale en niet-neurale componenten kunnen ontrafeld worden door gebruik te maken van systeemidentificatie en parameterschatting (SIPE). Voor deze technieken worden robots gebruikt die precieze verstoringen in de vorm van beweging of kracht op het gewricht uitoefenen (input) en tegelijkertijd de reactie hierop in respectievelijk kracht en beweging meten (output). Door te kijken naar de relatie tussen de opgelegde beweging of kracht en gemeten kracht of beweging kunnen systeemeigenschappen van een gewricht worden bepaald[18;25-27]. Door middel van modellen kunnen systeemeigenschappen vertaald worden naar onderliggende componenten (parameterschatting) zoals de neurale reflexstijfheid en de niet-neurale weefselstijfheid[18;28]. SIPE is reeds toegepast bij gezonde proefpersonen en patiënten[28-33]; echter met gebruikmaking van kleine verstoringen waarbij het systeem (gewrichts-) gedrag niet representatief is voor functionele condities, zoals lopen of het bewegen van een arm. In dit proefschrift worden “Parameter Estimation” (PE-) methoden beschreven die zijn ontwikkeld en toegepast voor het bepalen van gewrichtsstijfheid onder meer functionele condities[34]. De verstoringen die gebruikt worden, lijken op de klinische testen, zoals de Ashworth en Tardieu. De gemeten signalen (spieractiviteit, gewrichtshoek en –moment, i.e. kracht maal arm) worden gecombineerd, waarbij ook gebruik wordt gemaakt van spiermodellen voor de flexoren en

extensoren van het gewricht. Parameters in het spiermodel worden geoptimaliseerd zodat de gezamenlijke krachten rond het (enkel- of pols-) gewricht, ook wel netto gewrichtsmoment genoemd, en welke wordt gemeten met de robot, overeenkomt met het geschatte gewrichtsmoment door het model (Figuur 8.2). De waarden van parameters die vervolgens uit het model komen, bieden een schatting van onderliggende componenten zoals reflexstijfheid en weefselstijfheid.



Figuur 8.2: *Vereenvoudigde weergave van de in dit proefschrift gebruikte methode met de pols als voorbeeld voor het gewricht. Polshoek en spieractivatie (van de polsflexoren en -extensoren) zijn input voor het model. Het polsmodel berekent een polsmoment op basis van de (geschatte) parameters van het model. Dit geschatte moment wordt vergeleken met het moment gemeten door de polsrobot. De parameters van het model worden zo aangepast tot het verschil tussen het geschatte moment en gemeten moment minimaal is. De methode voor het schatten van de parameters van de enkel werkt vergelijkbaar met hier gepresenteerde methode voor de pols.*

Doelen van de onderzoeken beschreven in dit proefschrift zijn:

1. Het kwantificeren van neurale en niet-neurale eigenschappen van gewrichtsstijfheid bij patiënten na een CVA en met cerebrale parese om meer begrip te krijgen van de onderliggende mechanismen in het ontstaan en de ontwikkeling van gewrichtsstijfheid. Hiervoor is een methode ontwikkeld en gevalideerd (hoofdstuk 2, 3, 4).

2. De ontwikkelde methode is vervolgens gebruikt om functioneel herstel na een CVA beter te begrijpen en om het effect van therapie te onderzoeken. Voor het bereiken van dit doel zijn de volgende studies uitgevoerd:
    a) De neurale en niet-neurale eigenschappen van gewrichtsstijfheid werden gemeten gedurende de eerste 26 weken na een CVA bij groepen patiënten met verschillende combinaties van prognose voor functioneel herstel van de bovenste extremiteiten en het uiteindelijke functioneel herstel van de bovenste extremiteiten (hoofdstuk 5).
    b) Het effect van botuline toxine A injecties op de neurale en niet-neurale componenten van gewrichtsstijfheid werd onderzocht om een eerste stap te maken naar selectie voor patiënt-specifieke therapie (hoofdstuk 6).

Hoofdbevindingen

In hoofdstuk 2 van dit proefschrift worden de neurale en niet-neurale eigenschappen van gewrichtsstijfheid in patiënten met cerebrale parese beschreven[35]. Hiervoor werd gebruikt gemaakt van een PE-methode, Figuur 8.2. Patiënten met cerebrale parese lieten een hogere reflexactiviteit (neurale component) en een hogere weefselstijfheid (niet-neurale component) zien, vergeleken met gezonde proefpersonen. Bovendien werd meer variatie in de verhouding van reflexactiviteit en weefselstijfheid gezien in de patiënten dan in de gezonde proefpersonen. In patiënten met een beperkt bewegingsbereik van de enkel was de weefselstijfheid groter dan in patiënten met een groot bewegingsbereik. Deze studie liet zien, naast de mogelijkheid gewrichtsstijfheid te ontbinden in zijn neurale en niet-neurale componenten in patiënten met cerebrale parese, dat de verhouding neuraal/niet-neuraal per patiënt varieert, wat de basis is voor patiënt-specifieke therapie.

In hoofdstuk 3 werd het spiermodel verfijnd en uitgebreid met parameters om te bepalen of bij een patiënt met toegenomen weefselstijfheid sprake is van een verkorting of een verstijving van de spier. Hiervoor werden parameters aan het model toegevoegd en de spierlengte formules verfijnd voor het schatten van de passieve en actieve kracht-lengte relatie van de voetbuigers (kuitspieren, triceps surea) en voetheffers (tibialis anterior). De actieve kracht-lengte relatie geeft de mate weer waarin een spier kracht kan leveren bij een bepaalde lengte van de spier. Bij de optimale spierlengte kan de spier de meeste kracht leveren. Naast het bepalen van de reflexactiviteit, is het model nu in staat de optimale spierlengte, de rustlengte van de spier en de stijfheid van de spier te schatten. Het model bleek gevoelig voor het meten van de parameters bij verschillende kniehoeken. Op deze manier kan de bijdrage van de verschillende kuitspieren, de gastrocnemius spier (bi-articulair) en soleus spier (mono-articulair), gevarieerd worden.

In hoofdstuk 4 werd het enkelmodel vertaald naar een polsmodel dat in staat is om de eigenschappen van de strekkers (extensoren) en buigers (flexoren) van het polsgewricht te schatten[36]. Bij een groep patiënten met een CVA meer dan 6 maanden voorafgaand aan de meting (chronische fase na CVA), werd het model toegepast en werd toegenomen reflexactiviteit en toegenomen weefselstijfheid aangetoond met het model. Het bleek dat de weefselstijfheid samenging met een kleinere optimale spierlengte en kortere rustlengte van de spier, waaruit geconcludeerd werd dat de buigspieren van de pols bij de CVA patiënten waren verkort.

Veranderingen van de neurale en niet-neurale eigenschappen van de polsbuigers en -strekkers in de eerste 26 weken na een CVA worden beschreven in hoofdstuk 5. In deze studie werden de patiënten ingedeeld in groepen, gebaseerd op een goede of slechte prognose voor functionele uitkomst van de bovenste extremiteiten en een daadwerkelijk goed of slecht functioneel herstel van de bovenste extremiteiten na 26 weken. Dit resulteerde in drie groepen: patiënten met goede prognose en goed herstel, patiënten met een slechte prognose en goed herstel en patiënten met slechte prognose en slecht herstel. Bij patiënten met een slechte prognose voor functionele uitkomst na 26 weken en uiteindelijk ook een slecht functioneel herstel werd verkorting van polsbuigers waargenomen rond week 4 en 5 na het CVA[37]. De verkorting van spieren ging samen met een afgenomen rusthoek van de pols gevonden vanaf acht weken na het CVA[38]. Bij deze patiënten werd pas na twaalf weken een toegenomen neurale component gevonden[37]. Deze

resultaten laten zien dat de methode gebruikt kan worden in studies naar het verloop van onderliggende factoren van gewrichtsstijfheid en kan mogelijk ook bijdragen aan het ontwikkelen en evalueren van behandelingen om spierverkorting tegen te gaan.

Botuline toxine A injecties worden veel gegeven in overactieve spieren om zo de gewrichtsstijfheid tegen te gaan, het bewegingsbereik van het gewricht te vergroten en om ongewenste ruststand van het gewricht te herstellen[39-42]. Het effect van deze behandeling op de neurale en niet-neurale componenten van gewrichtsstijfheid van de enkel werd onderzocht in chronische CVA patiënten en beschreven in hoofdstuk 6. Het bewegingsbereik en de ruststand van de enkel werden verbeterd door toepassing van botuline toxine A injecties. Deze verbeteringen gingen samen met een verandering van de weefselstijfheid, spierrustlengte en spieractiviteit (op basis van elektromyografie, EMG) van de achterste kuitspier (m. soleus). Er werd echter geen relatie met reflexactiviteit gevonden. Deze resultaten onderbouwen de hypothese dat botuline toxine A niet zozeer op reflexactiviteit werkt, maar op de rustactiviteit van spieren. Deze rustactiviteit van de spieren is een neurale component die we nog niet kunnen schatten met het huidige model. Ook in deze studie is te zien dat klinisch waarneembare veranderingen, zoals toegenomen gewrichtsstijfheid, verminderd bewegingsbereik en ongewenste ruststand van de enkel, gerelateerd kunnen worden aan onderliggende neurale en niet-neurale weefseleigenschappen van het gewricht. Deze informatie is nuttig voor het begrip van deze drie klinisch waarneembare veranderingen, voor de diagnose en het monitoren ervan. De resultaten laten daarnaast zien dat de methode gebruikt kan worden bij patiënt-specifieke therapiekeuze en vaststellen van het behandeleffect.

Reflectie

Niet-neurale weefselveranderingen gaan vooraf aan neurale reflexieve veranderingen

De mate van functiebeperkingen in het bewegingsapparaat en het herstel na een CVA hangt samen met de plaats en omvang van de hersenschade en wordt bepaald door nog onbekende neurobiologische processen[43]. Van de groep patiënten met een slechte initiële prognose voor functioneel herstel van de bovenste extremiteiten zijn er die functioneel redelijk of goed herstellen, maar ook patiënten die een slecht functioneel herstel laten zien van de bovenste extremiteiten. De mechanismen die enerzijds een goed functioneel herstel en anderzijds de ontwikkeling van toegenomen gewrichtsstijfheid, veranderde ruststand van het gewricht en afgenomen bewegingsbereik bepalen, zijn nog onvoldoende begrepen en spelen zich voornamelijk af in de eerste acht weken na een CVA[44;45]. Een verminderde neurale aansturing van spieren resulteert mogelijk in het niet gebruiken en daardoor immobilisatie van spieren. Spieren die geïmmobiliseerd zijn in een verkorte positie gaan zich aanpassen aan deze verkorte spierlengte en verliezen sarcomeren (contractiele eenheden om spieren samen te trekken) om toch kracht te kunnen uitoefenen met deze kortere spierlengte[46-50]. Als gezonde proefpersonen vergeleken worden met CVA patiënten met verkorte spieren, op een vergelijkbare stand van het gewricht, zal de spanning in de spieren van patiënten veel hoger zijn en dus ook de weerstand bij bewegen, zoals ook beschreven door Lieber en Friden[51]. De verhoogde spanning in verkorte spieren kan bij rek ook bijdragen aan een hogere respons van spierspoeltjes. Spierspoeltjes zijn belangrijk in het genereren van reflexen. Verhoogde gevoeligheid van spierspoeltjes zal resulteren in een hogere reflexactiviteit[48]. Een verhoogde rustactivatie als gevolg van veranderde neurale input, zoals beschreven door Burne en collega's, kan ook leiden tot verhoogde reflexactiviteit[19]. In de longitudinale studie is gekeken naar verhoogde spieractiviteit op basis van EMG gemeten in rust. Er konden geen verschillen worden aangetoond in spieractiviteit tussen de verschillende groepen[37]. Dit is een mogelijke aanwijzing dat de verhoogde reflexactiviteit bij patiënten met slecht functioneel herstel niet werd veroorzaakt door verhoogde spieractiviteit in rust. Omdat spieractiviteit gemeten met EMG een relatieve maat is, is het wenselijk om de bijdrage van de neurale activatie leidend tot spieractiviteit in rust met het model te kunnen kwantificeren. Hiermee zou de hypothese over de bijdrage van rustactiviteit van de spier met meer zekerheid kunnen worden getoetst.

Verschillen in de niet-neurale eigenschappen bij de verschillende groepen op basis van de mate van functioneel herstel van de bovenste extremiteiten waren te zien vanaf vier tot vijf weken na het CVA[37]. Een belangrijk aandachtsgebied voor de revalidatiegeneeskunde in deze eerste weken, kan zijn het voorkomen van weefselveranderingen in de acute en subacute fase (< 6 maanden). In de praktijk betekent dat voorkomen van immobilisatie in flexiestand van het gewricht, waarbij verkorting van de spier wordt tegen gegaan, door op dag één na het CVA te starten met fysiotherapie, stimulatie van spieren en/of een splint of spalk om abnormale gewrichtsstand te voorkomen. De methode beschreven in dit proefschrift kan een belangrijke bijdrage leveren aan het monitoren van neurale en niet-neurale veranderingen en het ondersteunen bij het kiezen van de juiste behandeling gericht op de neurale en/of niet-neurale component op het juiste moment.

Botuline toxine A verlaagt rustactiviteit van de spier

Botuline toxine A wordt vaak toegepast in spieren om activatie van de spier te verminderen en zo de gewrichtsstijfheid te reduceren, het bewegingsbereik van het gewricht te vergroten en de rusthoek van het gewricht te corrigeren[39;40;52-57]. Voor een goed begrip van het effect van botuline toxine A is kennis nodig van de neurale en niet-neurale componenten van het gewricht en interactie(s) tussen beide componenten. De vraag is dan ook wat een verandering in één van deze componenten voor gevolgen heeft voor de andere component[58]. En dus ook wat het effect van een therapie voor invloed heeft op beide componenten. Deze kennis is een voorwaarde voor een optimaal gebruik van botuline toxine A voor het behandelen van bewegingsstoornissen na een CVA.

In een groep met CVA patiënten zagen we na behandeling met botuline toxine A in de kuitspieren dat het bewegingsbereik van de enkel verbeterde richting “normaal” en ook de rusthoek van de enkel normaliseerde. Deze veranderingen in het enkelgewricht gingen samen met veranderingen in weefselstijfheid, lengte van de kuitspieren en verandering in spieractivatie van de achterste kuitspier (soleus, op basis van EMG). Tegen de verwachting in bleek er geen verband tussen de reflexactiviteit en het bewegingsbereik en de rusthoek van de enkel.

Er werd een grote variatie in aanvankelijke weefselstijfheid en spierlengte tussen de patiënten gevonden en niet alle patiënten verbeterden in uitkomstparameters na botuline toxine A injecties. Patiënten met een hoge weefselstijfheid en/of korte lengte van de kuitspieren leken meer baat te hebben bij botuline toxine injecties. Door te "selecteren" op deze eigenschappen zou het succespercentage van botuline toxine A kunnen stijgen, onnodige behandelingen kunnen worden voorkomen en zo de zorgkosten verlaagd worden.

Botuline toxine A wordt over het algemeen toegediend om de reflexcomponent tegen te gaan. In deze studie werd aangetoond dat er een effect lijkt te zijn op de rustactivatie van de spier. De werking van botuline toxine A kan als volgt uitgelegd worden: Botuline toxine A verlaagt de rustactivatie van de spier. Dit zorgt ervoor dat de spier ontspant, waardoor de spierlengte in rust en het bewegingsbereik vergroten. Rustactivatie van de spier is experimenteel lastig vast te stellen en kan met het huidige model niet geschat worden. Omdat we de gemeten kracht zo goed mogelijk willen voorspellen met het model (Figuur 8.2), kan het zijn dat de andere componenten van het spiermodel, zoals de weefselstijfheid en rustlengte van de spier, deze rustactivatie gaan beschrijven. De lengte van de spier kan namelijk ook veranderen door een afname van de pennatiehoek van de spier door ontspanning van de spier[59;60]. Aangezien de rustactivatie van de spier belangrijk lijkt te zijn voor de mate van reflexactiviteit[19] en weerstand bij bewegen en tot nu toe alleen kan worden geschat op basis van het EMG, zal het kwantificeren van deze neurale component met het model een belangrijke volgende uitdaging zijn.

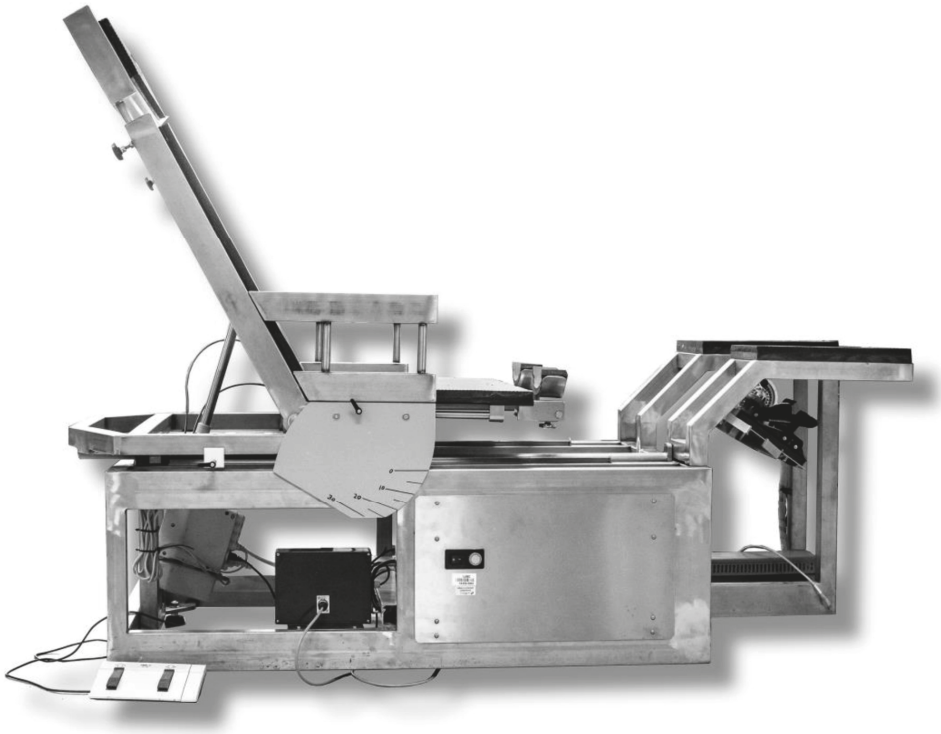
Ontwikkeling van gewrichtsstijfheid in CVA patiënten en patiënten met cerebrale parese

Dit proefschrift richt zich voornamelijk op patiënten na een CVA, maar toepasbaarheid van de methode is ook aangetoond in patiënten met cerebrale parese[35]. De ontwikkeling in de tijd van de neurale en niet-neurale componenten is onderzocht in CVA patiënten[37], maar dit is nog niet gedaan in patiënten met cerebrale parese. Leeftijd heeft in deze CP-groep mogelijk een effect op de verhouding van neurale en niet-neurale componenten[61] en een negatief effect op het bewegingsbereik van de enkel[62]. De invloed van leeftijd bij cerebrale parese dient nader onderzocht te worden om een beter inzicht te krijgen in de ontwikkeling van gewrichtsstijfheid en de mogelijke consequenties voor behandeling.

Toekomstperspectief

Toepassing in de klinische praktijk

De methode gebruikt in de studies kan toegepast worden bij patiënten met verschillende mate van afwijkende gewrichtsstand, afgenomen bewegingsbereik en toegenomen gewrichtsstijfheid. In dit proefschrift is de methode toegepast bij patiënten met cerebrale parese en CVA. De methode is veilig, comfortabel voor de patiënt en vereist geen vrijwillige aansturing van de spieren. In Figuur 8.3 is de huidige opstelling te zien voor het meten van enkelgewrichtsstijfheid.



Figuur 8.3: *Stoel Achilles (uit gebruikershandleiding (concept 12-03-2019) voor de Achillesstoelcombinatie 1.0, Facilitair Bedrijf, Instrumentele Zaken, ©Leids Universitair Medisch Centrum).*

De in het proefschrift toegepaste PE-methode maakt gebruik van op de klinische Ashworth en Tardieu test gebaseerde bewegingen over het hele bereik van het gewricht. Hierdoor is een vergelijk met klinische testen mogelijk, wat minder het geval zal zijn bij SIPE technieken waarbij met kleine bewegingen wordt gewerkt. Het passief bewegen van het gewricht wijkt wel af van actieve functionele taken zoals lopen.

Klinische toepasbaarheid kan vergroot worden door de voorbereidingstijd te verkorten. De voorbereidingstijd is twee tot drie keer langer dan de meettijd door het plakken van de electroden voor spieractiviteit (EMG) en door het goed positioneren van de patiënt in het apparaat. Er zijn ook methodes zonder EMG. Een voorbeeld hiervan is de NeuroFlexor. De NeuroFlexor laat betrouwbare waarden zien voor de neurale en niet-neurale component[63;64], maar maakt geen onderscheid in onderliggende eigenschappen zoals lengte en stijfheid van de spier. Echter, deze informatie is wel essentieel om onderliggende componenten van gewrichtsstijfheid te onderzoeken en de juiste behandeling te selecteren. Apparaten zoals de NeuroFlexor kunnen een goed alternatief zijn voor een eerste verkenning van de mate van toegenomen gewrichtsstijfheid.

Het spiermodel

De methode beschreven in dit proefschrift gaat uit van spiergroepen (bijvoorbeeld kuitspieren of buigspieren van de pols), maar nog niet van geïsoleerde spieren. Voor toediening van botuline toxine A kan het belangrijk zijn te weten welke spier in de spiergroep het meest bijdraagt aan de gewrichtsstijfheid. In hoofdstuk 3 is een eerste stap gezet door gebruik te maken van de selectieve bijdrage van de kuitspieren aan het enkelmoment bij verschillende kniehoeken. Op deze manier kan de bijdrage van de verschillende kuitspieren, de gastrocnemius spier (bi-articulair) en soleus spier (mono-articulair), gevarieerd worden.

Het model is een vereenvoudiging van de werkelijkheid en keuzes zijn gemaakt welke componenten en parameters essentieel zijn in het model. De belangrijkste twee elementen die onderzocht moeten worden of het meerwaarde heeft deze toe te voegen zijn de pennatiehoek van de spier en de spierpees. In gezonde proefpersonen leek toevoegen van een peesmodel geen significant effect te hebben op de modelparameters van de spier[65]. Echter, na een CVA of

cerebrale parese kan dit wel het geval zijn doordat de peeseigenschappen veranderd kunnen zijn[66]. De pennatiehoek van de spier kan veranderen door spierontspanning en -aanspanning, rustactivatie van de spier en spieratrofie[59;60;67]. Veranderingen in de pennatiehoek hebben invloed op de passieve en actieve kracht-lengte relatie van de spier en kunnen invloed hebben op de modelparameters “rustlengte van de spier”, “weefselstijfheid” en “optimale spierlengte”. Deze pennatiehoek kan door deze afhankelijkheid niet apart worden geschat met het model en zal dus als ‘input’ in het model moeten worden meegegeven. Echografie kan gebruikt worden om pennatiehoeken van de spieren te onderzoeken. Zoals eerder genoemd is het ook wenselijk om met het model de neurale component “rustactivatie van de spier” te schatten.

Klinische implicaties

De resultaten in dit proefschrift brengen ons een stap dichter bij het beantwoorden van de vraag “wanneer” behandeld moet worden, door in de tijd naar veranderingen in neurale en niet-neurale componenten van het gewricht te kijken. Ook geeft het proefschrift richting in het “hoe” we beter kunnen behandelen: welke behandeling is het beste voor welke patiënt? Door verder onderzoek te doen naar dosis, injectieplaats en -techniek en door botuline toxine A alleen te injecteren bij patiënten bij wie vooraf bepaald is dat het effect heeft, kunnen de kosten en gebruik van botuline toxine A mogelijk gereduceerd worden. Het kwantificeren van de neurale en niet-neurale componenten van toegenomen gewrichtsstijfheid bij patiënten is essentieel voor het begrijpen en behandelen van bewegingsbeperkingen met het doel functioneren in de dagelijkse praktijk en kwaliteit van leven te verbeteren.

Referenties

(1) Prevalence and characteristics of children with cerebral palsy in Europe. *Dev Med Child Neurol* 2002;44:633-640.

(2) Odding E, Roebroeck ME, Stam HJ. The epidemiology of cerebral palsy: incidence, impairments and risk factors. *Disabil Rehabil* 2006;28:183-191.

(3) Hersenstichting. 2019. Online Source.

(4) Murray CJ, Vos T, Lozano R et al. Disability-adjusted life years (DALYs) for 291 diseases and injuries in 21 regions, 1990-2010: a systematic analysis for the Global Burden of Disease Study 2010. *Lancet* 2012;380:2197-2223.

(5) Lozano R, Naghavi M, Foreman K et al. Global and regional mortality from 235 causes of death for 20 age groups in 1990 and 2010: a systematic analysis for the Global Burden of Disease Study 2010. *Lancet* 2012;380:2095-2128.

(6) World Health Organization. The top 10 causes of death. 24-5-2018. Online Source.

(7) Skolarus LE, Burke JF, Brown DL, Freedman VA. Understanding stroke survivorship: expanding the concept of poststroke disability. *Stroke* 2014;45:224-230.

(8) Crichton SL, Bray BD, McKevitt C, Rudd AG, Wolfe CD. Patient outcomes up to 15 years after stroke: survival, disability, quality of life, cognition and mental health. *J Neurol Neurosurg Psychiatry* 2016;87:1091-1098.

(9) van der Krogt HJ, Meskers CG, de Groot JH, Klomp A, Arendzen JH. The gap between clinical gaze and systematic assessment of movement disorders after stroke. *J Neuroeng Rehabil* 2012;9:61.

(10) VRA Nederlandse vereniging van revalidatieartsen. 2019. Online Source.

(11) World Health Organization. *International Classification of Functioning, Disability and Health: ICF*. 2011.

(12) Dressler D, Bhidayasiri R, Bohlega S et al. Defining spasticity: a new approach considering current movement disorders terminology and botulinum toxin therapy. *J Neurol* 2018;265:856-862.

(13) Sommerfeld DK, Gripenstedt U, Welmer AK. Spasticity after stroke: an overview of prevalence, test instruments, and treatments. *Am J Phys Med Rehabil* 2012;91:814-820.

(14) Lance JW. Spasticity: Disordered Motor Control. In: Feldman R, Young R, Koella W, eds. *Symposium Synopsis*. C: Year Book Medical Publishers; 1980;485-495.

(15) Dietz V, Sinkjaer T. Spastic movement disorder: impaired reflex function and altered muscle mechanics. *Lancet Neurol* 2007;6:725-733.

(16) Meskers CG, de Groot JH, de Vlugt E, Schouten AC. NeuroControl of movement: system identification approach for clinical benefit. *Front Integr Neurosci* 2015;9:48.

(17) van den Noort JC, Bar-On L, Aertbelien E et al. European consensus on the concepts and measurement of the pathophysiological neuromuscular responses to passive muscle stretch. *Eur J Neurol* 2017;24:981-e38.

(18) van der Helm FC, Schouten AC, de Vlugt E, Brouwn GG. Identification of intrinsic and reflexive components of human arm dynamics during postural control. *J Neurosci Methods* 2002;119:1-14.

(19) Burne JA, Carleton VL, O'Dwyer NJ. The spasticity paradox: movement disorder or disorder of resting limbs? *J Neurol Neurosurg Psychiatry* 2005;76:47-54.

(20) Ashworth B. Preliminary trial of carisoprodol in multiple sclerosis. *Practitioner* 1964;192:540-542.

(21) Tardieu C, Huet dlT, Bret MD, Tardieu G. Muscle hypoextensibility in children with cerebral palsy: I. Clinical and experimental observations. *Arch Phys Med Rehabil* 1982;63:97-102.

(22) Haugh AB, Pandyan AD, Johnson GR. A systematic review of the Tardieu Scale for the measurement of spasticity. *Disabil Rehabil* 2006;28:899-907.

(23) Lorentzen J, Grey MJ, Crone C, Mazevet D, Biering-Sorensen F, Nielsen JB. Distinguishing active from passive components of ankle plantar flexor stiffness in stroke, spinal cord injury and multiple sclerosis. *Clin Neurophysiol* 2010;121:1939-1951.

(24) Fleuren JF, Voerman GE, Erren-Wolters CV et al. Stop using the Ashworth Scale for the assessment of spasticity. *J Neurol Neurosurg Psychiatry* 2010;81:46-52.

(25) Kearney RE, Stein RB, Parameswaran L. Identification of intrinsic and reflex contributions to human ankle stiffness dynamics. *IEEE Trans Biomed Eng* 1997;44:493-504.

(26) van der Kooij H, van der Helm FC. Observations from unperturbed closed loop systems cannot indicate causality. *J Physiol* 2005;569:705.

(27) Schouten AC, de Vlugt E, Van Hilten JJ, van der Helm FC. Design of a torque-controlled manipulator to analyse the admittance of the wrist joint. *J Neurosci Methods* 2006;154:134-141.

(28) Schouten AC, Van de Beek WJ, Van Hilten JJ, van der Helm FC. Proprioceptive reflexes in patients with reflex sympathetic dystrophy. *Exp Brain Res* 2003;151:1-8.

(29) Meskers CG, Schouten AC, de Groot JH et al. Muscle weakness and lack of reflex gain adaptation predominate during post-stroke posture control of the wrist. *J Neuroeng Rehabil* 2009;6:29.

(30) Boonstra TA, Schouten AC, van Vugt JP, Bloem BR, van der Kooij H. Parkinson's disease patients compensate for balance control asymmetry. *J Neurophysiol* 2014;112:3227-3239.

(31) Engelhart D, Pasma JH, Schouten AC et al. Impaired standing balance in elderly: a new engineering method helps to unravel causes and effects. *J Am Med Dir Assoc* 2014;15:227.

(32) Pasma JH, Engelhart D, Maier AB et al. Reliability of System Identification Techniques to Assess Standing Balance in Healthy Elderly. *PLoS One* 2016;11:e0151012.

(33) Klomp A, de Vlugt E, de Groot JH, Meskers CGM, Arendzen JH, van der Helm FCT. Perturbation velocity affects linearly estimated neuromechanical wrist joint properties. *J Biomech* 2018;74:207-212.

(34) de Vlugt E, de Groot JH, Schenkeveld KE, Arendzen JH, van der Helm FC, Meskers CG. The relation between neuromechanical parameters and Ashworth score in stroke patients. *J Neuroeng Rehabil* 2010;7:35.

(35) de Gooijer-van de Groep KL, de Vlugt E, de Groot JH et al. Differentiation between non-neural and neural contributors to ankle joint stiffness in cerebral palsy. *J Neuroeng Rehabil* 2013;10:81.

(36) de Gooijer-van de Groep K, de Vlugt E., van der Krogt HJ et al. Estimation of tissue stiffness, reflex activity, optimal muscle length and slack length in stroke patients using an electromyography driven antagonistic wrist model. *Clin Biomech* 2016;35:93-101.

(37) de Gooijer-van de Groep KL, de Groot JH, van der Krogt H, de Vlugt E, Arendzen JH, Meskers CGM. Early Shortening of Wrist Flexor Muscles Coincides With Poor Recovery After Stroke. *Neurorehabil Neural Repair* 2018;1545968318779731.

(38) van der Krogt H. *Recovery of arm-hand function after stroke: developing neuromechanical biomarkers to optimize rehabilitation strategies* [2019.

(39) Ward AB. Spasticity treatment with botulinum toxins. *J Neural Transm (Vienna)* 2008;115:607-616.

(40) Brashear A, Gordon MF, Elovic E et al. Intramuscular injection of botulinum toxin for the treatment of wrist and finger spasticity after a stroke. *N Engl J Med* 2002;347:395-400.

(41) Simpson DM, Gracies JM, Graham HK et al. Assessment: Botulinum neurotoxin for the treatment of spasticity (an evidence-based review): report of the Therapeutics and Technology Assessment Subcommittee of the American Academy of Neurology. *Neurology* 2008;70:1691-1698.

(42) Rosales RL, Chua-Yap AS. Evidence-based systematic review on the efficacy and safety of botulinum toxin-A therapy in post-stroke spasticity. *J Neural Transm (Vienna)* 2008;115:617-623.

(43) Dobkin BH. Clinical practice. Rehabilitation after stroke. *N Engl J Med* 2005;352:1677-1684.

(44) Kwakkel G, Kollen B. Predicting improvement in the upper paretic limb after stroke: a longitudinal prospective study. *Restor Neurol Neurosci* 2007;25:453-460.

(45) van Kordelaar J, van Wegen E, Kwakkel G. Impact of time on quality of motor control of the paretic upper limb after stroke. *Arch Phys Med Rehabil* 2014;95:338-344.

(46) Tabary JC, Tabary C, Tardieu C, Tardieu G, Goldspink G. Physiological and structural changes in the cat's soleus muscle due to immobilization at different lengths by plaster casts. *J Physiol* 1972;224:231-244.

(47) Williams PE, Goldspink G. Changes in sarcomere length and physiological properties in immobilized muscle. *J Anat* 1978;127:459-468.

(48) Gracies JM. Pathophysiology of spastic paresis. I: Paresis and soft tissue changes. *Muscle Nerve* 2005;31:535-551.

(49) Kelleher AR, Gordon BS, Kimball SR, Jefferson LS. Changes in REDD1, REDD2, and atrogene mRNA expression are prevented in skeletal muscle fixed in a stretched position during hindlimb immobilization. *Physiol Rep* 2014;2:e00246.

(50) Wisdom KM, Delp SL, Kuhl E. Use it or lose it: multiscale skeletal muscle adaptation to mechanical stimuli. *Biomech Model Mechanobiol* 2015;14:195-215.

(51) Lieber RL, Friden J. Spasticity causes a fundamental rearrangement of muscle-joint interaction. *Muscle Nerve* 2002;25:265-270.

(52) Sheean G. Botulinum toxin treatment of adult spasticity. *Expert Rev Neurother* 2003;3:773-785.

(53) Sheean G. Botulinum toxin should be first-line treatment for poststroke spasticity. *J Neurol Neurosurg Psychiatry* 2009;80:359.

(54) Simpson DM, Gracies JM, Graham HK et al. Assessment: Botulinum neurotoxin for the treatment of spasticity (an evidence-based review): report of the Therapeutics and Technology Assessment Subcommittee of the American Academy of Neurology. *Neurology* 2008;70:1691-1698.

(55) Rosales RL, Chua-Yap AS. Evidence-based systematic review on the efficacy and safety of botulinum toxin-A therapy in post-stroke spasticity. *J Neural Transm (Vienna)* 2008;115:617-623.

(56) Rosales RL, Efendy F, Teleg ES et al. Botulinum toxin as early intervention for spasticity after stroke or non-progressive brain lesion: A meta-analysis. *J Neurol Sci* 2016;371:6-14.

(57) Wu T, Li JH, Song HX, Dong Y. Effectiveness of Botulinum Toxin for Lower Limbs Spasticity after Stroke: A Systematic Review and Meta-Analysis. *Top Stroke Rehabil* 2016;23:217-223.

(58) Kwakkel G, Meskers CG. Botulinum toxin A for upper limb spasticity. *Lancet Neurol* 2015.

(59) Tok F, Ozcakar L, Safaz I, Alaca R. Effects of botulinum toxin-A on the muscle architecture of stroke patients: the first ultrasonographic study. *J Rehabil Med* 2011;43:1016-1019.

(60) Kawano A, Yanagizono T, Kadouchi I, Umezaki T, Chosa E. Ultrasonographic evaluation of changes in the muscle architecture of the gastrocnemius with botulinum toxin treatment for lower extremity spasticity in children with cerebral palsy. *J Orthop Sci* 2018;23:389-393.

(61) Pierce SR, Prosser LA, Lauer RT. Relationship between age and spasticity in children with diplegic cerebral palsy. *Arch Phys Med Rehabil* 2010;91:448-451.

(62) Hagglund G, Wagner P. Spasticity of the gastrosoleus muscle is related to the development of reduced passive dorsiflexion of the ankle in children with cerebral palsy. *Acta Orthop* 2011;82:744-748.

(63) Gaverth J, Sandgren M, Lindberg PG, Forssberg H, Eliasson AC. Test-retest and inter-rater reliability of a method to measure wrist and finger spasticity. *J Rehabil Med* 2013;45:630-636.

(64) Scholte L. *Validation of the NeuroFlexor method for obtaining the neural and intrinsic component of wrist hyper-resistance post stroke*. TU Delft, The Netherlands; 2018.

(65) van de Poll KD. *Estimating ankle muscle parameters*. TU Delft, The Netherlands; 2016.

(66) Zhao H, Ren Y, Wu YN, Liu SQ, Zhang LQ. Ultrasonic evaluations of Achilles tendon mechanical properties poststroke. *J Appl Physiol* 2009;106:843-849.

(67) Ramsay JW, Buchanan TS, Higginson JS. Differences in Plantar Flexor Fascicle Length and Pennation Angle between Healthy and Poststroke Individuals and Implications for Poststroke Plantar Flexor Force Contributions. *Stroke Res Treat* 2014;2014:919486.

List of publications

Karin L. de Gooijer-van de Groep, Jurriaan H. de Groot, Hanneke J. van der Krogt, Erwin de Vlugt, J. Hans Arendzen, Carel G.M. Meskers. *Early shortening of wrist flexor muscles coincides with poor recovery after stroke.* Neurorehabil Neural Repair. 2018 Jun;32(6-7):645-654.

Karin L. de Gooijer-van de Groep, Erwin de Vlugt, Hanneke J. van der Krogt, Áróra Helgadóttir, J. Hans Arendzen, Carel G.M. Meskers, Jurriaan H. de Groot. *Estimation of tissue stiffness, reflex activity, optimal muscle length and slack length in stroke patients using an electromyography driven antagonistic wrist model.* Clinical Biomechanics 35 (2016) 93–101

Lizeth H. Sloot, Marjolein M. van der Krogt, **Karin L. de Gooijer-van de Groep**, Stijn van Eesbeek , Jurriaan H. de Groot, Annemieke I. Buizer, Carel G. M. Meskers, Jules G. Becher, Erwin de Vlugt, Jaap Harlaar. *The validity and reliability of modelled neural and tissue properties of the ankle muscles in children with cerebral palsy.* Gait Posture. 2015 Jun;42(1):7-15.

Karin L de Gooijer-van de Groep, Erwin de Vlugt, Jurriaan H de Groot, Hélène CM van der Heijden-Maessen, Dennis HM Wielheesen, Rietje (M) S van Wijlen-Hempel, J Hans Arendzen, Carel GM Meskers. *Differentiation between non-neural and neural contributors to ankle joint stiffness in cerebral palsy.* J Neuroeng Rehabil 2013 Jul 23; 10:81

Karin L. de Gooijer-van de Groep, Frans S. Leijten, Cyrille H. Ferrier, Geertjan J Huiskamp. *Inverse modeling in magnetic source imaging: Comparison of MUSIC, SAM(g2), and sLORETA to interictal intracranial EEG.* Hum Brain Mapp. 2013 Sep;34(9):2032-44.

Karin L. de Gooijer-van de Groep, Zaloa Agirre-Arrizubieta, Geertjan J Huiskamp, Cyrille H. Ferrier, Alexander C. van Huffelen, Frans S. Leijten. *Seizure onset detection in the electrocorticogram by a frequency analysis algorithm versus human observers.* Nov 2009 Epilepsia. 50, p. 174-175 2 p.

Dankwoord

En dan is het proefschrift eindelijk daar! Blij met het resultaat dat nooit tot stand had kunnen komen zonder de hulp en steun van een heleboel mensen die ik graag wil bedanken.

Hans Arendzen, Jurriaan de Groot, Carel Meskers en Erwin de Vlugt. De vele discussies en gesprekken die we gevoerd hebben, jullie enthousiasme en kritische blik hebben mij enorm geholpen. Ik heb inhoudelijk en persoonlijk veel geleerd van dit traject. En ondanks dat we allen op een andere locatie zaten, hebben we elkaar gelukkig (bijna) elke week kunnen spreken. Fijn dat jullie hier elke keer weer tijd voor maakten.

Graag wil ik de leden van de promotiecommissie bedanken voor het beoordelen van het manuscript.

Er hebben veel vrijwilligers meegedaan aan het onderzoek. Zonder jullie was dit proefschrift er niet geweest. Hartelijk dank voor jullie bijdrage!

Ook dank aan de afdeling revalidatie van het LUMC en dan met name de revalidatieartsen, het secretariaat, collega (ex)promovendi, arts-assistenten en studenten voor het ondersteunen in de metingen en meedenken over het onderwerp. Daarnaast de afdeling Instrumentele Zaken van het LUMC voor het ontwikkelen van de Achilles stoel.

Dank aan de overige betrokkenen van het ROBIN project: de onderzoekers en specialisten van de TU Delft en het VU medisch centrum en de betrokken bedrijven. En natuurlijk Stijn en Lizeth. Het was leerzaam en prettig met jullie samenwerken.

Inmiddels werk ik met veel plezier in het value based healthcare team van het St. Antonius ziekenhuis met collega's binnen en buiten ons ziekenhuis. Het heeft mijn blik verruimd om vanuit verschillende kanten de zorg te zien. Bedankt voor de prettige samenwerking. En fijn om ook op het vlak van promoveren ervaringen uit te kunnen wisselen.

Onze vrienden uit Barneveld, Nijkerk, Enschede en Haarlem; Confetti-Gub en V6 vriendinnen: Jullie zijn ons dierbaar! Bedankt voor jullie steun en interesse. Hopelijk hebben we nu weer meer tijd om af te spreken.

En dan natuurlijk mijn paranimfen. Marian, dit jaar beleven we ons 30-jarig jubileum. Als kleuters is onze vriendschap begonnen en dit is zo gebleven. Dank je wel voor je trouwe vriendschap, gezellige momenten en nog zoveel meer!

Jetske, wie had ooit kunnen denken dat we na onze spannende rondrit in Barneveld 15 jaar geleden, nu gezellig bij elkaar op de koffie kunnen en elke week sporten in datzelfde dorp. Zonder jouw inbreng was dat waarschijnlijk niet gebeurd… Bedankt!

Willeke, Arjan, André en Mieke, het is lang geleden dat we bij elkaar in één huis woonden, maar ik kijk terug op een mooie tijd. Inmiddels is mijn/onze familie een heel stuk groter geworden. Al mijn zwagers, schoonzussen, neefjes en nichtjes: Wat fijn om zo'n grote en gezellige familie te hebben!

Bijzonder en dankbaar dat mijn oma van 95 jaar dit mee mag maken!

Pa en ma de Gooijer, ik heb het getroffen met zulke fijne schoonouders! Dank jullie wel voor jullie interesse en dat jullie altijd voor ons klaar staan. En natuurlijk voor jullie bijdrage als proefpersoon.

Pap en mam, jullie betekenen erg veel voor me. Doorzettingsvermogen en er voor gaan is iets dat jullie ons hebben meegegeven en dat kwam met dit proefschrift goed van pas. Maar ook hebben jullie ons geleerd wat echt belangrijk is in dit leven. Dank jullie wel voor jullie liefde en zorgzaamheid.

Lieve Harm, dit proefschrift had ik nooit zonder jouw steun kunnen maken. Gelukkig hebben we nu weer veel meer tijd om met z'n tweeën en vijven leuke dingen te gaan doen. Wie weet gaan we nu weer net als vroeger echte bergen trotseren!

Nathan, Elise en Amélie, woorden schieten tekort om te zeggen hoeveel jullie voor me betekenen. Jullie zijn verreweg het beste wat me is overkomen in de jaren dat dit proefschrift tot stand kwam.

Curriculum vitae

Karine Lamberthe van de Groep werd op 22 november 1984 geboren in Nijkerk. In 2003 voltooide zij haar VWO aan de GSG Guido de Brès in Amersfoort, waarna zij Technische Geneeskunde ging studeren aan de Universiteit van Twente. Na haar bachelor specialiseerde zij zich in “medical signaling”. Ze liep klinische stages op de afdelingen klinische neurofysiologie en de intensive care van het Medisch Spectrum Twente, op de afdeling kinderurologie van het Wilhelmina Kinderziekenhuis in Utrecht en de afdelingen thoraxchirurgie en cardiologie van het Leids Universitair Medisch Centrum. Voor haar masterthesis deed zij een klinische specialisatiestage in het Universitair Medisch Centrum Utrecht op de afdeling klinische neurofysiologie. Haar masterthesis was genaamd “Optimizing the delineation of focal epilepsy”. Karin voltooide haar master Technical Medicine in 2009 en begon daarna aan een 1-jarig onderzoeksproject naar multi-unit microneurografie, een samenwerking tussen de Universiteit Twente, Technische Universiteit Delft en het Universitair Medisch Centrum Utrecht. In december 2010 begon zij haar promotietraject in het ROBIN project op de afdeling revalidatiegeneeskunde in het Leids Universitair Medisch Centrum onder begeleiding van Prof. Dr. J.H. Arendzen, Dr. Ir. J.H. de Groot, Dr. C.G.M. Meskers en Dr. Ir. E. de Vlugt. Het ROBIN project was een samenwerking tussen het Leids Universitair Medisch Centrum, de Technische Universiteit Delft en het VU Medisch Centrum. Sinds maart 2016 is zij werkzaam als data-analist in het value based healthcare team van het St. Antonius Ziekenhuis. Karin is getrouwd met Harm de Gooijer. Samen hebben zij drie kinderen: Nathan, Elise en Amélie.

Identification of neural and non-neural contributors to joint stiffness in upper motor neuron disease *Novel tools for diagnosis and follow-up*

Karin L. de Gooijer - van de Groep